

Copyright
by
Heather Renae Wilson
2017

**The Thesis Committee for Heather Renae Wilson
Certifies that this is the approved version of the following thesis:**

**Investigation of Corbels Designed According to
Strut-and-Tie and Empirical Methods**

**APPROVED BY
SUPERVISING COMMITTEE:**

Oguzhan Bayrak, Supervisor

Trevor Hrynyk

**Investigation of Corbels Designed According to
Strut-and-Tie and Empirical Methods**

by

Heather Renae Wilson, B.S.C.E.

Thesis

Presented to the Faculty of the Graduate School of

The University of Texas at Austin

in Partial Fulfillment

of the Requirements

for the Degree of

Master of Science in Engineering

The University of Texas at Austin

May 2017

Dedication

To my friends, my family, and Mark, for all of your love and support. Thank you all.

Acknowledgements

First, I would like to thank Dr. Bayrak for his support and insight throughout this project. Your willingness to share your expertise has helped me become better prepared for my future career. I have learned a lot over the past two years and believe that my experience at The University of Texas would not have been the same without the opportunity to work on both the MPR project and the corbel project. Thank you.

To all of the past and present staff at Ferguson Lab, thank you. This project would not have been completed without all of your help. Michael Brown, thank you for your insight into the steps to make this project happen and for helping me learn how to use power tools. David Braley, thank you for helping me with the welding done on the reinforcing cages and for your advice and lessons in the lab. Dennis Phillip, thank you for your assistance with the transportation of specimens on the lab floor. Thank you Michelle Damvar, Liz Clayton, and Deanna Mueller for your help with logistics and your support throughout this process. Thanks also to Joel Arredondo and John Bacon for your assistance with specimen instrumentation. Thank you to all of my peers who helped cast the “mini-Texas” or “mini-airplanes”; while they were small, they would not have been cast without your help.

Hossein Yousefpour, thank you so much for the long hours that you put in during the revision process of this thesis. Your insight and specificity helped me to write and format this thesis in a manner that is better than it would have been without your help. You made the writing process a lot more fluid. Thank you so much for your constant selflessness with your time, knowledge, and experience. For your help, not just with research, but with classes and life, I am extremely grateful.

Thank you to my church group, friends, and family for your love, prayers, and support. Thank you to everyone in AveNEW who prayed for me to get through this semester, especially Leigh, who prayed for my thesis to be less painful than I was thinking it would be (it was). Thank you to my mom and dad for listening to me when I needed a break from writing. John, thank you for the hours of mutual understanding spent writing in the computer lab. Carmen, thank you for your understanding and for your long distance support.

And finally Mark. Thank you for all of the support that you gave me both in person and from afar. I cannot express how much your love, words of encouragement, and your hugs –as well as the ice cream- meant to me while I was finishing my writing. Thank you for being the wonderful, supportive boyfriend you are.

Abstract

Investigation of Corbels Designed According to Strut-and-Tie and Empirical Methods

Heather Renae Wilson, M.S.E.

The University of Texas at Austin, 2017

Supervisor: Oguzhan Bayrak

Corbels are short, typically shear-controlled, cantilevers that transfer loads to columns in structures. Currently, ACI 318-14 provisions allow the structural design of shear-controlled corbels through either an empirical design method or the strut-and-tie method (STM). The objective of this thesis is to evaluate STM as an independent design method for corbels and investigate the differences stemming from the use of STM compared with the empirical design method. Four full-scale double-corbel specimens were designed, fabricated, and tested at Ferguson Structural Engineering Laboratory. Two specimens were designed using the empirical method and two specimens were designed using STM, with and without crack-control reinforcement. Measured load-carrying capacities exceeded the capacities calculated using STM for all specimens, and no signs of premature failure were observed in the corbel detailed merely based on STM. The results of this study suggest that STM can be used independently for corbels and the empirical detailing requirements specific to corbels might not be necessary when using STM.

Table of Contents

List of Tables	x
List of Figures	xiii
Chapter 1. Introduction	1
1.1 Overview	1
1.2 Research Significance	7
1.3 Thesis Organization	8
Chapter 2. Experimental Program	9
Chapter 3. Results and Discussion	21
3.1. Cracking Patterns	22
3.2. Load-Deflection Behavior	25
3.3. Stresses in the Reinforcement	27
3.4. Failure and Post-Failure Conditions	31
3.5. Discussion of Test Results	33
Chapter 4. Summary and Conclusions	40
Appendix A. Materials	43
A.1 Overview	43
A.2 Explanation of the Notation Used in This Appendix	43
A.3 Modulus of Elasticity, Tensile Strength, and Concrete Compressive Strength for Each Specimen	44
A.4 Concrete Batching Details	47
A.5 Mechanical Properties of Reinforcement	49
Appendix B. Crack Patterns	52
Appendix C. Load vs. Strain Plots	55
Appendix D. Experimental Procedures	61
D.1. Overview	61
D.2. Experimental Procedure	62

D.3. Instrumentation Calibration	69
D.4. Test Records.....	70
Appendix E. Capacity calculations	74
E.1 Overview.....	74
E.2 Notation.....	74
E.3 Capacity Calculations: ACI 318-14 Empirical Method.....	79
E.4 Specimen Calculations: ACI 318-14 STM	87
E.5 Specimen calculations: AASHTO LRFD STM ($\nu = 0.45$).....	103
E.6 Specimen Calculations: AASHTO STM ($\nu > 0.45$).....	112
References.....	119
Vita	121

List of Tables

Table 2-1. Specimen design parameters	11
Table 2-2. Concrete mixture properties	17
Table 2-3. Summary of measured mechanical properties.....	18
Table 3-1. Loads corresponding to cracking, yielding, and ultimate strength of the specimens.....	21
Table 3-2. Comparison of predicted and measured capacities of the specimens.....	34
Table A-1. Modulus of elasticity data for each test specimen	44
Table A-2. Splitting tensile strength data for each test specimen.....	44
Table D-1. Calibration factors	69
Table D-2. Specimen C0 test record	70
Table D-3. Specimen C1 test record.....	71
Table D-4. Specimen C2 test record	72
Table D-5. Specimen C3 test record.....	73
Table E-1. Specimen C0 properties used in the empirical method.....	79
Table E-2. Specimen C0 empirical method calculations	80
Table E-3. Specimen C1 properties used in the empirical method.....	81
Table E-4. Specimen C1 empirical method calculations	82
Table E-5. Specimen C2 properties used in the empirical method.....	83
Table E-6. Specimen C2 empirical method calculations	84
Table E-7. Specimen C3 properties used in the empirical method.....	85
Table E-8. Specimen C3 empirical method calculations	86

Table E-9. Specimen C0 properties used in the ACI STM.....	87
Table E-10. Specimen C0 ACI STM (part 1 of 3).....	88
Table E-11. Specimen C0 ACI STM (part 2 of 3).....	89
Table E-12. Specimen C0 ACI STM (part 3 of 3).....	90
Table E-13. Specimen C1 properties used in the ACI STM.....	91
Table E-14. Specimen C1 ACI STM (part 1 of 3).....	92
Table E-15. Specimen C1 ACI STM (part 2 of 3).....	93
Table E-16. Specimen C1 ACI STM (part 3 of 3).....	94
Table E-17. Specimen C2 properties used in the ACI STM.....	95
Table E-18. Specimen C2 ACI STM (part 1 of 3).....	96
Table E-19. Specimen C2 ACI STM (part 2 of 3).....	97
Table E-20. Specimen C2 ACI STM (part 3 of 3).....	98
Table E-21. Specimen C3 properties used in the ACI STM.....	99
Table E-22. Specimen C3 ACI STM (part 1 of 3).....	100
Table E-23. Specimen C3 ACI STM (part 2 of 3).....	101
Table E-24. Specimen C3 ACI STM (part 3 of 3).....	102
Table E-25. Specimen C0 properties used in AASHTO STM calculations ($\nu = 0.45$)..	104
Table E-26. Specimen C0 AASHTO STM calculations ($\nu = 0.45$) ..	105
Table E-27. Specimen C1 properties used in AASHTO STM calculations ($\nu = 0.45$)..	106
Table E-28. Specimen C1 AASHTO STM calculations ($\nu = 0.45$) ..	107
Table E-29. Specimen C2 properties used in AASHTO STM calculations ($\nu = 0.45$)..	108

Table E-30. Specimen C2 AASHTO STM calculations ($\nu = 0.45$)	109
Table E-31. Specimen C3 properties used in AASHTO STM calculations ($\nu = 0.45$)..	110
Table E-32. Specimen C3 AASHTO STM calculations ($\nu = 0.45$)	111
Table E-33. Specimen C0 properties used in AASHTO STM calculations ($\nu > 0.45$)..	113
Table E-34. Specimen C0 AASHTO STM calculations ($\nu > 0.45$)	114
Table E-35. Specimen C1 properties used in AASHTO STM calculations ($\nu > 0.45$)..	115
Table E-36. Specimen C1 AASHTO STM calculations ($\nu > 0.45$)	116
Table E-37. Specimen C2 properties used in AASHTO STM calculations ($\nu > 0.45$)..	117
Table E-38. Specimen C2 AASHTO STM calculations ($\nu > 0.45$)	118

List of Figures

Figure 1-1. Typical corbel configuration	1
Figure 2-1. Specimen design with reinforcement detailing	10
Figure 2-2. Strut-and-tie model.....	12
Figure 2-3. Specimen and fabrication details	14
Figure 2-4. Instrumentation details	16
Figure 2-5. Double-corbel test setup.....	19
Figure 3-1. Load vs. midpoint displacement plots for the specimens	22
Figure 3-2. Crack patterns at service-level loads.....	23
Figure 3-3. Crack patterns immediately prior to failure	24
Figure 3-4. Load vs. deflection comparison of specimens C0, C1, and C2.....	26
Figure 3-5. Estimated stress levels in the reinforcement at service-level loads	28
Figure 3-6. Estimated stress levels in the reinforcement at peak load.....	29
Figure 3-7. Post-failure conditions of the specimens.....	32
Figure A-1. Concrete compressive strength for C0	45
Figure A-2. Concrete compressive strength for C1	45
Figure A-3. Concrete compressive strength for C2	46
Figure A-4. Concrete compressive strength for C3	46
Figure A-5. Concrete batching ticket for Specimen C0.....	47
Figure A-6. Concrete batching for Specimens C1, C2, and C3	48
Figure A-7. Stress-strain plots for No. 4 bars used in C0 (secondary reinforcement).....	49
Figure A-8. Stress-strain plots for No. 4 bars used in C1, C2, & C3 (secondary reinforcement).....	49
Figure A-9. Stress-strain plots for No. 8 bars used in C0 (primary reinforcement)	50

Figure A-10. Stress-strain plots for No. 8 bars used in C1, C2, & C3 (primary reinforcement).....	50
Figure A-11. Stress-strain plots for No. 9 bars used in C0 (column bars).....	51
Figure A-12. Stress-strain plots for No. 9 bars used in C1, C2, & C3 (column bars)	51
Figure B-1. Crack patterns at service-level loads	53
Figure B-2. Crack patterns at peak loads	54
Figure C-1. C0 total load vs. strains in primary reinforcement	56
Figure C-2. C0 total load vs. strains in secondary reinforcement (T1 & T2).....	56
Figure C-3. C0 total load vs. strains in secondary reinforcement (T3 & T4).....	57
Figure C-4. C1 total load vs. strains in primary reinforcement	57
Figure C-5. C1 total load vs. strains in secondary reinforcement (T1 & T2).....	58
Figure C-6. C1 total load vs. strains in secondary reinforcement (T3).....	58
Figure C-7. C2 total load vs. strains in primary reinforcement	59
Figure C-8. C2 total load vs. strains in secondary reinforcement (T1 & T2).....	59
Figure C-9. C2 total load vs. strains in secondary reinforcement (T3 & T4).....	60
Figure C-10. C3 total load vs. strains in primary reinforcement	60
Figure D-1. Fabrication of formwork and reinforcing cages	62
Figure D-2. Fabrication of specimens: typical casting procedures.....	63
Figure D-3. Specimen movement into setup.....	64
Figure D-4. Double-corbel test setup.....	64
Figure D-5. Specimen C0 after the test.....	65
Figure D-6. Specimen C1 after the test.....	66
Figure D-7. Specimen C2 after the test.....	67
Figure D-8. Specimen C3 after the test.....	68

CHAPTER 1. INTRODUCTION

1.1 OVERVIEW

Corbels are short, typically shear-controlled, cantilevers used to transfer concentrated loads to columns in structures. Figure 1-1 shows typical configuration of a reinforced concrete corbel and some of the relevant nomenclature. Because of the change in geometry and the presence of a concentrated load, corbels demonstrate nonlinear strain distribution and are categorized as “discontinuity (D-) regions,” in which the “*plane sections remain plane*” assumption of the flexural theory is not valid (Marti, 1985) and (Schlaich et al., 1987).

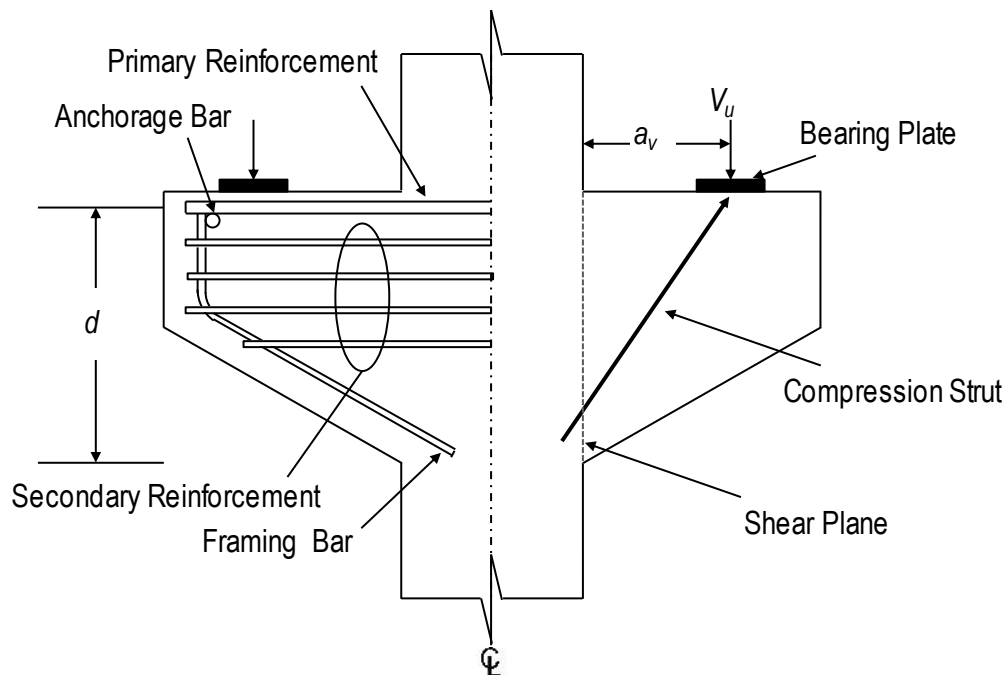


Figure 1-1. Typical corbel configuration

The load-carrying capacity of corbels is governed by a variety of failure modes (Kriz & Raths, 1965) and (Park & Paulay, 1975), the most common being yielding of the primary reinforcement and crushing of the inclined compression strut. Other failure modes include sliding shear at the column-corbel interface and localized failure in the vicinity of the bearing plate. In previous studies by Mattock et al. (1976), increased secondary reinforcement has been shown to shift the failure mode of corbels toward a beam-shear failure behavior, characterized by the widening of cracks throughout the compression strut and crushing of the concrete in compression zones.

ACI 318-14 (2014) provisions allow the design of corbels through two different design methodologies. When the shear span-to-depth ratio (a_v/d) is less than 1, the empirical method, found in Chapter 16 of these provisions, can be used for design. On the other hand, Chapter 23, the strut-and-tie method, can be used for the design of corbels with any a_v/d ratio less than 2. Therefore, corbels with an a_v/d less than 1 may be designed using either method.

In the empirical method of corbel design in ACI 318-14, the load-carrying capacity of the corbel is calculated at the critical shear plane, i.e. the interface between the column and the corbel. The reinforcement in the corbel is designed to provide sufficient sectional moment capacity as well as shear-friction resistance at this shear plane. Sectional moment capacity is calculated using the flexural theory based on the plane section assumption. Shear friction, as a design model, is based on the assumption that shear force is transferred across a cracked interface due to friction, which is generated by normal forces that are

equivalent to the component of the tensile forces in the reinforcement crossing that interface (Birkeland & Birkeland, 1966). According to Section 22.9 of ACI 318-14, if the reinforcement is perpendicular to the shear plane, the shear-friction strength is taken as $\mu A_{vf} f_y$, where A_{vf} and f_y are the area and yield strength of reinforcement crossing the shear plane, respectively, and μ is the coefficient of friction, equal to 1.4 in monolithically placed concrete.

For corbels not subjected to horizontal forces, the area of primary reinforcement in the empirical method is determined as the greatest of: 1) the area of steel needed to resist flexural demands; 2) $2/3$ of the area of shear-friction reinforcement; and 3) $0.04(f'_c/f_y)(b_w d)$, where f'_c is the compressive strength of concrete, f_y is the yield strength of steel, and b_w and d are the width and effective depth of the corbel, respectively. The secondary reinforcement needs to be uniformly distributed over a distance of $(2/3)d$ from the primary reinforcement and must have a total area equal to at least half of the area of primary reinforcement if the corbel is not subjected to any horizontal loads. A set of dimensional restrictions is also specified in Section 16.5.2.4 of ACI 318-14, which limits the total capacity of corbels based on the area of the shear plane. According to these provisions, the shear strength of a corbel cannot exceed $(k + 0.08f'_c)b_w d$, where k is equal to 480 if f'_c is in psi or 3.3 if f'_c is in MPa.

This legacy method is primarily based on the research by Mattock et al. (1976), which involved an experimental study of 28 double-corbel specimens to investigate the structural response of corbels under various combinations of vertical and horizontal

loading. Results from specimens with a wide range of horizontal reinforcement, loading configurations, specimen geometries, and a_v/d ratios showed that the load-carrying capacity of corbels could be estimated as the lesser of the load corresponding to the sectional moment capacity of the shear plane and the shear-friction resistance at the column face.

Prior to Mattock et al., another comprehensive experimental study was conducted by Kriz and Rath (1965). In this study, 195 full-scale double-corbel specimens were investigated to identify the parameters that affect corbel behavior. The variables included reinforcement ratio, concrete strength, a_v/d ratio, amount of secondary reinforcement, corbel dimensions, and ratio between horizontal and vertical loading. The findings of this research provided major contributions to the detailing practices for corbel reinforcement and dimensional restrictions to prevent secondary failures such as splitting of the tip of the corbel or bearing failure. In addition to these two comprehensive investigations, Yong et al. (1985), Fattuhi (1994), Foster et al. (1996), Fattuhi & Hughes (1989), and Campione et al. (2007) have conducted other experimental studies on the behavior of corbels, in which the effects of using high-strength or fiber-reinforced concrete in corbels with various secondary reinforcement were investigated.

The strut-and-tie method (STM) is a design tool for reinforced concrete elements with origins that date back to 1899 (Ritter, 1899) or earlier. In 1987, Schlaich et al. (1987) published a landmark paper that revitalized interest in STM in North America. The methodology presented by Schlaich et al. formed the basis for years of extensive research

that led to the development of current STM provisions in ACI 318-14. In this method, D-regions, such as corbels, are designed using hypothetical trusses that transfer forces from the location of the concentrated loads to the supports. These trusses are made of compressive elements (struts) and tensile elements (ties) that meet at pinned joints (nodes). Designing the D-regions according to ACI 318-14 involves providing sufficient capacities for struts, ties, and all node faces. The strength of struts is determined based on the compressive strength of concrete and a strut coefficient (β_s), which depends on whether the stresses can spread out in the middle of the strut and whether the strut has sufficient distributed reinforcement to control the width of cracks and prevent premature failure (ACI Committee 318, 2014). The most common struts are bottle-shaped struts, i.e. struts in which the compressive zone can spread out at the mid-length of the strut. According to Section 23.5.2 of ACI 318-14, for bottle-shaped struts, if the total area of the distributed reinforcement projected in the direction of the strut exceeds 0.30 percent of the cross-sectional area of the strut, β_s is taken as 0.75. Otherwise, β_s is equal to 0.60. The strength of a tie is dependent on the yield strength and the total area of the reinforcement comprising that tie. The compressive strength of each node is determined based on the compressive strength of concrete and a nodal zone coefficient, β_n , which is taken as 1.0 for nodes with no ties (CCC nodes), 0.80 for nodes with one tie (CCT nodes), and 0.60 for nodes with two or more ties (CTT nodes).

The empirical method and the STM design procedure lead to different reinforcement and detailing requirements for corbels, especially for the secondary

reinforcement. Generally, the STM provisions provide more flexibility regarding the secondary reinforcement and also make it possible to analyze corbels that are not compliant with the detailing requirements prescribed by the empirical design provisions. However, concerns have been raised regarding potential deficiencies in the behavior of corbels that are detailed merely using STM. Moreover, Section 23.2.9 in ACI 318-14 provisions requires that when STM is used for designing corbels, the area of primary reinforcement be greater than $0.04 (f'_c/f_y)(b_w d)$ and some of the requirements of the empirical method, i.e. Sections 16.5.2 and Section 16.5.6, remain satisfied. The requirements in Section 16.5.2 are dimensional limits established in previous research by Mattock et al. (1976) and Kriz and Raths (1956) to prevent premature failures due to geometrical insufficiencies. Section 16.5.6, which covers the detailing of reinforcement, requires that the secondary reinforcement be located within $(2/3)d$. This detailing requirement is not consistent with the crack-control reinforcement requirements of STM, which result in evenly distributed reinforcement over the entire depth of the member. It is also not clear whether STM can be used independently to analyze existing corbels that do not comply with the secondary reinforcement requirements of Section 16.5.6.

Similar to ACI 318-14, AASHTO LRFD Bridge Design Specifications (2016) allow the design of shear-controlled corbels using either an empirical method, which is almost identical to that in Chapter 16 of ACI 318-14, or STM provisions. However, Article 5.13.2.4.2 of AASHTO LRFD provisions requires that in corbels designed based on STM, the primary and secondary reinforcement areas be greater than those required according to

the flexural and shear-friction requirements of the empirical method. These specifications clearly discourage the use of STM for corbels, as no benefits can be gained from the use of this method in reinforcement area or flexibility of detailing.

The goal of this thesis is to examine whether strut-and-tie design methodology can be used for corbels independently of the empirical design requirements specified in Chapter 16 of ACI 318-14. Four full-scale specimens were designed using these two methodologies and fabricated at the Ferguson Structural Engineering Laboratory. The observed behavior of the specimens under applied loads was evaluated until failure to identify differences in behavior due to the use of different secondary reinforcement and the necessity of the detailing requirements specified in the empirical method.

1.2 RESEARCH SIGNIFICANCE

The two corbel design methods currently available in ACI 318-14 result in different reinforcement requirements. Recently, there have been questions regarding the efficacy of STM as an independent method for designing corbels, and concerns have been raised regarding the necessity of satisfying the legacy requirements of the empirical method when using STM. This thesis aims to address these concerns through a comparative experimental study on corbels that were designed according to these two methods. The findings of this research provide important contributions towards optimizing the use of STM, which leads to significant flexibility in the design of new corbels and the analysis of existing ones.

1.3 THESIS ORGANIZATION

This thesis is divided into four chapters, including this introduction. Chapter 2 describes the experimental program and presents specimen design and fabrication, specimen instrumentation, test setup, and test procedures. Chapter 3 provides the results of the experimental program along with discussion of the results. Conclusions and further research options are given in Chapter 4. Additional details of the test program are provided in five appendices, as follows:

- Appendix A includes detailed information regarding the mechanical properties of materials,
- Appendix B contains cracking patterns observed in the experimental program,
- Appendix C provides strain gage data,
- Appendix D demonstrates additional information about the experimental procedures, and
- Appendix E includes detailed calculations for estimating the load-carrying capacities of the specimens using ACI 318-14 and AASHTO LRFD provisions.

CHAPTER 2. EXPERIMENTAL PROGRAM

Four double-corbel specimens, identified herein as C0 through C3, were designed based on ACI 318-14 (2014) provisions. The geometry of the specimens and the reinforcement detailing used within each specimen are shown in Figure 2-1. All specimens shared the same dimensions, with a width of 14 in. (356 mm), a corbel height of 24 in. (610 mm), a corbel length of 20 in. (508 mm), and an extended column height of 12 in. (305 mm). Note that the specimens in Figure 2-1 are shown in the-orientation in which they were tested.

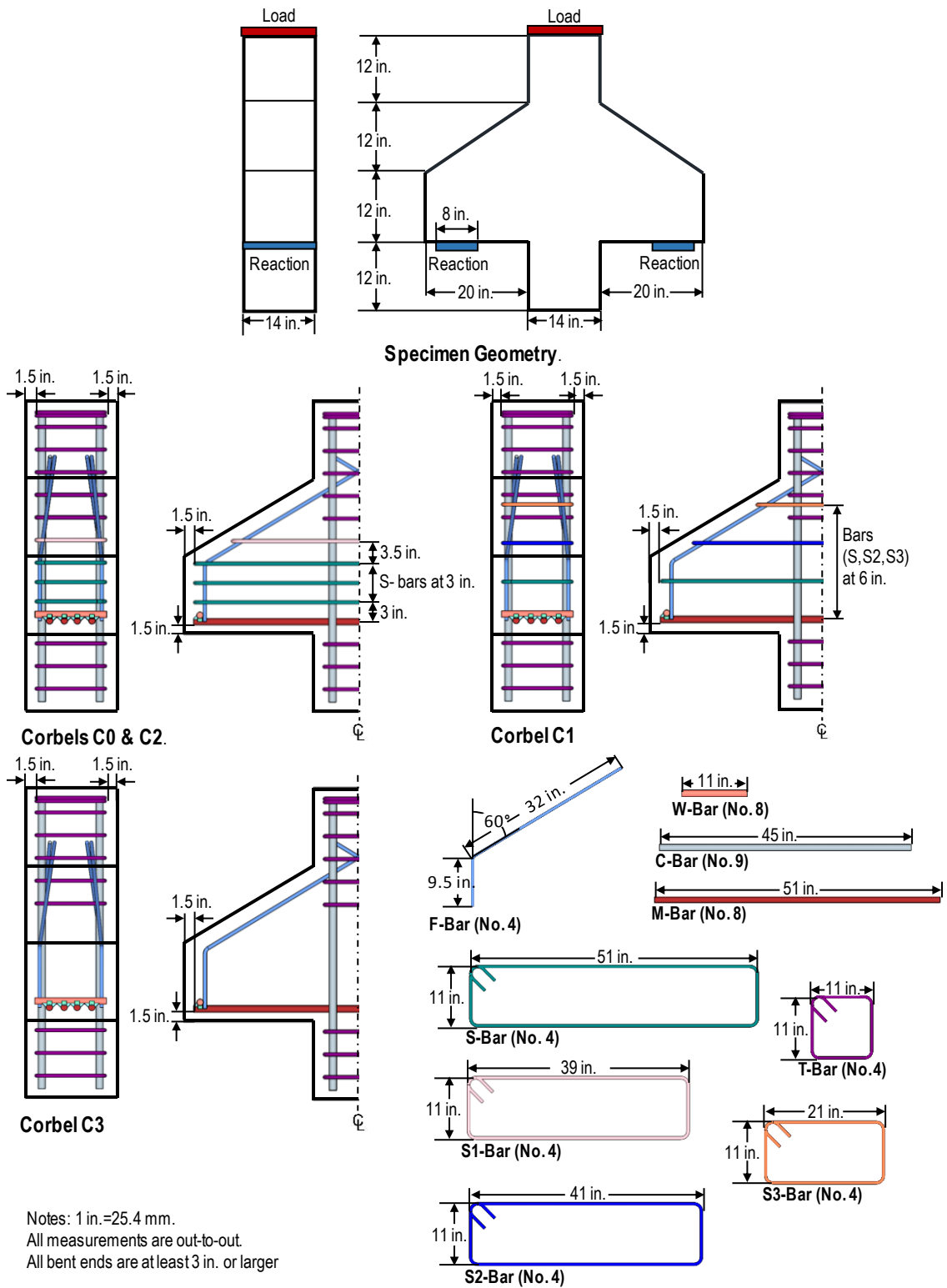


Figure 2-1. Specimen design with reinforcement detailing

To simplify the test setup, the specimens were designed to resist only vertical loading, and no horizontal tensile forces were considered in design. The specimens were designed to require identical primary reinforcement (four No. 8 bars) but different secondary reinforcement depending on the design method used. The design concrete strength (f'_c) and the yield strength of the reinforcement (f_y) were assumed equal to 5 ksi (34.5 MPa) and 60 ksi (413.7 MPa), respectively. The design assumptions, expected failure modes, and the predicted capacities for the specimens are listed in Table 2-1.

Table 2-1. Specimen design parameters

	C0	C1	C2	C3
Design method	Empirical	STM	Empirical	STM
Shear span-to-depth ratio, a_v/d	0.66	0.59		
Design capacity, kips	523	421	523	418
Predicted failure mode	---	Yielding of AA'	---	Crushing of AB and A'B'

Note: 1 in. = 25.4 mm; 1 kip = 4.45 kN.

Specimens C0 and C2 were designed according to the empirical provisions in Chapter 16 of ACI 318-14, which require designing the corbels for moment and shear-friction capacity at the column face. These specimens had identical detailing; however, C0 was tested at a greater shear span-to-depth (a_v/d) ratio than all other specimens.

The secondary reinforcement used in C0 and C2 was detailed according to Articles 16.5.5.2 and 16.5.6.6 of ACI 318-14. Since no horizontal forces were assumed in design, the total area of secondary reinforcement was taken as half of the area of the primary reinforcement. The No. 4 bars comprising the secondary reinforcement in these two

specimens were uniformly distributed within $2/3$ of the effective depth of the corbel at the face of the column.

Specimens C1 and C3 were designed based on STM provisions in Chapter 23 of ACI 318-14. The strut-and-tie truss model used to design these specimens is shown in Figure 2-2. The horizontal locations of Nodes A and A' were aligned with the center of the bearing plates. Since the column was subjected to pure compression, Nodes B and B' were positioned at the quarter points within the column width. The vertical location of Nodes B and B' was determined as the middle of the rectangular compression block at the column face. The design process involved checking the yield strength of Tie AA', the compressive strength of Struts AB, A'B', BB', BC, and B'C', and the back, bearing, and inclined faces of Nodes A, A', B, and B'.

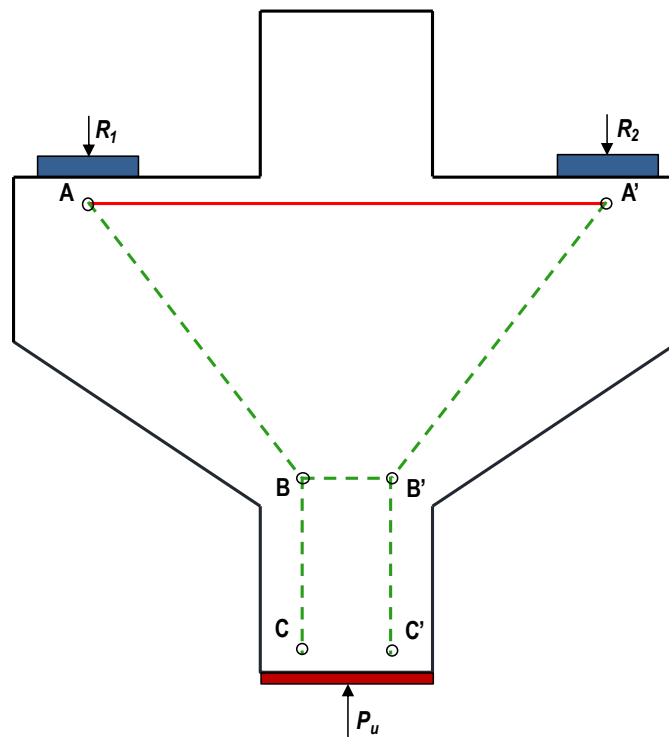


Figure 2-2. Strut-and-tie model

The secondary reinforcement in C1 was designed according to the crack-control reinforcement requirements described in Section 23.5 of ACI 318-14. The No. 4 bars comprising the secondary reinforcement in this specimen were evenly distributed across the inclined strut. As a result, the strut coefficient (β_s) was taken as 0.75 when designing this specimen using STM.

Specimen C3 was designed without any crack-control, i.e. secondary, reinforcement. Therefore, a lower β_s value of 0.60 was implemented in the strut-and-tie capacity calculations. Designing new corbels that are not reinforced to control cracking is not recommended for any application. However, this specimen was designed to investigate the failure mechanisms governing the corbel capacity and the performance of STM provisions in assessing the strength of existing corbels that do not comply with the recommended design practice.

All four specimens contained symmetric primary reinforcement anchored by a No. 8 cross bar welded at each end, as recommended in Section 16.5.6.3 of ACI 318-14. All specimens also contained No. 4 reinforcing ties spaced at 3.5 in. (89 mm) in the column region to prevent premature failure of the specimens.

The specimens were fabricated at Ferguson Structural Engineering Laboratory (FSEL). Specimen C0 was constructed prior to the other specimens to verify the suitability of fabrication and testing procedures. Specimens C1, C2, and C3 were cast together to minimize the potential effects of variable mechanical properties of concrete on observed specimen behavior. Wooden formwork was used in the fabrication of all specimens, as shown in Figure 2-3 (a).

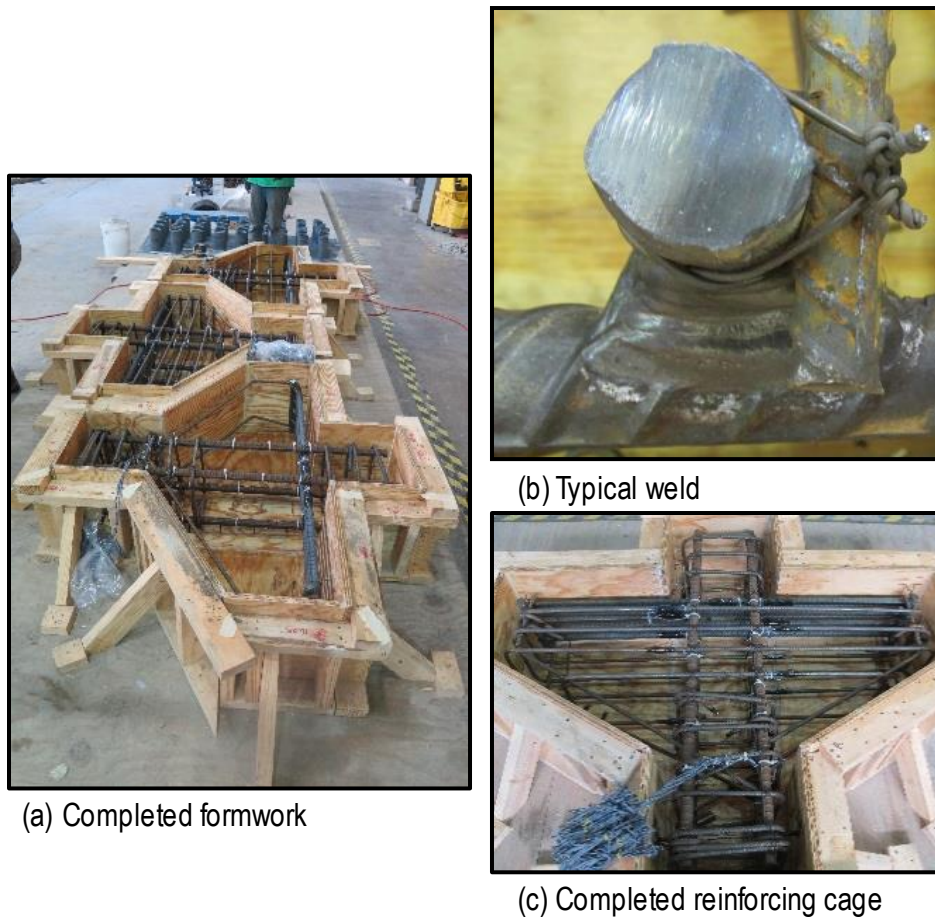
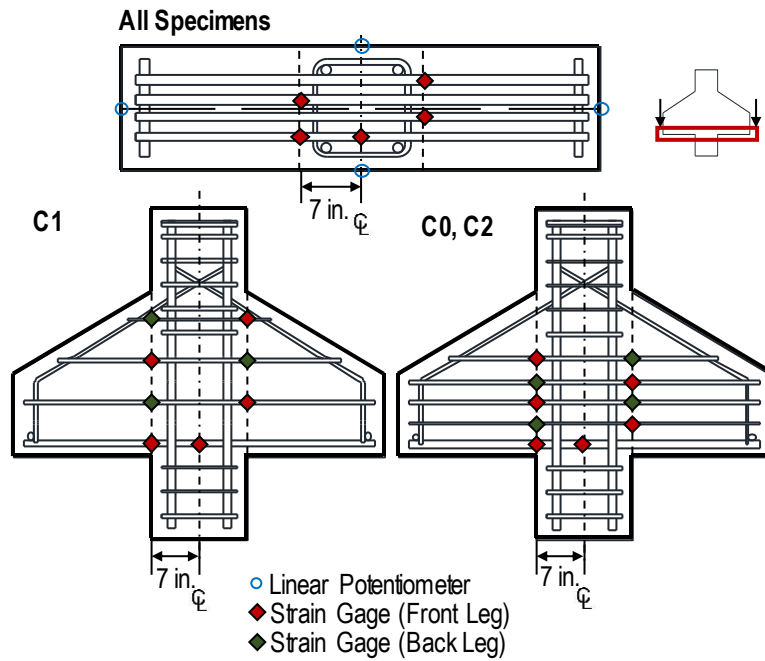


Figure 2-3. Specimen and fabrication details

The No. 8 cross bars (W-bars in Figure 2-1) were welded across the four No. 8 bars of the primary reinforcement (M-bars), resulting in a base section for the remaining cage. A typical weld detail is shown in Figure 2-3 (b). No. 9 column bars (C-bars in Figure 2-1) were then tied onto the primary reinforcing bars. Next, the remaining No. 4 bars in the corbel and column areas were tied. Figure 2-3 (c) shows a completed reinforcement cage.

To determine the strains in the reinforcement during the test, each specimen was instrumented with electrical resistance strain gages (SGs) on the primary reinforcing bars, as shown in Figure 2-4 (a). The SGs had a gage length of 0.2 in. (5 mm). The secondary

reinforcement in Specimens C0, C1, and C2 was also instrumented, as shown in the figure. Two SGs were installed on each tie comprising the secondary reinforcement, located diagonally opposite from each other. The instrumented leg alternated from one tie to the next. The location of the SGs coincided with the interface between the column and the corbel. An example of the installation of a SG before the application of protective layers is shown in Figure 2-4 (b).



(a) Strain gage and linear potentiometer locations
 Note: 1 in.=25.4 mm.



(b) Strain gage application

Figure 2-4. Instrumentation details

The properties of the concrete mixtures used for the fabrication of the specimens are provided in Table 2-2. Corresponding batch tickets can be found in Appendix A.

Crushed limestone with a nominal maximum aggregate size of 1 in. (25 mm) was used in all mixtures. The mixtures for all specimens were batched and mixed at a local ready-mix concrete supplier and transported to FSEL. Each specimen was cast in two layers and internal vibrators were used after each layer was placed to ensure sufficient concrete consolidation. After the concrete was placed and finished, the specimens were covered with plastic sheeting for a minimum of 7 days for curing.

Table 2-2. Concrete mixture properties

		C0	C1	C2	C3
Mixture components	Portland cement, lb/yd ³	423	410		
	Fly ash, lb/yd ³	140	150		
	Coarse aggregate, lb/yd ³	1947	1940		
	Coarse aggregate type	Crushed limestone, Maximum size: 1 in.			
	Fine aggregate, lb/yd ³	1440	1467		
	Water, lb/yd ³	175	211		
	Super plasticizer, oz/yd ³	28			
	Retarder, oz/yd ³	6			
	Water-cementitious ratio	0.31	0.38		

Note: 1 lb/yd³ = 0.6 kg/m³; 1 oz/yd³ = 38.7 mL/m³; 1 in. = 25.4 mm.

A series of 4- by 8-in. (100- by 200- mm) concrete cylinders was cast together with the double-corbel specimens to obtain mechanical properties of the concrete comprising each specimen. The cylinders were tested according to ASTM-compliant procedures to determine the compressive strength of concrete at 28 days and the compressive strength, modulus of elasticity, and splitting tensile strength of the concrete on each double-corbel specimen's test day. The cylinders were stored in the same environment as the double-

corbel specimens to ensure similar strength gain between the cylinders and the specimens. Mechanical properties of the primary and secondary reinforcing bars were also measured using ASTM-compliant tests. Measured mechanical properties of the concrete and reinforcing bars are summarized in Table 2-3.

Table 2-3. Summary of measured mechanical properties

Property		Test method	C0	C1	C2	C3
Concrete	$f'_{c,28}$, ksi	ASTM C39	4.6	6.5		
	f'_c , ksi	ASTM C39	5.3	6.5	6.8	5.6
	E_c , ksi	ASTM C469	4,920	6,300	6,480	4,980
	f_t , ksi	ASTM C496	0.55	0.61	0.64	0.66
No. 4 bars	f_y , ksi	ASTM A370	69.3	67.2		
	f_u , ksi		99.0	95.8		
No. 8 bars	f_y , ksi		73.4	70.6		
	f_u , ksi		101.6	99.3		
No. 9 bars	f_y , ksi		74.0	71.9		
	f_u , ksi		107.5	105.7		

Note: 1 ksi = 6.9 MPa; f'_c, E_c, f_t = compressive strength, modulus of elasticity, and splitting tensile strength of concrete on test day; $f'_{c,28}$ = 28-day compressive strength of concrete; f_y, f_u = yield and ultimate strength of the reinforcement.

The specimens were tested in an inverted configuration, using the test setup shown in Figure 2-5. Load was applied by means of an 800-kip (3,560-kN) hydraulic ram, which was pressurized through a pneumatically controlled hydraulic pump. The specimens were supported by a roller support fixture on one side and a tilt-saddle (i.e. spherical seat) support fixture on the other side. The bearing area on these fixtures was 8- by 14 in. (203-

by 356 mm). The support fixtures also contained load cells, allowing the measurement of reaction forces during the test. As shown in Figure 2-4 (a), the specimens were also instrumented using four 1-in. (26-mm) linear potentiometers (LPs), one on either end of the specimen and two under the load application point, one on either side. These LPs were used to measure the specimen deformation under loading.

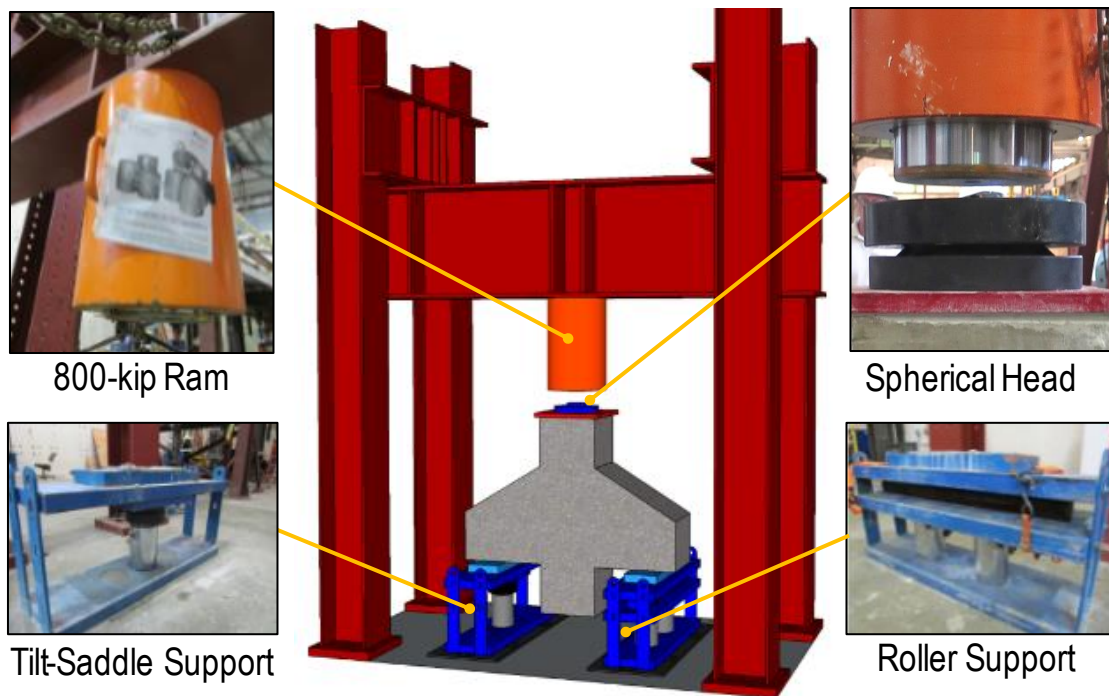


Figure 2-5. Double-corbel test setup

Specimen C0 was tested at a shear span of 14.5 in. (368 mm), resulting in a shear-span-to-depth ratio of 0.66. Section 16.5.2.3 in ACI 318-14 provision requires that no part of the bearing area project farther from the face of support than both the end of the straight portion of the primary reinforcement and the interior face of the transverse bar welded to the primary reinforcement to provide anchorage. With the configuration used for C0, the end of the primary reinforcement was outside the bearing region, but the bearing plate

extended beyond the interior face of the transverse bar. In other specimens, a shorter shear span of 13.0 in. (343 mm), corresponding with a shear-span-to-depth ratio of 0.59, was used to satisfy the requirements of ACI 318-14.

The specimens were loaded in increments that were smaller than 10 percent of the predicted capacity of each specimen based on nominal material properties. Each increment was applied at a load rate of 600 lb (2.67 kN) per second or less. After each load increment, the cracking pattern in the specimen was traced and documented. Upon reaching the load corresponding to 75 percent of the calculated nominal capacity, the specimen was continuously loaded to failure, which was identified by a loss in the load-carrying capacity.

CHAPTER 3. RESULTS AND DISCUSSION

Figure 3-1 shows the plots of load versus midpoint displacement for all four specimens. In this figure, the points corresponding to cracking, first detected yielding, yielding of all primary reinforcing bars, and the ultimate capacity of each specimen are identified. A summary of observations from the experimental program is also presented in Table 3-1. Detailed results of the test program are discussed in the following sections. In all of the discussions provided in this chapter, the reported load values are the total loads applied to the specimen and therefore represent twice the shear force applied to each corbel.

Table 3-1. Loads corresponding to cracking, yielding, and ultimate strength of the specimens

		C0	C1	C2	C3
P_{cr} , kips	North	144-168	150-180	48-96	90-120
	South	144-168	150-180	96-144	90-120
$P_{cr,st}$, kips		110	79	80	85
P_{y1} , kips		-	629	646	596
$P_{y,all}$, kips		-	751	724	669
P_{max} , kips		641	754	802	694
P_{y1}/P_{max}		-	0.834	0.805	0.858
$P_{y,all}/P_{max}$		-	0.996	0.902	0.963

Note: 1 kip = 4.45 kN.

P_{cr} = Load at first observed cracking;

$P_{cr,st}$ = Load corresponding to change in stiffness;

P_{y1} = Load at first detected yielding; $P_{y,all}$ = Load corresponding to yielding of all primary reinforcing bars; P_{max} = Peak applied load.

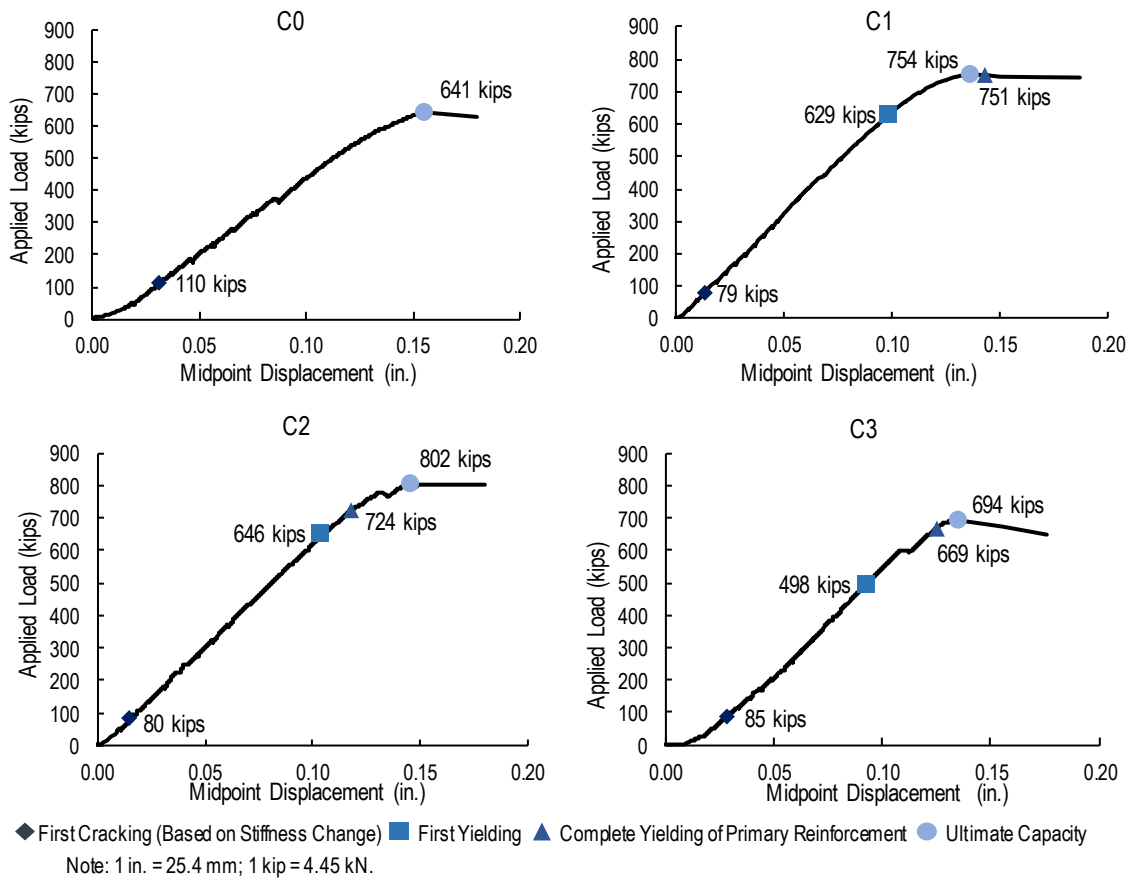


Figure 3-1. Load vs. midpoint displacement plots for the specimens

3.1. CRACKING PATTERNS

Before each test, the specimen was closely examined for existing cracks potentially due to shrinkage or damage during handling and transportation. None of the specimen had cracks in the test region, i.e. the region between each support plate and the column face, prior to loading.

Figure 3-2 and Figure 3-3 show the progression of cracking within each specimen until the service-level load and immediately prior to failure, respectively. To estimate the service-level load for each specimen, the design capacity of the specimen was divided by 1.4. In reality service loads may be slightly greater or somewhat smaller than the values obtained through the use of this estimation. Nevertheless, for the purposes of discussion this estimation is deemed appropriate. The cracking patterns shown in both figures were observed on one face of each specimen (the north face). Similar figures illustrating the cracks observed on the opposite (south) face of the specimens are provided in Appendix B.

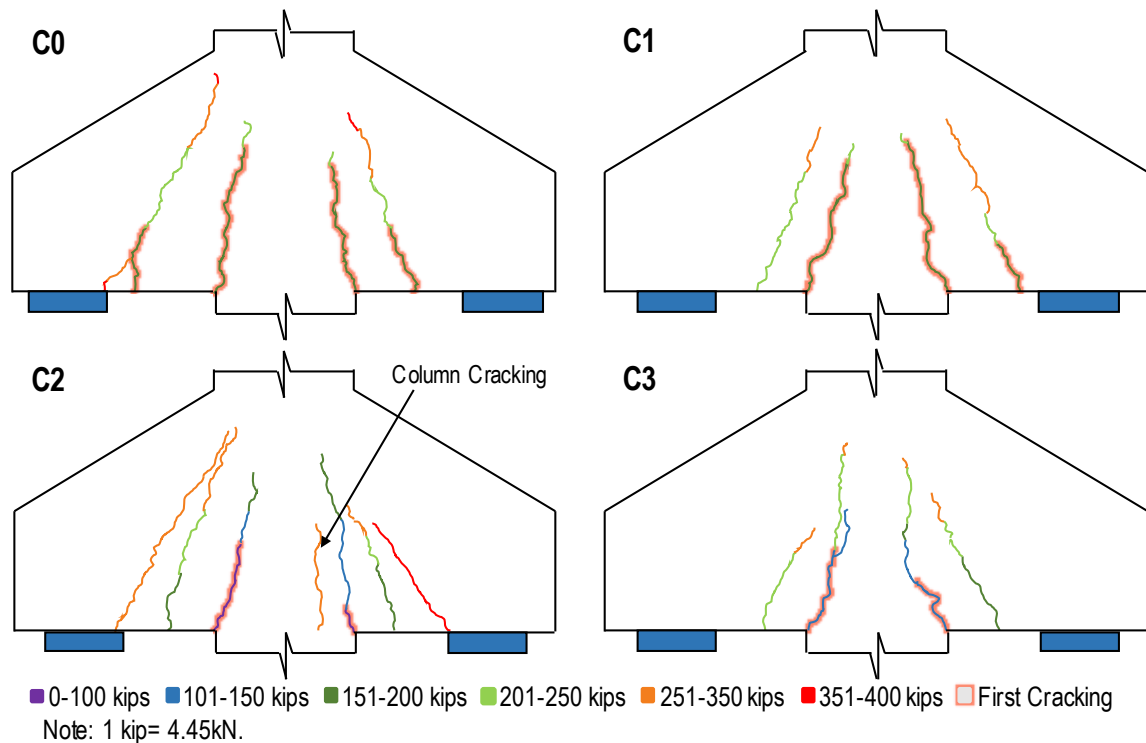


Figure 3-2. Crack patterns at service-level loads

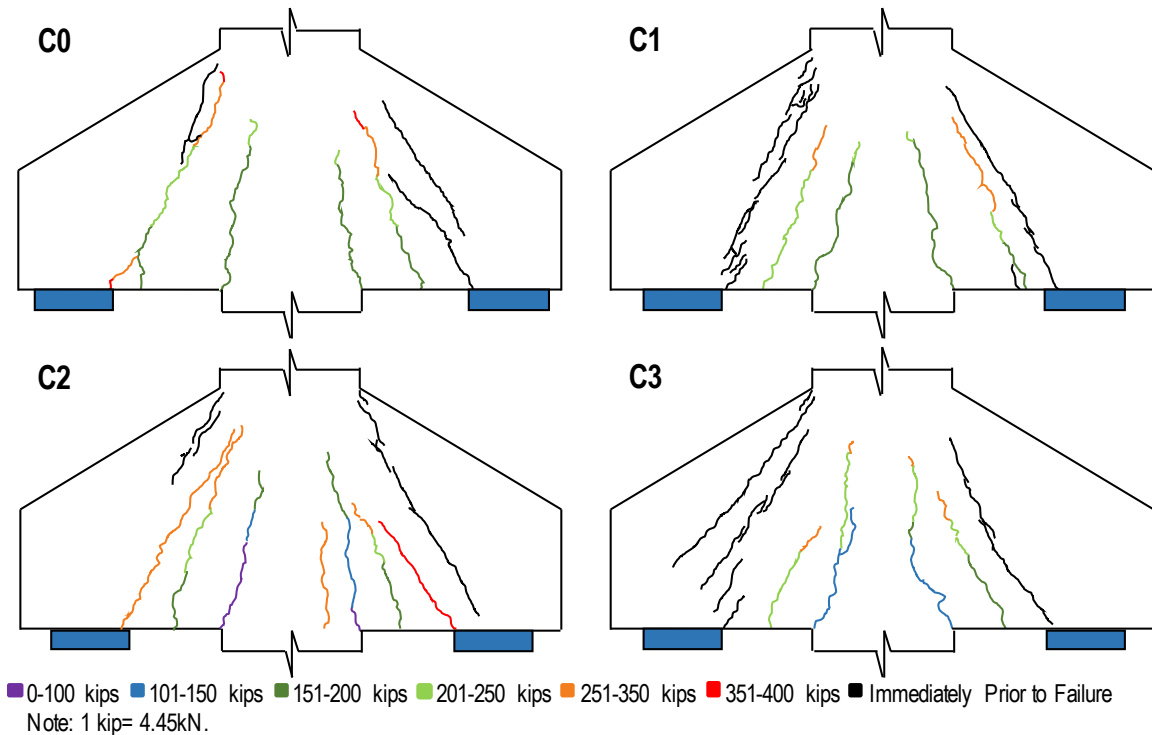


Figure 3-3. Crack patterns immediately prior to failure

The load corresponding to the first observation of cracks in each specimen is reported in Table 3-1. As indicated in Figure 3-2, the first cracks in all specimens appeared at the corner between the column and the horizontal face of the corbel, consistent with the assumed critical shear plane in the empirical method.

At their service-level loads, corbels designed based on STM experienced slightly less crack propagation than those designed and detailed using the empirical method. In all specimens, the cracks generally extended beyond the corbel region, into the column. In

Specimen C2, which demonstrated the most extensive cracking at its service-level load, a crack developed completely in the column, as indicated in Figure 3-2.

Large shear cracks appeared on the surface of each specimen prior to failure. Specimens C1 and C3 had more extensive cracking than Specimens C0 and C2 immediately prior to failure. The cracks on Specimen C3, in particular, covered a broader area than those on all other specimens. Unlike other specimens, the cracks formed in this specimen extended beyond the triangular region between the support plate and the column. As expected, eliminating the secondary reinforcement in this specimen led to an increase in the extent of cracking.

No crack width measurements were taken from the specimens. It is likely that the cracks in Specimen C3 were wider than those in other specimens because there was no clamping force in this specimen to restrain the growth of cracks. However, general observations with the naked eye did not reveal a significant difference in crack widths among the other three specimens, which contained secondary reinforcement.

3.2. LOAD-DEFLECTION BEHAVIOR

Since the initial portions of the load-displacement plots are affected by support deformations, occurrence of first cracking in the specimens is not visually identified in the plots shown in Figure 3-1. To exclude the effects of support deformations, the measurements obtained from the LPs at the supports were subtracted from the midpoint displacements. The result is shown in Figure 3-4. During the structural testing of C3, one

of the LPs used to measure the support deformations malfunctioned. Therefore, C3 is not included in Figure 3-4.

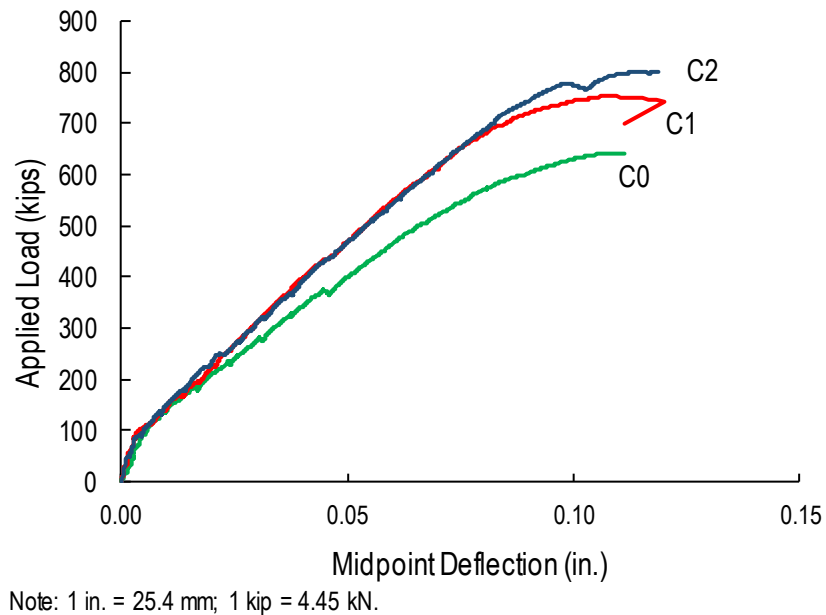


Figure 3-4. Load vs. deflection comparison of specimens C0, C1, and C2

As can be seen in Figure 3-4, the first cracking of the specimens was accompanied by a noticeable decrease in stiffness, i.e. change in the slope of the load-deflection plot. The change in stiffness typically occurred before cracks became visible to the naked eye. As presented in Table 2-3, Specimens C1 and C2 had greater concrete compressive strength and modulus of elasticity and were tested at a smaller shear-span-to-depth ratio compared with C0. Therefore, C1 and C2 showed a slightly greater stiffness than C0, before and after cracking.

Figure 3-4 also shows that the difference in the overall load-deflection behavior of C1 and C2 was negligible until the last stages of loading. While these specimens experienced extensive cracking before failure, differences in secondary reinforcement between these two specimens do not appear to noticeably affect the stiffness before or after cracking.

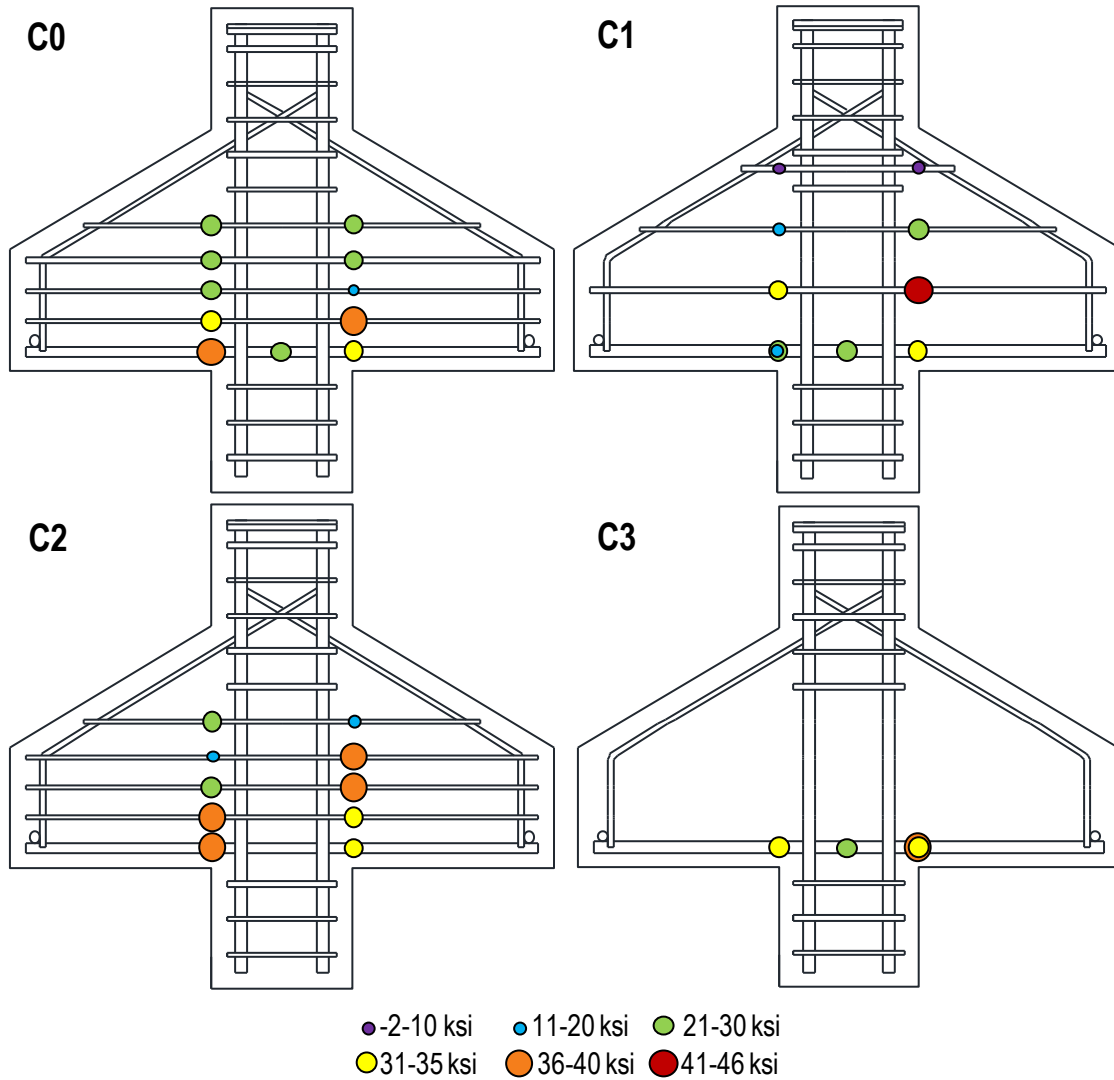
The ultimate strength of each corbel is indicated in Figure 3-1 and Table 3-1. Among the specimens with similar shear-span-to-depth ratios and compressive strengths of concrete, i.e. C1, C2, and C3, the ultimate strength of the corbel correlated with the amount of the secondary reinforcement.

3.3. STRESSES IN THE REINFORCEMENT

The stresses in the reinforcing bars were inferred from strain gage measurements, assuming a modulus of elasticity of 29,000 ksi (200 GPa). Figure 3-5 and Figure 3-6 show the stresses in the reinforcing bars at service-level and peak loads, respectively. Corresponding load-strain plots are provided in Appendix C for the reinforcing bars in all specimens. In developing these figures, it is assumed that the stress in each leg of the ties comprising the secondary reinforcement was equal to the stress in the other leg.

All specimens except C0 showed reinforcement yielding during the test. The first yielding occurred in the primary reinforcing bars in C1 and C3 but in the secondary reinforcement closest to the primary reinforcement in C2. The load corresponding to the

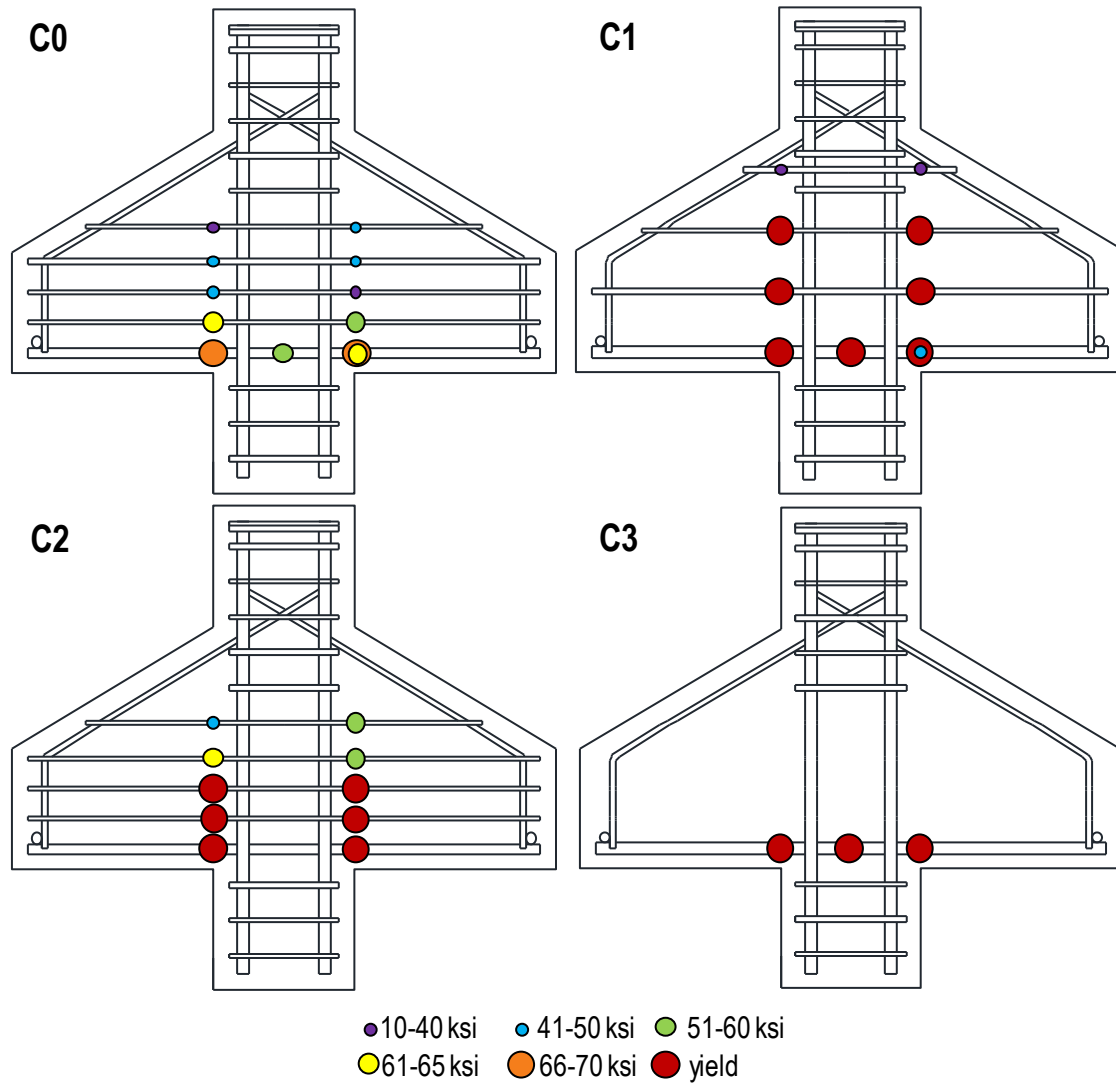
first yield and the ratio of this load to the ultimate strength correlated with the amount of secondary reinforcement provided.



Note: 1 ksi = 6.9 MPa.

Figure 3-5. Estimated stress levels in the reinforcement at service-level loads

Figure 3-5 shows that overall differences in stresses in the secondary reinforcement were not significant among the specimens at their service-level loads. Specimen C1 showed slightly smaller stresses in the primary reinforcement compared to other specimens but the largest stresses in the secondary reinforcement were observed in this specimen.



Note: 1 ksi = 6.9 MPa.

Figure 3-6. Estimated stress levels in the reinforcement at peak load

As visible in Figure 3-6, at peak load, all reinforcing bars were in tension. In Specimens C0 and C2, maximum tensile stresses were observed in the primary reinforcement, and the stress level in the secondary reinforcement decreased with an increase in distance from the primary reinforcement. This observation is consistent with the simplified flexural analysis of the corbel that is used as part of the empirical design method. Additional secondary reinforcement in C2 appears to increase the overall capacity of this specimen compared to C1. However, in both C1 and C2, all of the bars that were distributed within the 8 in. (203mm) distance from the bearing face of the corbel had yielded prior to failure. One of the primary reinforcing bars in C1 yielded after reaching the peak load.

Table 3-1 presents both P_{y1}/P_{max} and $P_{y,all}/P_{max}$ ratios for the specimens, where P_{y1} is the load at first detected yielding, $P_{y,all}$ is the load at complete yielding of the primary reinforcement, and P_{max} is the peak load. As can be seen in this table, while first yielding in Specimen C1 was detected at a smaller load compared to C2, complete yielding of the primary reinforcement occurred at a greater load in C1. However, Specimen C1 failed almost immediately after all bars comprising the primary reinforcement yielded, whereas C2 could carry an additional 78-kip (347-kN) load before failure. Similar to C1, C3 failed soon after complete yielding of the bars comprising the primary reinforcement of this specimen.

Stresses on the order of 64 ksi (441 MPa) were detected in the primary reinforcement of C0. However, none of the strain measurements from the bars in this

specimen revealed yielding of the reinforcement. As shown in Table 2-3, the yield strength of primary and secondary reinforcement in this specimen was slightly greater than that of the other three specimens. Moreover, as previously noted, a longer shear span was also used for testing C0 compared to the other three specimens, resulting in the bearing plate's being extended beyond the interior face of the transverse anchorage bar. This configuration could potentially result in diminished stress development in the primary reinforcement of this specimen, preventing this reinforcement from being completely utilized. However, no evidence of insufficient reinforcement anchorage was observed in this specimen.

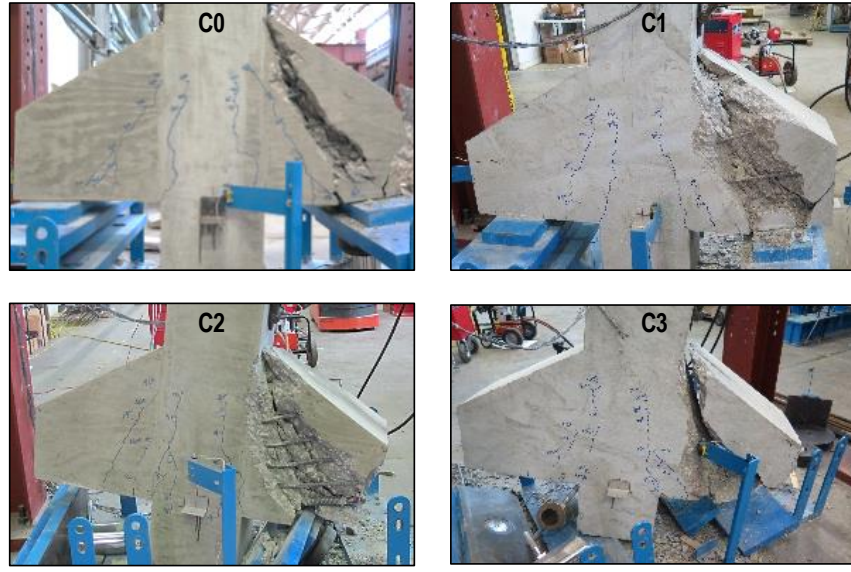
3.4. FAILURE AND POST-FAILURE CONDITIONS

Failure of all specimens was identified as a sudden loss of load accompanied by the occurrence of significant damage to the specimens in a brittle, explosive manner. Specimen C0 was the only specimen in which compression failure of the inclined strut occurred before detected yielding of the reinforcement. All other specimens failed through yielding of the primary reinforcement, followed by failure of the inclined strut.

Figure 3-7 shows the post-failure condition of the specimens. Additional figures from the experimental program are provided in Appendix D. All specimens failed on the corbel placed over the tilt-saddle support. The strut failures in C0, C1, and C2 were relatively similar, showing clear signs of compression failure, with noticeable spalling of the cover concrete on the inclined strut. In C3, however, the strut showed a splitting-type failure due to tensile stresses perpendicular to the inclined crack.



(a) North



(b) South

Figure 3-7. Post-failure conditions of the specimens

For specimen C0, the failure crack, which developed along the inclined strut between the column and the inside edge of the bearing area, was the second to appear and

grew in length and width throughout the rest of the test. For specimens C1, C2, and C3, the crack along which failure occurred was not present until later stages of the test, i.e. after reaching approximately 75 percent of the predicted capacity when the cracks were no longer marked. The failure crack in C3 formed at a shallower angle compared to those of C0, C1, and C2. This crack started at the outside edge of the bearing plate, which is different than the observations from the other three specimens.

3.5. DISCUSSION OF TEST RESULTS

To evaluate the performance of different design provisions in predicting the load-carrying capacities of the specimens, the measured mechanical properties of materials comprising each specimen were used to calculate the ultimate strength of that specimen according to: 1) the empirical method in Chapter 16 provisions of ACI 318-14; 2) STM according to the Chapter 23 provisions of ACI 318-14; and 3) STM according to Section 5.6.3 of AASHTO LRFD Bridge Design Specifications. All load and resistance factors were taken equal to 1. Details of the calculations according to each method are provided in Appendix E. A summary of the results is provided in Table 3-2.

Table 3-2. Comparison of predicted and measured capacities of the specimens

	C0	C1	C2	C3
P_{max} , kips	641	754	802	694
$P_{ACI,Emp}$, kips	555	615	632	571
$P_{ACI,STM}$, kips	448	556	558	468
$P_{AASHTO,0.45}$, kips	426*	556*	558*	477*
v_{AASHTO}	0.58**	0.53**	0.51**	0.45
$P_{AASHTO,v}$, kips	519*	556	558	477*
$P_{max}/P_{ACI,Emp}$	1.16	1.23	1.27	1.22
$P_{max}/P_{ACI,STM}$	1.43	1.36	1.44	1.49
$P_{max}/P_{AASHTO,0.45}$	1.50	1.36	1.44	1.45
$P_{max}/P_{AASHTO,v}$	1.24	1.36	1.44	1.45

Note: 1 kip = 4.45kN.

$P_{ACI,Emp}$, $P_{ACI,STM}$ = Capacities according to Chapters 16 and 23 of ACI 318-14, respectively; v_{AASHTO} = Concrete efficiency factor according to AASHTO LRFD for the strut-to-node interface;

$P_{AASHTO,0.45}$ = Capacity according to AASHTO LRFD, assuming $v=0.45$; $P_{AASHTO,v}$ = Capacity according to AASHTO LRFD, ignoring the crack-control reinforcement requirements.

* Without considering the back face of Nodes A and A'.

** Ignoring the requirements in Article 5.6.3.6 of AASHTO LRFD.

The reinforcement detailing used within Specimens C1 and C3 did not comply with the requirements of the empirical method in ACI 318-14. However, the nominal shear and flexural strengths of these specimens were calculated according to the provisions of Section 16.5.4 in ACI 318-14 to estimate the load-carrying capacity for comparison purposes. In other words, the provisions of Section 16.5.5 regarding the required amount of secondary

reinforcement were ignored when using the empirical method for Specimens C1 and C3. For all four specimens, the capacity estimates according to the empirical method were governed by the provisions of Section 16.5.2.4 in ACI 318-14.

The STM provisions of ACI 318-14 predicted the failure of Specimen C0 to occur in the back face of the CCT node (Node A in Figure 2-2). According to these provisions, the governing mode for Specimens C1 and C2, as well as the second governing mode for C0, was yielding of the primary tie reinforcement. In Specimen C3, however, failure of the inclined strut (Strut AB in Figure 2-2) was the governing failure mode.

The STM provisions in AASHTO LRFD are generally similar to ACI 318-14 provisions, with a few key differences. First, the strut strength is assumed to be governed by the strength of the node faces to which the strut is connected. Therefore, only the node faces are examined, without checking the strut separately. Second, AASHTO LRFD specifications are clear that checking the capacity of smeared nodes, i.e. nodes not bounded by a bearing plate, such as Node B in Figure 2-2, is unnecessary. The crack-control reinforcement provisions are also more stringent in AASHTO LRFD, requiring distributed reinforcement in both orthogonal directions to enable the use of a concrete efficiency factor greater than 0.45.

Two sets of results are presented in Table 3-2 for AASHTO LRFD specifications, varying in the assumed concrete efficiency factor for checking the nodes. None of the specimens meet the crack-control reinforcement requirements of AASHTO LRFD, as they did not contain any vertical reinforcement in the corbels. In a conservative interpretation

of these specifications, the concrete efficiency factor should be taken as 0.45 for all four specimens, resulting in strength values that are reported as $P_{AASHTO,0.45}$ in Table 3-2. For comparison, an alternative set of ultimate strengths was also calculated according to AASHTO LRFD specifications for specimens other than C3. In these calculations, the lack of vertical secondary reinforcement was ignored, and greater concrete efficiency factors, according to Table 5.6.3.5.3a-1 of AASHTO LRFD, were used. The resulting strength values are reported as $P_{AASHTO,\nu}$ in Table 3-2. Due to the lack of secondary reinforcing bars in Specimen C3, the efficiency factor was always taken as 0.45 for this specimen.

According to Article 5.6.3.5.3b of AASHTO LRFD specifications, the bond stresses of adequately developed bars do not need to be applied to the back face of the node. For the specimens in this test program, a transverse bar is welded to develop the primary reinforcing bars relatively close to the back face of the CCT nodes (Nodes A and A' in Figure 2-2). As a result, the back face might be completely or partially subjected to bond stresses, and it might be prudent to apply the tie force to the back face of these nodes. Checking the back face of the CCT nodes would control the load-carrying capacity of all specimens when using a concrete efficiency factor of 0.45, and that of Specimens C0 and C3 when using the greater concrete efficiency factors shown in Table 3-2. However, since no experimental evidence of back face damage was observed in any of the specimens, it appears unnecessary to check the back face of the CCT node for corbels with configurations similar to specimens used in this test program. The capacity estimates that are indicated with an asterisk in Table 3-2 were calculated without checking the back face of the CCT

nodes. When this strength check is not considered, the capacities of Specimens C0 and C3 are governed by the strength of the inclined face of Nodes A and A' whereas yielding of the primary reinforcement governs the capacities of Specimens C1 and C2.

Table 3-2 also presents the ratios of the maximum load measured during the structural test to the capacities predicted using each of the design procedures described above. The load-carrying capacities of all specimens exceeded their predicted capacities based on all calculation procedures, meaning that all of the methods provide a safe estimate for the ultimate strength of the corbels investigated in this test program. The most conservative estimates were obtained from the STM provisions of ACI 318-14 and those of AASHTO LRFD assuming the lower concrete efficiency factor of 0.45. The use of both of these methods was consistent with the amount of secondary reinforcement provided within the specimens, without ignoring any detailing requirements.

Comparison between the $P_{max}/P_{ACI,Emp}$ and $P_{max}/P_{ACI,STM}$ ratios shows that the strut-and-tie method was more conservative than the empirical method of the ACI 318-14 provisions for estimating the capacities of all specimens, including those detailed according to the requirements of the empirical method. The $P_{max}/P_{ACI,STM}$ ratios were greater for Specimens C0 and C2 compared with C1. This observation is expected, as these specimens contained greater amounts of steel than required by the STM provisions of ACI 318-14. The additional secondary reinforcement, while beneficial to the load-carrying capacity, is not considered in calculating the capacities of these specimens. Due to a similar reason, the $P_{max}/P_{AASHTO,0.45}$ ratio was greater for C0 and C2 compared with C1.

Failure of Specimens C1 and C2 was predicted to be governed by yielding of the primary reinforcement in all STM calculations (with the aforementioned exclusion of the back face check for AASHTO LRFD). As a result, equal capacities were predicted for these specimens in all STM procedures. For Specimen C3, the STM provisions of ACI 318-14 provided a capacity estimate that was more conservative than that of AASHTO LRFD.

Unlike ACI 318-14, AASHTO LRFD specifications do not require checking the strength of struts if the nodal strengths are sufficient. When using the STM provisions of ACI 318-14 for Specimen C3, failure of the inclined strut corresponds to a noticeably smaller load than the load associated with failure of the inclined face of Nodes A and A'. The more conservative estimate for the capacity of this specimen by ACI 318-14 provisions appears to be a result of this additional check. However, the data obtained from this study are too limited for making general conclusions regarding the necessity of performing independent strength checks for struts. Despite the predictions of AASHTO LRFD and ACI 318-14, yielding of the tie reinforcement was eventually confirmed in Specimen C3, which shows that both provisions are very conservative in taking the concrete strength into account for corbels without crack-control reinforcement. Considering the variability of concrete strength and the potential brittle failure of corbels without crack-control reinforcement, this observed conservatism is desirable.

The observations from this test program clearly shows the merits of STM according to Chapter 23 of ACI 318-14 in providing safe estimates of the capacity of corbels, independently of the empirical provisions provided in Chapter 16. All four specimens,

containing different amounts of secondary reinforcement, exceeded their strength predictions according to the STM provisions. However, the capacity estimates from these provisions were reasonably accurate and not excessively conservative. Moreover, slightly less service-level cracking was observed in the specimens that were designed and detailed according to the STM provisions compared to those detailed based on the empirical method. The use of corbels without crack-control reinforcement is not recommended, due to the possibility of sudden, brittle failures. However, the ACI 318-14 STM provisions could conservatively estimate the capacity of Specimen C3, indicating the potential suitability of these provisions for estimating the capacity of existing corbels with poor or unclear detailing of distributed reinforcement.

The empirical method, while still providing conservative estimates of the load-carrying capacity, was not as effective as the STM provisions. Development of cracks and the observed failure modes in the specimens did not correspond to the flexural and shear-friction failure modes governing the empirical method. Moreover, the use of the empirical method results in restrictive detailing requirements that make this method ineffective for estimating the capacities of many existing corbels.

CHAPTER 4. SUMMARY AND CONCLUSIONS

Four full-scale double-corbel specimens were designed according to the provisions of ACI 318-14 and fabricated at the Ferguson Structural Engineering Laboratory. Two specimens were designed according to the empirical provisions of Chapter 16 and the other two were designed using the STM provisions of Chapter 23. The specimens were tested to investigate the efficacy of STM provisions in comparison with the empirical method. Strains in the primary and secondary reinforcement and cracking conditions of the specimens were extensively monitored. Measured load-carrying capacities of the specimens were compared with the capacities calculated according to the two aforementioned methods as well as the STM provisions of AASHTO LRFD. The primary conclusions from this study were as follows:

- **Overall Corbel Behavior:** Specimens C1, which was detailed according to STM, showed a very similar load-deflection behavior compared to that of Specimen C2, which was designed according to the empirical method. All specimens developed significant shear cracks in the inclined strut regions prior to failure. At their service-level loads, specimens designed using STM showed slightly less cracking. However, the overall differences in cracking conditions immediately prior to failure were not significant among the three specimens that contained secondary reinforcement.
- **Reinforcement Requirements:** The crack-control reinforcement requirements in Chapter 23 of ACI 318-14 appear sufficient to prevent premature failure of corbels

designed according to STM. Yielding of the primary tie reinforcement was confirmed in Specimen C1, which was detailed merely based on Chapter 23 provisions and did not meet the detailing requirements of the empirical method in Chapter 16 of ACI 318-14.

- **Performance of STM Provisions:** The STM provisions in ACI 318-14 provided conservative estimates of the capacities of all specimens. For specimens that complied with the detailing requirements of the empirical method, the capacities estimated using STM were more conservative than those predicted using the empirical method. The specimens did not satisfy the crack-control reinforcement requirements of AASHTO LRFD. However, these STM design provisions also provided conservative lower-bound estimates of the ultimate strengths of the specimens.
- **Evaluating Non-Compliant Designs:** STM provisions of ACI 318-14 and AASHTO LRFD provided conservative estimates of the capacity of Specimen C3, which did not contain any secondary reinforcement. It is not recommend to design new corbels without secondary reinforcement because limited redistribution capability in such corbels might lead to premature, brittle failures. However, these results show that STM provisions can be used to obtain a lower-bound estimate of the capacity of existing corbels in which secondary reinforcement detailing is unknown or does not comply with code requirements.

The results of this study suggest that STM provisions may be independently used to design new corbels and evaluate the strength of existing corbels that do not necessarily

comply with code requirements. It is recommended that similar tests be conducted on more specimens with various geometries, concrete strengths, amounts of reinforcement, and horizontal loads to confirm the validity of observations from this testing program for different conditions in which corbels might be used.

APPENDIX A. MATERIALS

A.1 OVERVIEW

This appendix provides information on the materials comprising each specimen and details on the material testing results. Testing of concrete cylinders and reinforcement samples was completed according to ASTM-compliant procedures at Ferguson Structural Engineering Laboratory (FSEL).

A.2 EXPLANATION OF THE NOTATION USED IN THIS APPENDIX

D = measured diameter of the cylinder,

E_c = modulus of elasticity of concrete,

f'_c = concrete compressive strength,

f_t = splitting tensile strength of concrete,

f_u = ultimate tensile strength of steel reinforcement,

f_y = yield strength of steel reinforcement, and

L = measured length of the cylinder.

A.3 MODULUS OF ELASTICITY, TENSILE STRENGTH, AND CONCRETE COMPRESSIVE STRENGTH FOR EACH SPECIMEN

Table A-1. Modulus of elasticity data for each test specimen

Specimen	Cylinder ID	Age (days)	Date	L _{avg} (in.)	D (in.)	L/D	E _c (ksi)
C0	16	30	20-05-2016	7.9	4.01	1.97	5,180
C0	17	30	20-05-2016	7.9	4.01	1.97	4,730
C0	18	30	20-05-2016	7.9	4.01	1.97	4,840
C1	13	28	24-08-2016	7.9	4.01	1.97	7,400
C1	14	28	24-08-2016	7.9	4.01	1.97	5,130
C1	15	28	24-08-2016	7.9	4.01	1.97	6,380
C2	22	44	09-09-2016	7.8	4.01	1.95	6,800
C2	23	44	09-09-2016	7.9	4.01	1.97	4,060
C2	24	44	09-09-2016	7.9	4.01	1.97	6,160
C3	31	63	28-09-2016	7.9	4.01	1.97	4,800
C3	32	63	28-09-2016	7.8	4.01	1.95	6,940
C3	33	63	28-09-2016	7.9	4.02	1.97	5,150

Table A-2. Splitting tensile strength data for each test specimen

Specimen	Cylinder ID	Age (days)	Date	L _{avg} (in.)	D _{avg} (in.)	L/D	f _t (psi)
C0	19	30	20-05-2016	7.9	4.01	1.97	570
C0	20	30	20-05-2016	7.9	4.01	1.97	545
C0	21	30	20-05-2016	7.9	4.01	1.97	525
C1	16	28	24-08-2016	7.9	4.01	1.97	565
C1	17	28	24-08-2016	7.9	4.01	1.97	595
C1	18	28	24-08-2016	7.9	4.01	1.97	660
C2	25	44	09-09-2016	7.9	4.01	1.97	625
C2	26	44	09-09-2016	7.9	4.01	1.97	660
C2	27	44	09-09-2016	7.9	4.01	1.97	635
C3	31	63	28-09-2016	7.9	4.02	1.97	660
C3	32	63	28-09-2016	7.9	4.01	1.97	630
C3	33	63	28-09-2016	7.9	4.02	1.97	695

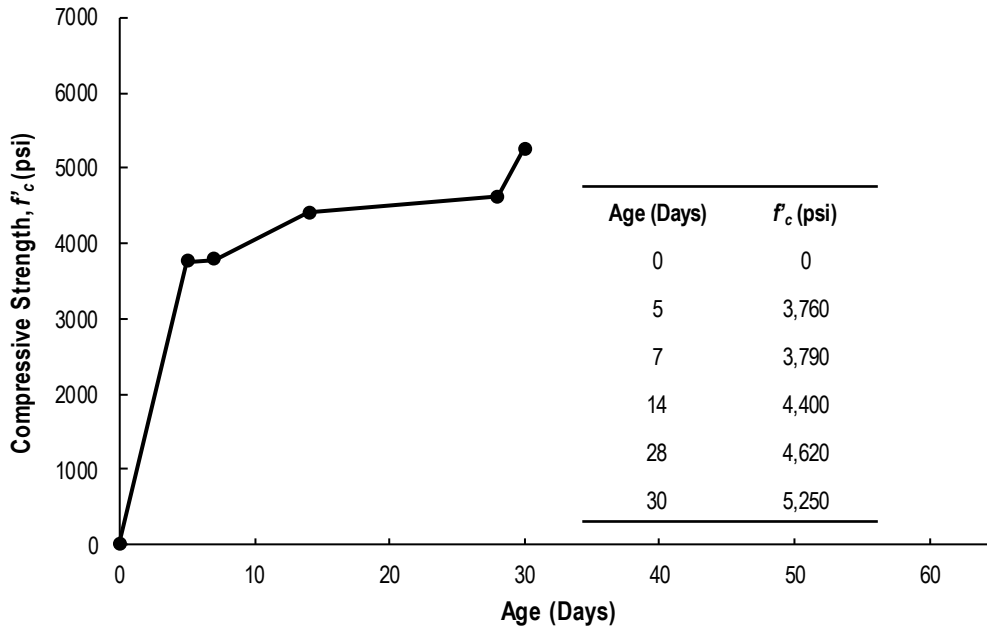


Figure A-1. Concrete compressive strength for C0

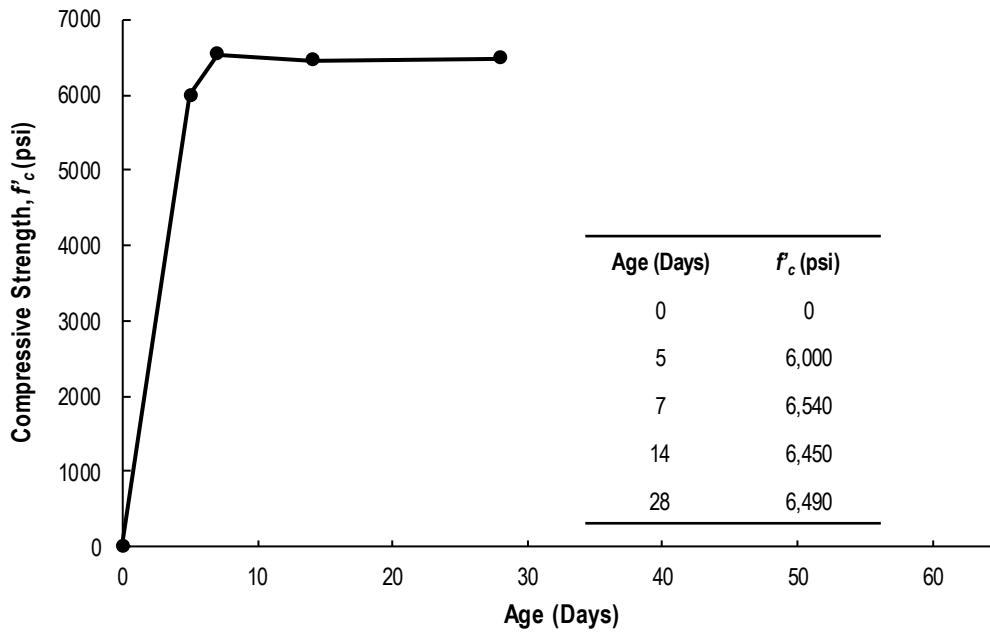


Figure A-2. Concrete compressive strength for C1

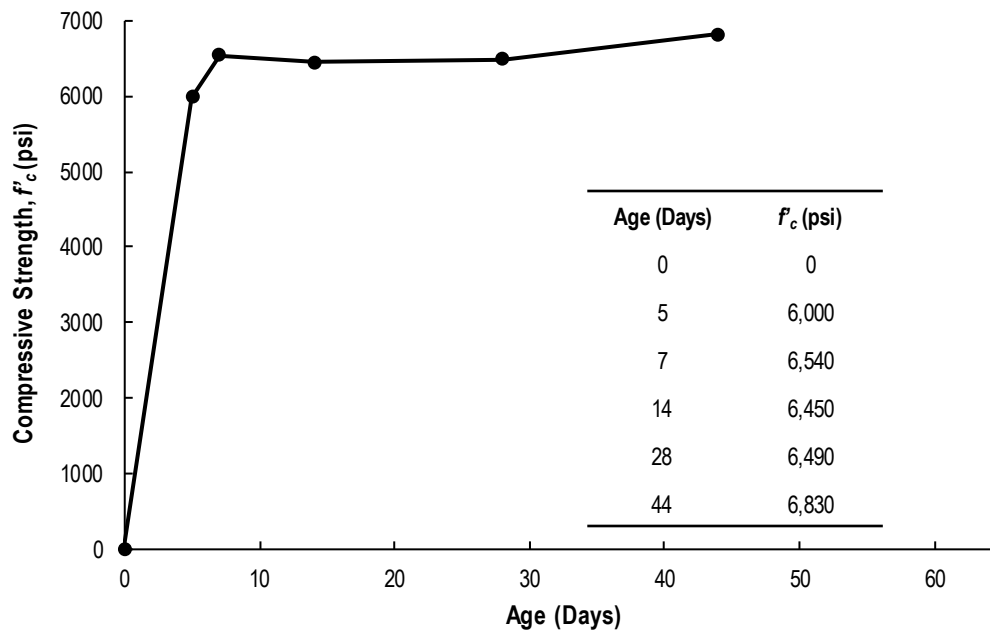


Figure A-3. Concrete compressive strength for C2

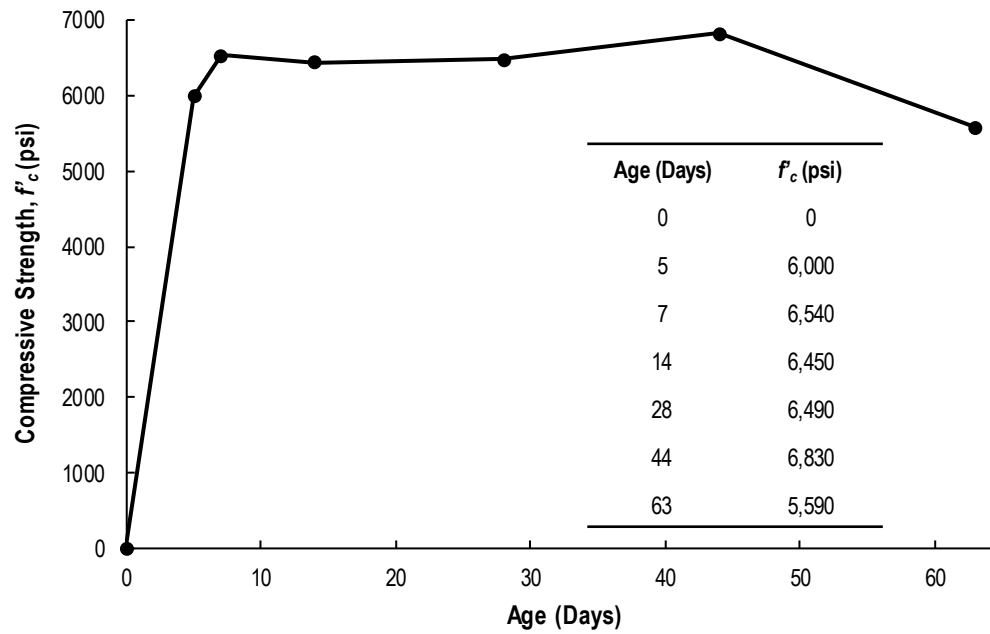



Figure A-4. Concrete compressive strength for C3

A.4 CONCRETE BATCHING DETAILS

SAFETY FIRST
THANK YOU FOR HELPING
OUR DRIVERS ENTER AND
EXIT JOB SITES SAFELY



1320 Arrow Point Drive, Suite 600
 Cedar Park, Texas 78613
 Tel: 512.385.3838

GET OUT AND LOOK
 JOB SITE CONDITIONS:
 FAIR WINDY
 RAIN
 OTHER *inside*

ORIGINAL DELIVERY TICKET

DATE	LEAVE PLANT	ARRIVE JOB	START POUR	FINISH POUR	LEAVE JOB	ARRIVE PLANT	ORDER NUMBER
04/20/2016	12:05 PM						7

U T Ferguson Lab
10100 Burnet Rd

10100 BURNETT RD


CUSTOMER NUMBER	SOURCE	TRUCK	DRIVER	CUSTOMER PURCHASE ORDER NUMBER
242889	089	0722	SYLVESTER MIMS	

PRODUCT CODE	QUANTITY	DESCRIPTION	U/M	PRICE	AMOUNT
6025102S	3.00	6.0 SK 25% FA 1" CLS W/HRWR			
8104	1.00	ENVIRONMENTAL WASTE CHARGE			
Origin : 8900 Ramirez Lane Austin, TX 78742					
UNDER 6 YARDS					

WATER ADDED ON SITE PER CUSTOMER REQUEST		Customer assumes all responsibility for the affect that added water may have on product quality, including without limitation strength, durability, appearance, air content, etc.			SUB TOTAL	
GALLONS OF WATER ADDED	ESTIMATED SLUMP				SALES TAX	
8		CONCRETE USED FOR		PLEASE PAY THIS AMOUNT		
601 test		ORDERED SLUMP	YARDS ORDERED	TOTAL YARDS	DELIVERY REQUEST TIME	
		8.00	3.00	3.00	13:02	

1. Ready Mix Concrete: Texas Concrete Materials 1001 50 Burnet Austin, Texas 78721, (512) 861-7100. Do not breathe dust/fume/gas/mist/vapor/spray. Wash hands thoroughly after handling. Wear protective gloves/protective clothing/eye protection/face protection. Contaminated work clothing must not be allowed out of the workplace. Use only outdoors or in a well-ventilated area. Description of first aid measures: If swallowed, rinse mouth. Do NOT induce vomiting. Immediately call a poison center/doctor. If on skin (or hair), take off immediately all contaminated clothing. Rinse skin with water/shower. Wash contaminated clothing before reuse. Immediately call a poison center/doctor. If inhaled, remove person to fresh air and keep comfortable for breathing. Immediately call a poison center/doctor. If in eyes, rinse cautiously with water for several minutes. Remove contact lenses, if present and easy to do. Continue rinsing. Immediately call a poison center/doctor. If exposed or concerned, seek medical advice/attention. Store locked up. Store in a well-ventilated place. Keep container(s) tightly closed. Dispose of contents/container in accordance with all local, regional, national, and international regulations.

THANK YOU FOR YOUR BUSINESS

Signature: *Adrian Cite* Print Name: _____ 2-202897 

Truck	Load Size	Mix Code	Disp Ticket Num	Time	Date
0722	3.00	CYDS 6025102S	8936589	12:05 PM	4/20/16

Material	Design Qty	Required	Batched	% Var	% Moisture	Actual	Wet
CEMENT	423.0 lb	1269.0 lb	1270.0 lb	0.08%			
FLYASHF	141.0 lb	423.0 lb	420.0 lb	-0.71%			
SAND	1343 lb	4331 lb	4320 lb	-0.26%	7.50% M	36 gl	
1"MFCLS	1950 lb	5865 lb	5840 lb	-0.42%	0.25% M	2 gl	
HRWR	28.20 oz	84.60 oz	84.00 oz	-0.71%			
WRRETARD	5.64 oz	16.92 oz	17.00 oz	0.47%			
WATER	29.0 gl	26.0 gl	25.2 gl	0.51%		25.2 gl	

Load	12066 lb	Design W/C:	0.429	Water/Cement:	0.311	A	Design	87.0 gl	Actual	63.0 gl	To Add:	24.0
Slump:	8.00 in	Water in Truck:	0.0 gl	Adjust Water:	0.0 gl / Load		Trim Water:	-8.0 gl / CYDS				

Figure A-5. Concrete batching ticket for Specimen C0

SAFETY FIRST
THANK YOU FOR HELPING
OUR DRIVERS ENTER AND
EXIT JOB SITES SAFELY

TEXAS
 CONCRETE MATERIALS
 1320 Arrow Point Drive, Suite 600
 Cedar Park, Texas 78613
 Tel: 512.385.3838

- GET OUT AND LOOK
- JOB SITE CONDITIONS:
- FAIR WINDY
- RAIN
- OTHER

ORIGINAL DELIVERY TICKET

DATE	LEAVE PLANT	ARRIVE JOB	START POUR	FINISH POUR	LEAVE JOB	ARRIVE PLANT	ORDER NUMBER
07/27/2016	9:20 AM						13



U T Ferguson Lab 10100 Burnet Rd	10100 BURNETT RD
-------------------------------------	------------------

CUSTOMER NUMBER	SOURCE	TRUCK	DRIVER	CUSTOMER PURCHASE ORDER NUMBER		
242889	089	0457	MOISES RAMIREZ	GOMEZ		
PRODUCT CODE	QUANTITY	DESCRIPTION		U/M	PRICE	AMOUNT
6025102S	3.00	6.0 SK 25% FA 1" CLS W/HRWR				
8104	1.00	ENVIRONMENTAL WASTE CHARGE				
AU495L	Origin : 8900 Ramirez Lane Austin, TX 78742 UNDER 6 YARDS 183 TRN RT ON BURNETT RD TO JJ PICKLE RESEARCH CENTER BLDG 24					
WATER ADDED ON SITE PER CUSTOMER REQUEST				SUB TOTAL		
GALLONS OF WATER ADDED ESTIMATED SLUMP				SALES TAX		
Customer assumes all responsibility for the affect that added water may have on product quality, including without limitation strength, durability, appearance, air content, etc.				PLEASE PAY THIS AMOUNT		
CONCRETE USED FOR		ORDERED SLUMP	YARDS ORDERED	TOTAL YARDS	DELIVERY REQUEST TIME	
		7.00	3.00	3.00	10:01	

1. Ready Mix Concrete. Texas Concrete Materials 1001 Ed Bluebell Austin, Texas 78721, (512) 861-7100. Do not breathe dust/fume/gas/mist/vapor/spray. Wash hands thoroughly after handling. Wear protective gloves/protective clothing/eye protection/face protection. Contaminated work clothing must not be allowed out of the workplace. Use only outdoors or in a well-ventilated area. Description of first aid measures: If swallowed, rise mouth. Do NOT induce vomiting. Immediately call a poison center/doctor, if on skin (or hair), take off immediately all contaminated clothing. Rinse skin with water/shower. Wash contaminated clothing before reuse. Immediately call a poison center/doctor, if inhaled, remove person to fresh air and keep comfortable for breathing. Immediately call a poison center/doctor, if in eyes, rinse cautiously with water for several minutes. Remove contact lenses, if present and easy to do. Continue rinsing. Immediately call a poison center/doctor, if exposed or concerned, seek medical advice/attention. Store locked up. Store in a well-ventilated place. Keep container(s) tightly closed. Dispose of concrete/container in accordance with all local, regional, national, and international regulations.



THANK YOU FOR YOUR BUSINESS

- 2. Concrete is NOT guaranteed against freezing. Claims of shortages will not be allowed and will be deemed waived unless made at the time the material is delivered. In accordance with ASTM C84, Texas Concrete Materials shall be provided with the results of any acceptance test on plastic or hardened concrete.
- 3. Only Texas Concrete Materials employees may have access to concrete delivery truck. Non-Texas Concrete Materials employees may drive, climb on or in any way access the Texas Concrete Materials truck. Any violation of this provision will be deemed trespass.
- 4. Customer is responsible to specify and provide a location on the job site for concrete washout. Trucks MAY NOT wash out into storm drains.
- 5. Customer and/or Owner will be responsible to direct Texas Concrete Materials employees as to proper ingress and egress of the property, if such required. To the extent such direction is followed or that no direction is given, Customer and/or Owner acknowledges that Texas Concrete Materials will not be liable and will be indemnified by them for damage of any nature or kind incurred by moving Texas Concrete Materials' truck past curb line or right of way limits, including without limitation damage to property, curbs, gutters, sidewalks, etc. Customer will also pay all towing and repair costs for Texas Concrete Materials' truck damage results from access directions or job site conditions. Mud and debris track out control and remediation is the responsibility of Customer and/or Owner.
- 6. NOTICE TO PROPERTY OWNER: Failure of Customer to pay for the materials being provided herewith may result in the filing of a mechanic's lien on the property pursuant to Texas Property Code Chapter 53. All of the terms of any other written agreement between Seller and Customer, including those terms set forth in credit agreements, material sales terms and conditions or other contracts, are not superseded by the matters set forth in this delivery ticket.
- 7. STANDBY AND UNLOADING TIME: Excess truck time will be assessed at the current rate per minute for orders exceeding 5 minutes per yard PLUS an additional 15 minutes per load.
- 8. The undersigned acknowledges that he/she is the Customer or an authorized agent for the Customer and agrees, on behalf of the Customer, to all of the terms and conditions set forth herein. Failure or refusal to sign this delivery ticket BUT acceptance of material constitutes agreement with terms and conditions above.

Signature: [Signature] Print Name: M D BROWN



Truck	Load Size	Mix Code	Disp Ticket Num	Time	Date	
0457	3.00	CYDS 6025102S	8945624	9:20 AM	7/27/16	
Material	Design Qty	Required	Batched	% Var % Moisture	Actual	Wat
CEMENT	423.0 lb	1269.0 lb	1230.0 lb	- 3.07%		
FLYASHF	141.0 lb	423.0 lb	450.0 lb	> 6.38%		
SAND	1343 lb	4230 lb	4400 lb	> 4.01%	5.00% M	25 gl
1"MFCLS	1950 lb	5850 lb	5820 lb	-0.51%	M	
HRWR	28.20 oz	84.60 oz	84.00 oz	-0.71%		
WRRETARD	5.64 oz	16.92 oz	17.00 oz	0.47%		
WATER	29.0 gl	50.9 gl	50.9 gl	0.14%		50.9 gl
Load	12331 lb	Design W/C: 0.429	Water/Cement: 0.378 A	Design	87.0 gl	Actual 76.0 gl To Add: 11.0
Slump:	7.00 in	# Water in Truck: 0.0 gl	Adjust Water: 0.0 gl / Load	Trim Water:	-4.0 gl / CYDS	

Figure A-6. Concrete batching for Specimens C1, C2, and C3

A.5 MECHANICAL PROPERTIES OF REINFORCEMENT

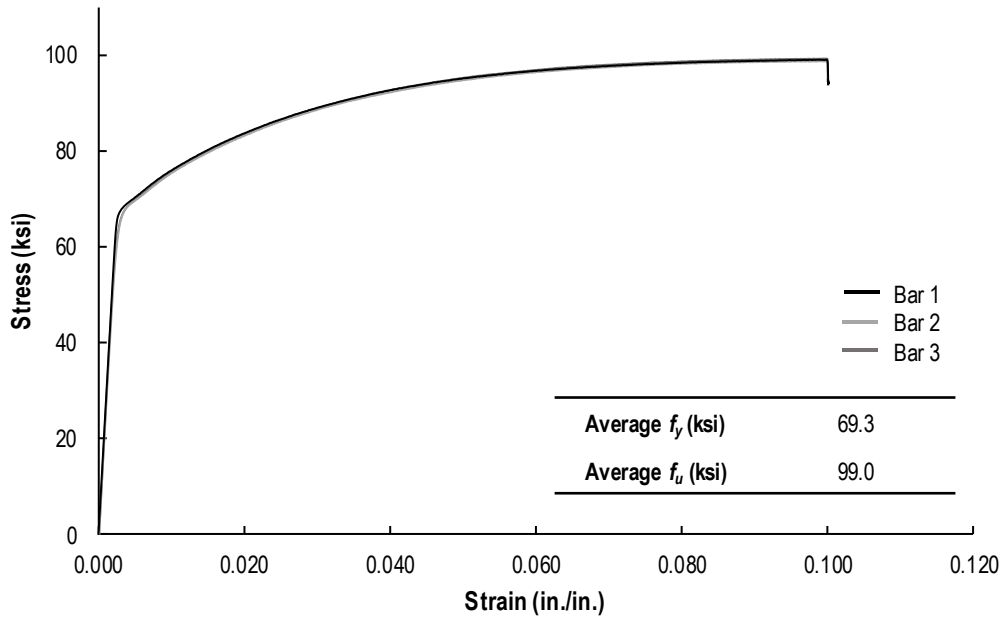


Figure A-7. Stress-strain plots for No. 4 bars used in C0 (secondary reinforcement)

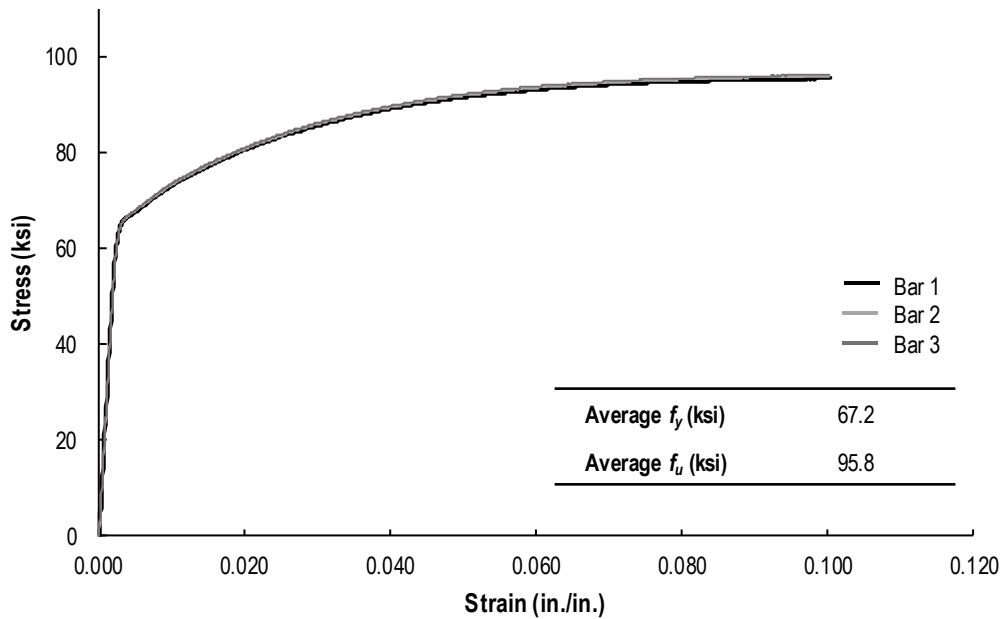


Figure A-8. Stress-strain plots for No. 4 bars used in C1, C2, & C3 (secondary reinforcement)

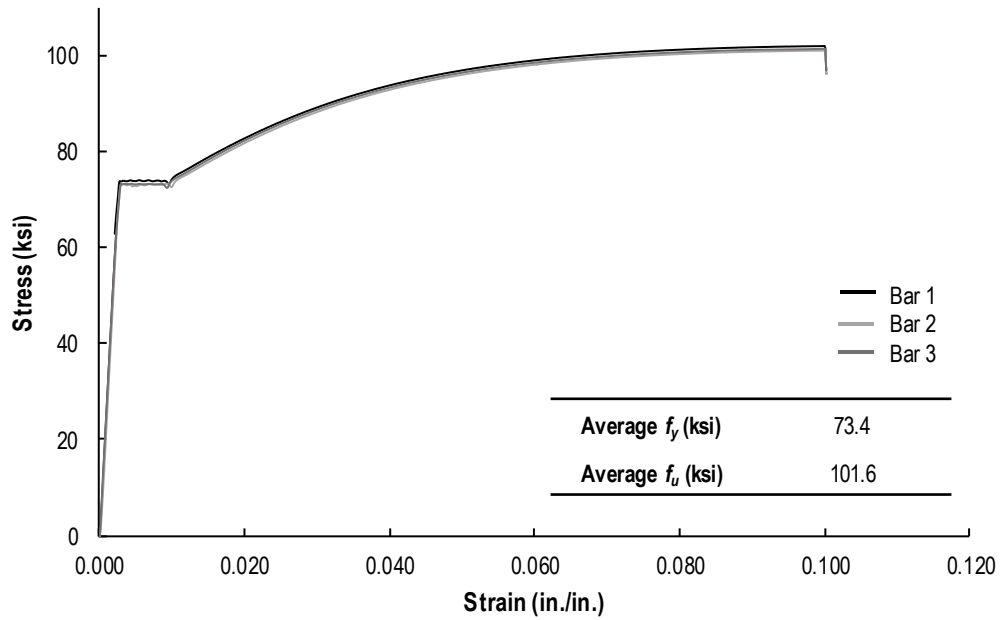


Figure A-9. Stress-strain plots for No. 8 bars used in C0 (primary reinforcement)

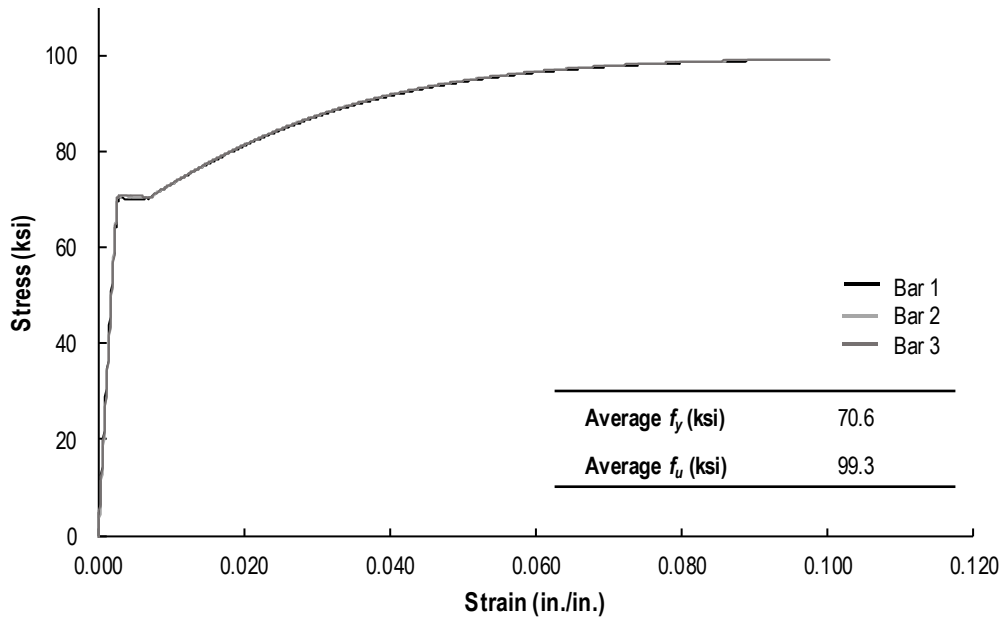


Figure A-10. Stress-strain plots for No. 8 bars used in C1, C2, & C3 (primary reinforcement)

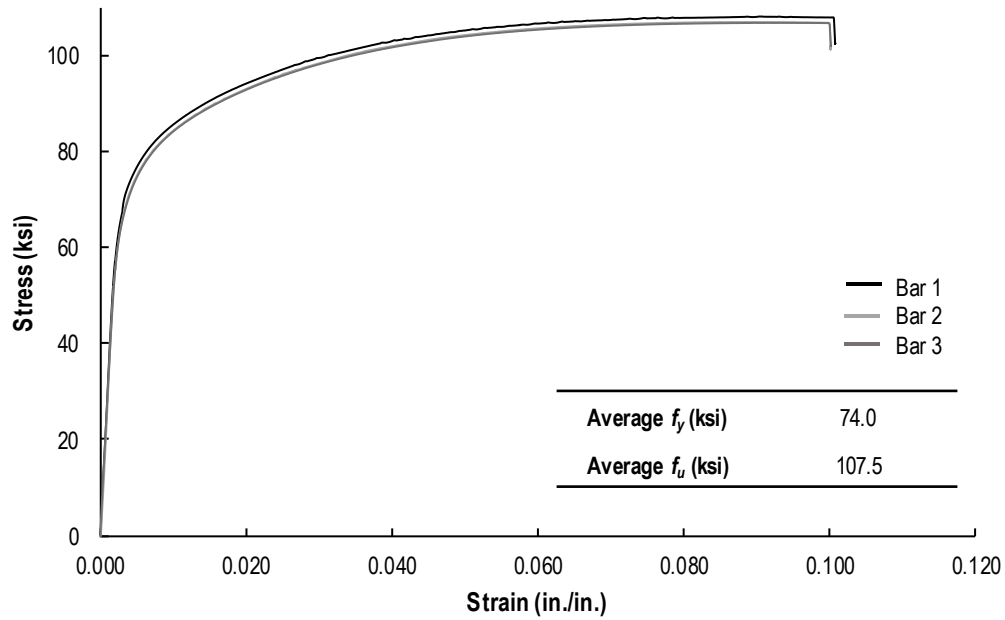


Figure A-11. Stress-strain plots for No. 9 bars used in C0 (column bars)

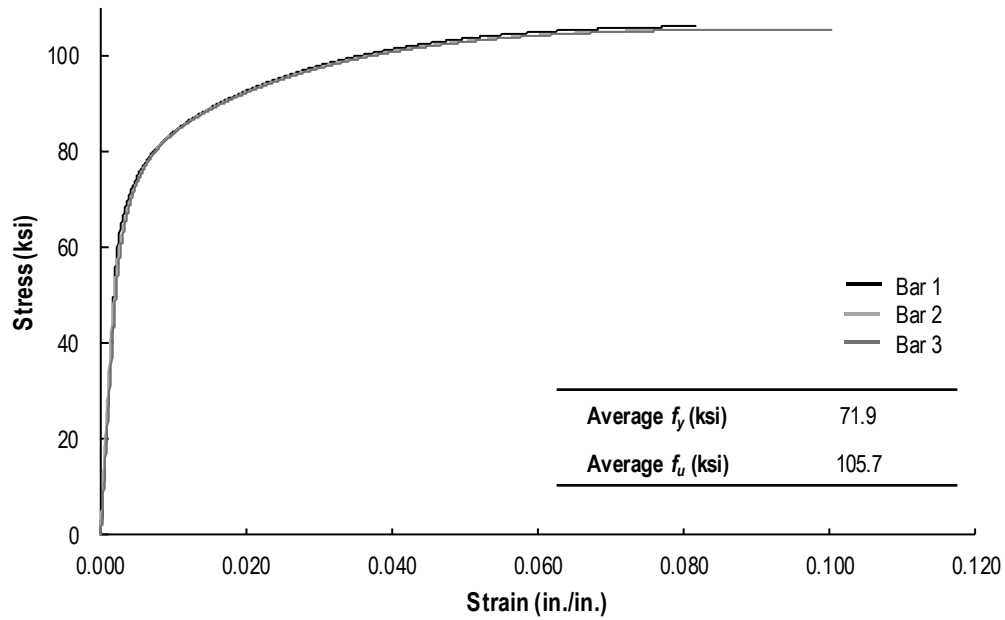


Figure A-12. Stress-strain plots for No. 9 bars used in C1, C2, & C3 (column bars)

APPENDIX B. CRACK PATTERNS

This appendix shows the cracking patterns on the south side of all specimens. Figure B-1 and Figure B-2 show cracking at service-level and peak loads for all specimens, respectively.

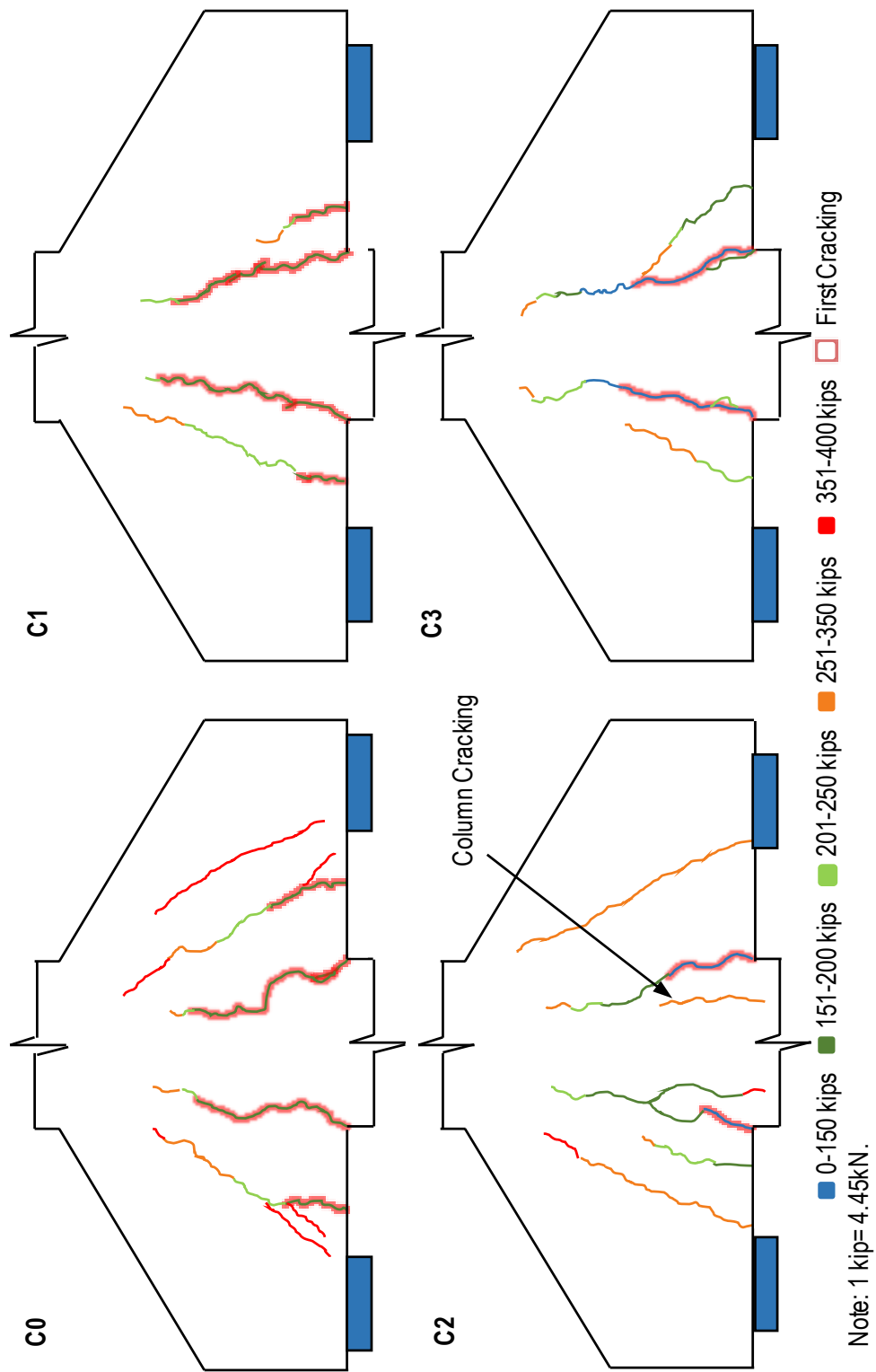


Figure B-1. Crack patterns at service-level loads

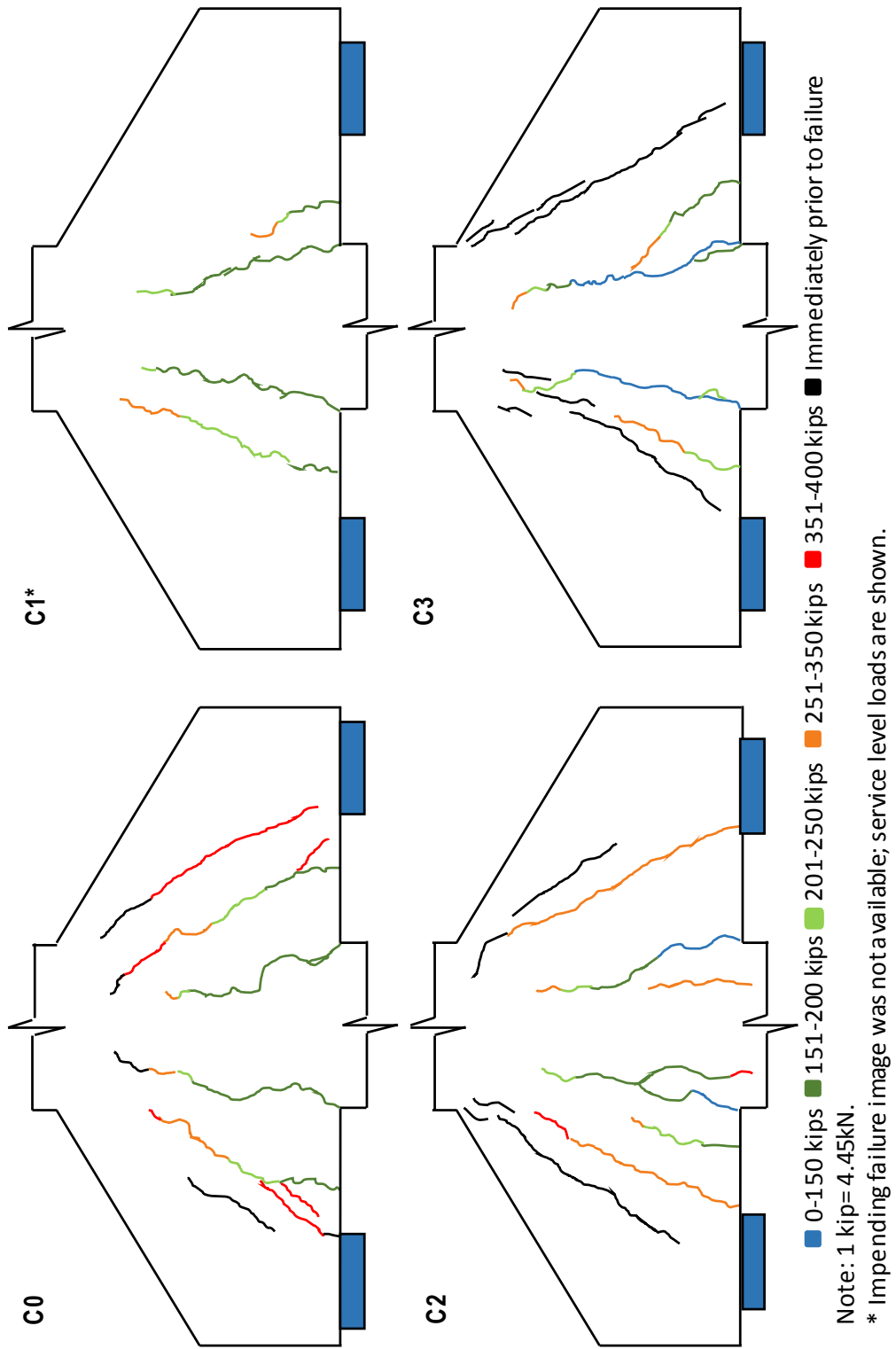


Figure B-2. Crack patterns at peak loads

APPENDIX C. LOAD VS. STRAIN PLOTS

This appendix provides experimental results that were not included in Chapter 3.

These results are presented in plots of load versus strain, as follows:

- *C0 total load vs. strains in primary reinforcement:* Figure C-1
- *C0 total load vs. strains in secondary reinforcement (T1 & T2):* Figure C-2
- *C0 total load vs. strains in secondary reinforcement (T3 & T4):* Figure C-3
- *C1 total load vs. strains in primary reinforcement:* Figure C-4
- *C1 total load vs. strains in secondary reinforcement (T1 & T2):* Figure C-5
- *C1 total load vs. strains in secondary reinforcement (T3):* Figure C-6
- *C2 total load vs. strains in primary reinforcement:* Figure C-7
- *C2 total load vs. strains in secondary reinforcement (T1 & T2):* Figure C-8
- *C2 total load vs. strains in secondary reinforcement (T3 & T4):* Figure C-9
- *C3 total load vs. strains in primary reinforcement:* Figure C-10

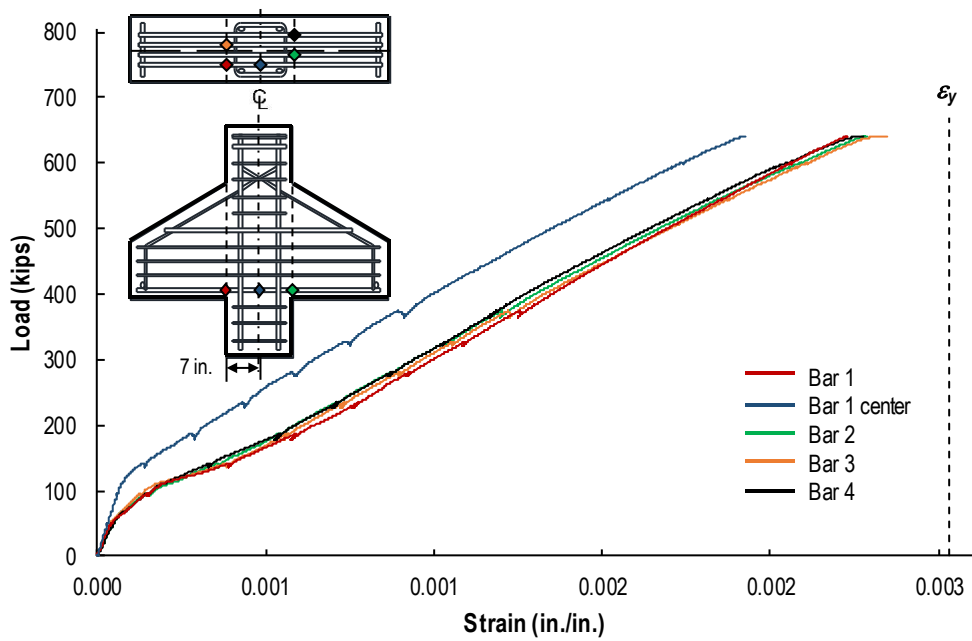


Figure C-1. C0 total load vs. strains in primary reinforcement

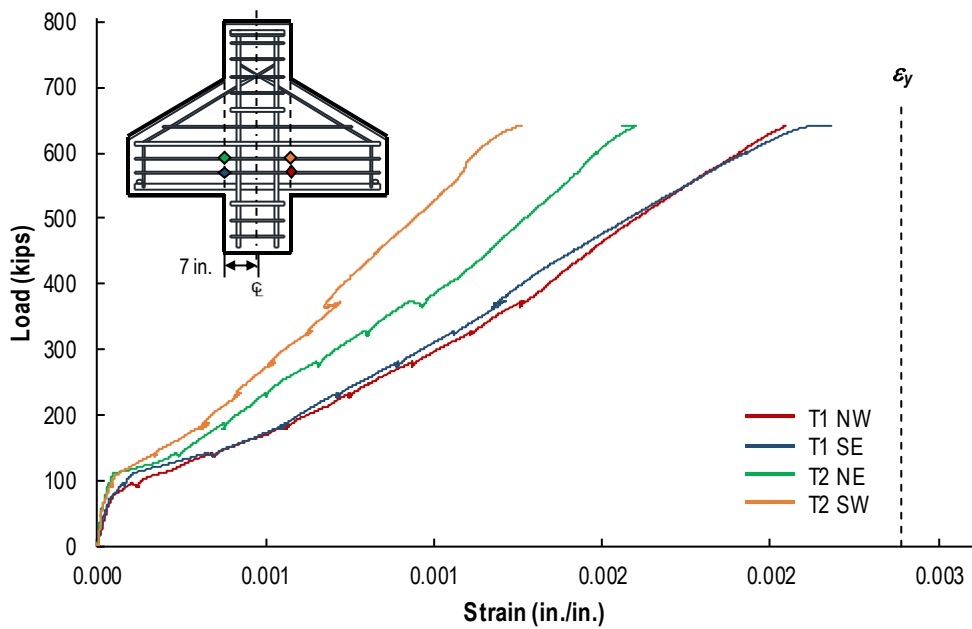


Figure C-2. C0 total load vs. strains in secondary reinforcement (T1 & T2)

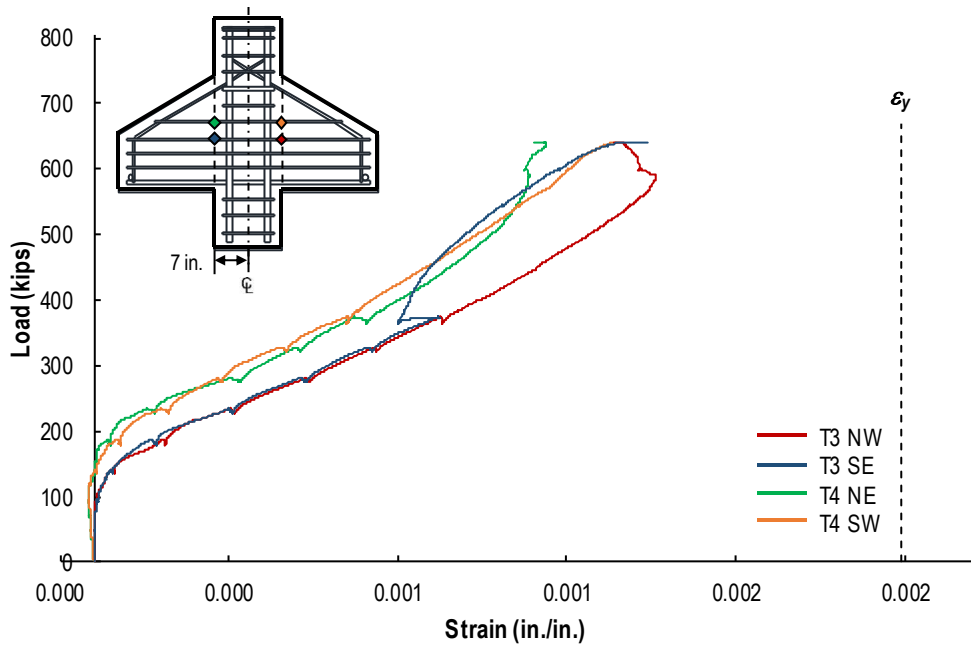


Figure C-3. C0 total load vs. strains in secondary reinforcement (T3 & T4)

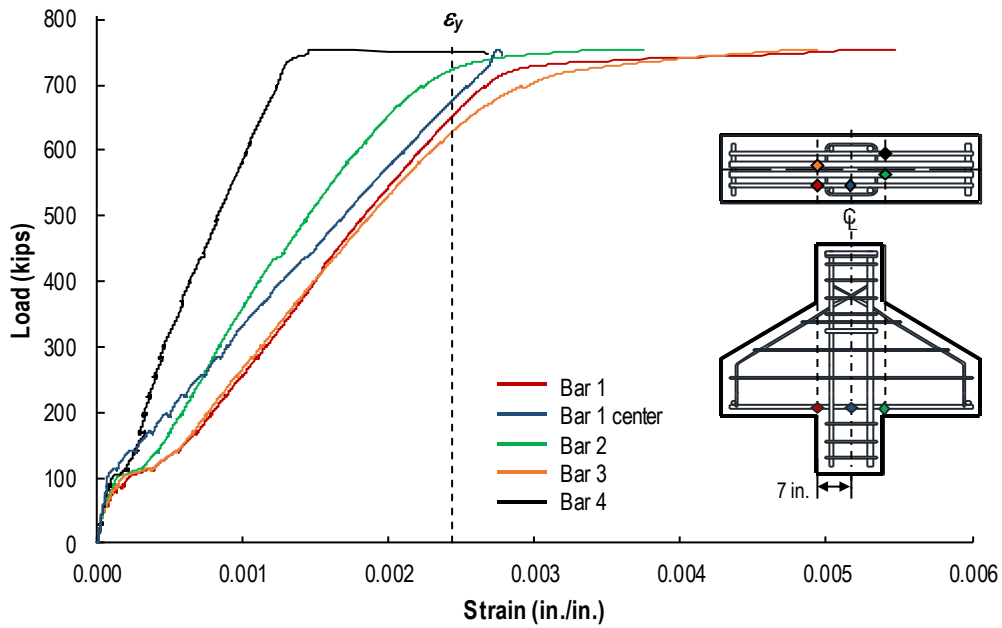


Figure C-4. C1 total load vs. strains in primary reinforcement

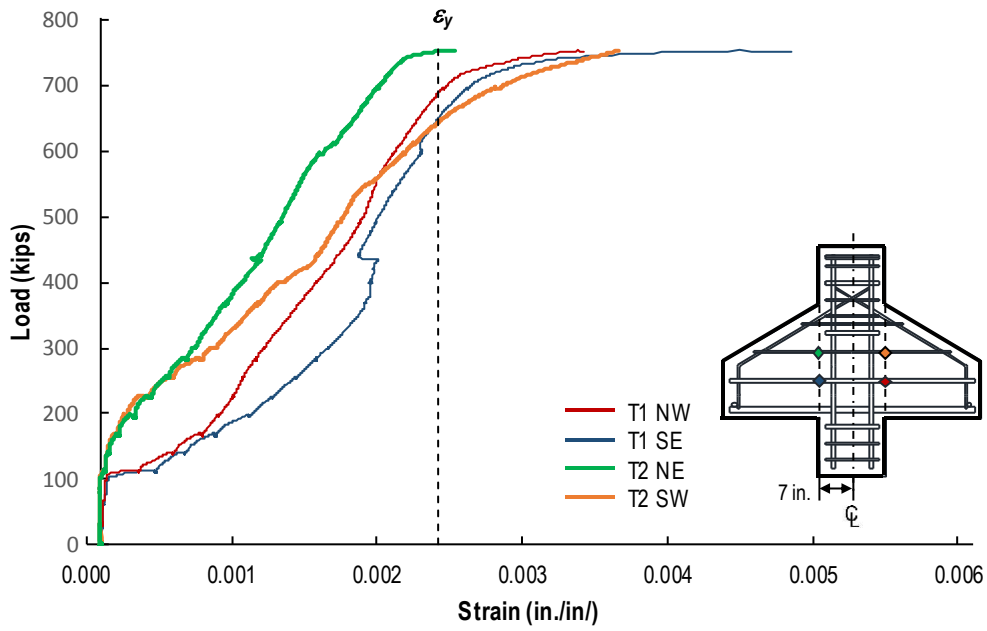


Figure C-5. C1 total load vs. strains in secondary reinforcement (T1 & T2)

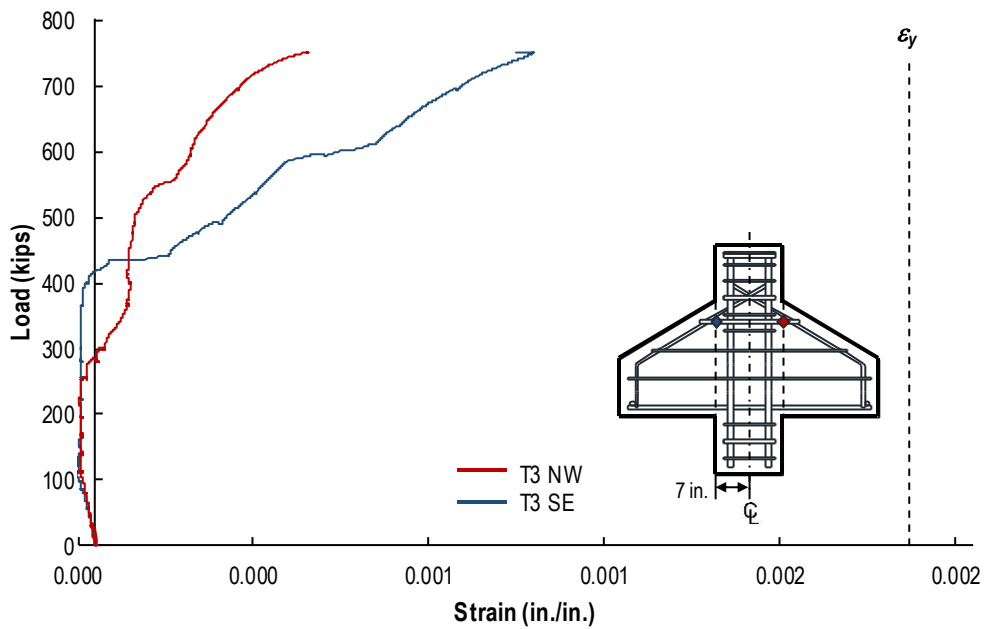


Figure C-6. C1 total load vs. strains in secondary reinforcement (T3)

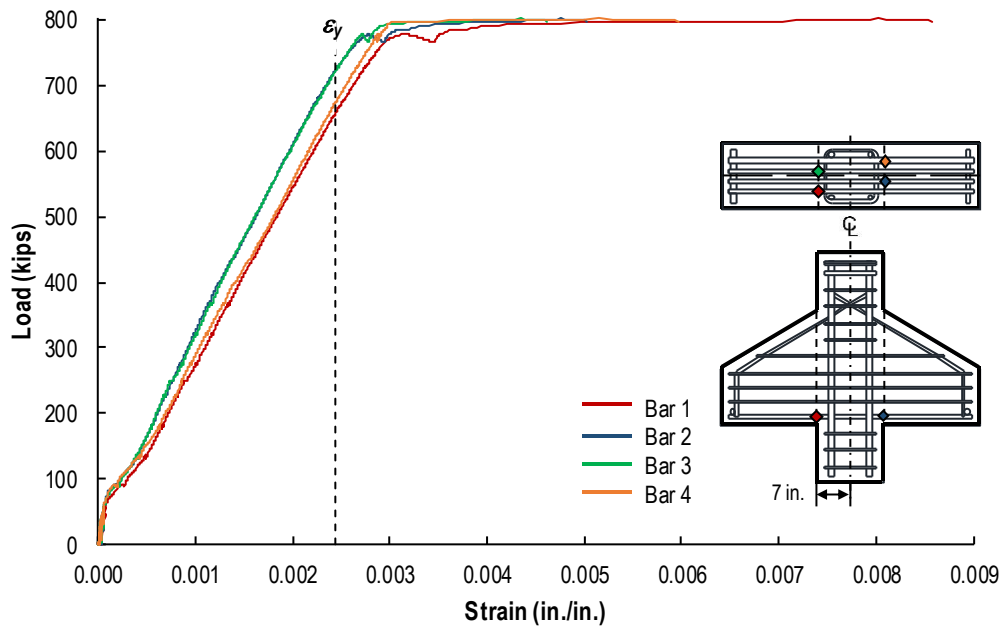


Figure C-7. C2 total load vs. strains in primary reinforcement

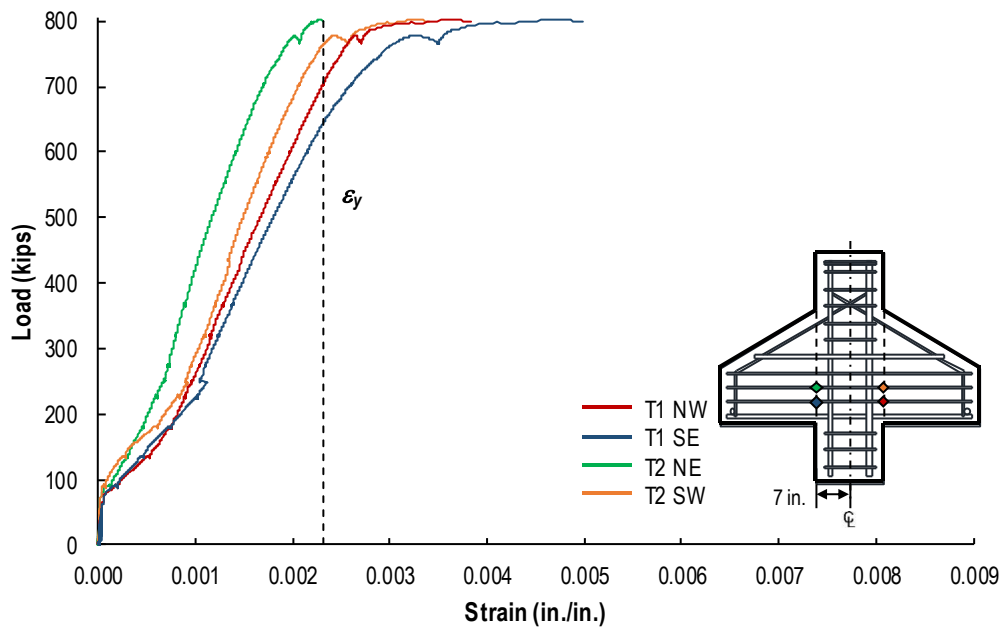


Figure C-8. C2 total load vs. strains in secondary reinforcement (T1 & T2)

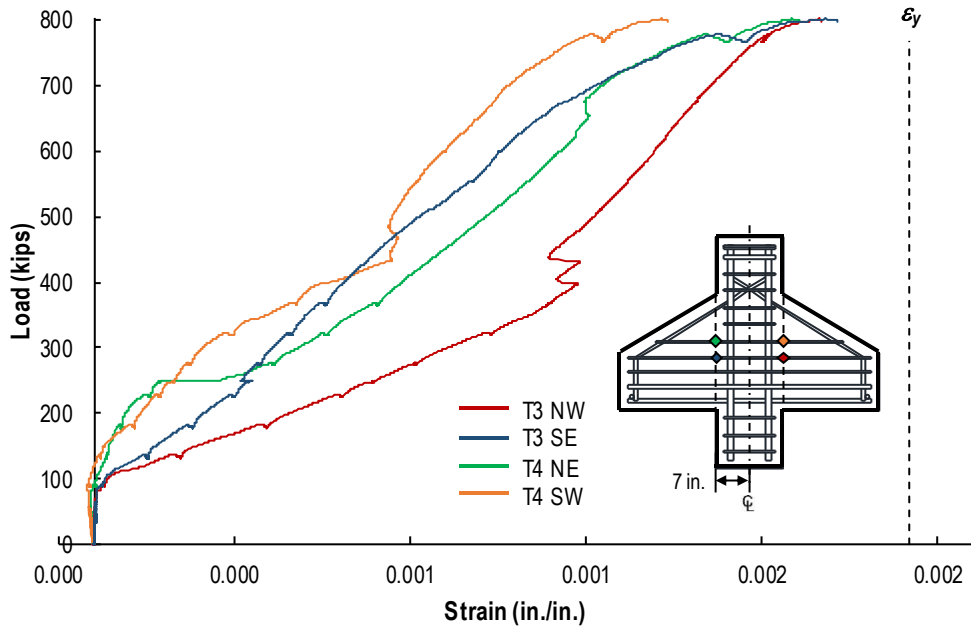


Figure C-9. C2 total load vs. strains in secondary reinforcement (T3 & T4)

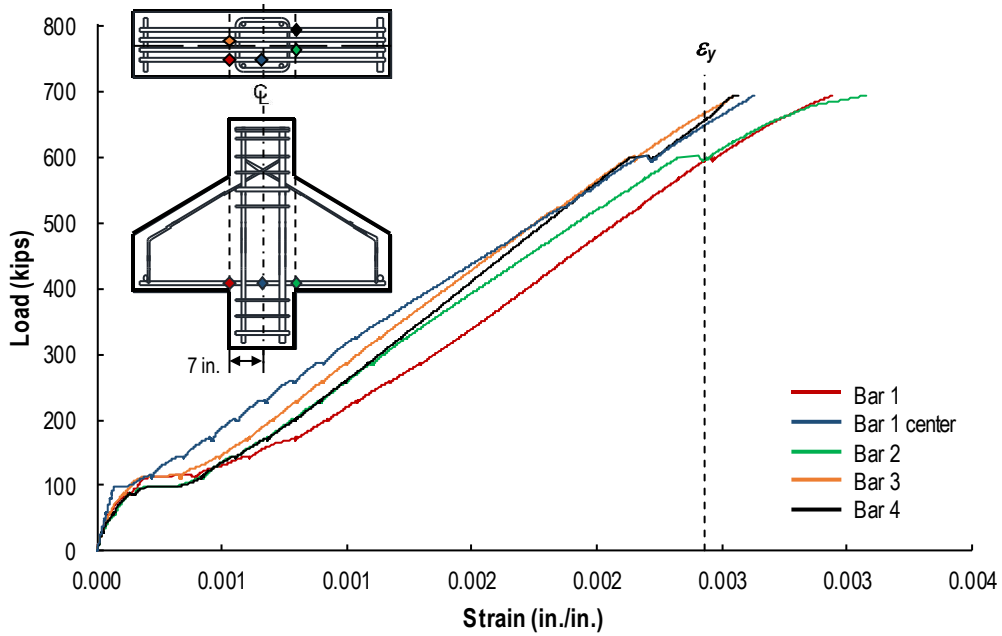


Figure C-10. C3 total load vs. strains in primary reinforcement

APPENDIX D. EXPERIMENTAL PROCEDURES

D.1. OVERVIEW

Appendix D presents more details of the experimental procedures and the calibration information for the instrumentation used during the test program. The following sections provide details of the experimental procedures for the specimens:

- Section D.2 depicts the experimental procedures with figures,
- Section D.3 explains the calibration factors for each instrument, and
- Section D.4 includes the notes reflecting the events during testing of each specimen.

D.2. EXPERIMENTAL PROCEDURE

D.2.1. Fabrication



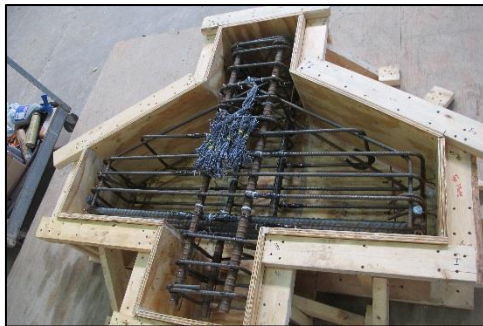
(a) Finished Forms



(b) Lowering the Cage



(c) Formwork for Specimen C0 (Side View)



(d) Reinforcing Cage in the Formwork (C0)

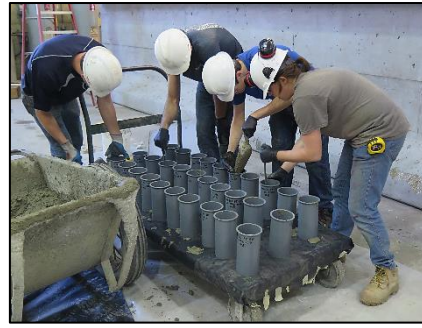


(e) Specimens C1, C2, and C3 in Forms

Figure D-1. Fabrication of formwork and reinforcing cages



(a) Slump Test



(b) Cylinder Preparation



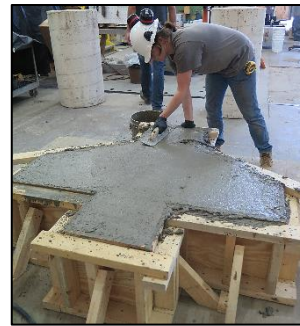
(c) Concrete Placement



(d) Internal Vibration



(e) Screeding



(f) Finishing the Surface



(g) Finished Specimen (C0)



(h) Covering the Surface for Curing

Figure D-2. Fabrication of specimens: typical casting procedures

D.2.2. Test Setup



Figure D-3. Specimen movement into setup



(a) North View



(b) East View



(c) South View



(d) West View

Figure D-4. Double-corbel test setup

D.2.3. Post-Test Photos



(a) North View



(b) East View



(c) South View

Figure D-5. Specimen C0 after the test



(a) North View



(b) East View



(c) South View

Figure D-6. Specimen C1 after the test



(a) North View



(b) East View



(c) South View

Figure D-7. Specimen C2 after the test



(a) North View



(b) South View

Figure D-8. Specimen C3 after the test

D.3. INSTRUMENTATION CALIBRATION

Calibration factors for linear potentiometers (LPs), load cells (LCs), and strain gages (SGs) are provided in the following table. LCs 070310 and 070312 were both used for all specimens. Due to a brittle failure that damaged the connection on LC 070311, this load cell was replaced with LC 070309 for testing Specimen C3.

Table D-1. Calibration factors

FSEL ID	Location	Type	Use	Calibration Factor
177	South	LP (1 in. Stroke)	Displacement Measurement	1.060
181	West			1.059
186	East			1.060
191	North			1.055
070309	East (C3)	LC (500 kip Capacity)	Load Measurement	2.270
070310	Southwest			2.279
070311	East (C0, C1, C2)			2.271
070312	Northwest			2.276
---	Primary and Secondary Reinforcement	SG	Strain Measurement	2.130

D.4. TEST RECORDS

The following tables document the observations during the structural testing of the specimens. In these tables, the shear force, i.e. the load that would be experienced by half of the specimen, are recorded. These forces represent half of the total load on the specimen.

Table D-2. Specimen C0 test record

Time	Target Shear Force	Actual Shear Force	Comments and Observations
11:50 AM	---	---	Test start
11:55 AM	---	---	Unloaded due to leakage of hydraulic fluid from the pump
12:06 PM	---	---	Second test start
12:07 PM	24 kips	24.39 kips	No cracks
12:12 PM	48 kips	48.15 kips	No cracks
12:16 PM	72 kips	72.15 kips	No cracks
12:20 PM	96 kips	96.19 kips	North face: four significant cracks; South face: four significant cracks
12:27 PM	120 kips	120.04 kips	Extensions on all existing cracks
12:33 PM	144 kips	144.22 kips	Six crack extensions
12:39 PM	168 kips	168.21 kips	Three crack extensions
12:44 PM	192 kips	192.21 kips	Eight crack extensions and two new cracks
---	261.5 kips	327.54 kips	Failure over tilt-saddle support

Table D-3. Specimen C1 test record

Time	Target Shear Force	Actual Shear Force	Comments and Observations
10:54 AM	15 kips	15.98 kips	No cracks
11:19 AM	---	---	Unloaded to inspect linear potentiometers; test restarted
11:20 AM	15 kips	15.52 kips	No cracks
11:25 AM	30 kips	30.19 kips	No cracks
11:29 AM	45 kips	45.16 kips	No cracks
11:35 AM	60 kips	60.90 kips	No cracks
11:38 AM	75 kips	75.01 kips	No cracks
11:42 AM	90 kips	90.45 kips	North face: three cracks; South face: four cracks
11:50 AM	105 kips	105.10 kips	North face: one crack, three crack extensions; South face: three crack extensions
11:58 AM	120 kips	120.19 kips	North face: one crack extension; South face: two crack extensions
12:03 PM	135 kips	136.01 kips	North face: two crack extensions; South face: two crack extensions
12:09 PM	150 kips	150.55 kips	North face: two crack extensions; South face: two crack extensions
---	---	155.00 kips	North face, east side: third major shear crack
---	---	158.50 kips	North face, west side: third major shear crack
12:40 PM	210.5 kips	377.00 kips	Failure over tilt-saddle support

Table D-4. Specimen C2 test record

Time	Target Shear Force	Actual Shear Force	Comments and Observations
10:29 AM	---	---	Test start
10:31 AM	24 kips	24.00 kips	No cracks
10:29 AM	---	---	Restart test due to leakage of hydraulic fluid from the pump
11:07 AM	---	---	Unloaded due to leakage of hydraulic fluid from the pump
11:18 AM	---	---	Restart the test
11:19 AM	24 kips	27.70 kips	No cracks
11:24 AM	48 kips	48.37 kips	North face: two cracks; South face: no cracks
11:30 AM	72 kips	72.15 kips	North face: two crack extensions; South face: two cracks
11:36 AM	96 kips	96.11 kips	North face: two cracks and two crack extensions; South face: one crack and two crack extensions
11:46 AM	120 kips	120.00 kips	North face: two crack extensions; South face: three crack extensions
11:53 AM	144 kips	144.60 kips	North face: one crack, one crack extensions; South face: two cracks, one crack extension
12:01 PM	168 kips	168.19 kips	North face: one crack, two crack extensions; South face: one crack, two crack extensions
12:09 PM	192 kips	192.09 kips	North face: one crack, one crack extension; South face: two crack extensions
12:18 PM	---	---	Start loading to failure
12:22 PM	---	---	Additional crack Northwest
12:24 PM	261.5 kips	261.5 kips	Surpasses calculated specimen capacity
12:26 PM	---	309.00 kips	Some bars have yielded
12:41 PM	261.5 kips	401.10 kips	Failure over tilt-saddle support

Table D-5. Specimen C3 test record

Time	Target Shear Force	Actual Shear Force	Comments and Observations
11:16 AM	---	---	Test start
11:18 AM	15 kips	15.20 kips	No cracks
11:23 AM	30 kips	30.08 kips	No cracks
11:27 AM	45 kips	45.08 kips	No cracks
11:31 AM	60 kips	60.13 kips	North face: two cracks; South face: two cracks
11:36 AM	75 kips	75.32 kips	North face: two crack extensions; South face: two crack extensions
11:42 AM	90 kips	90.10 kips	North face: one crack, one crack extension; South face one crack, one crack extension
11:49 AM	105 kips	105.17 kips	North face: one crack, three crack extensions; South face: one crack, four crack extensions
11:57 AM	120 kips	120.01 kips	North face: two crack extensions; South face: two crack extensions
12:09 PM	135 kips	135.10 kips	North face: three crack extensions; South face: one crack extension
12:15 PM	150 kips	150.11 kips	North face: four crack extensions
12:22 PM	---	---	Start loading to failure
12:32 PM	---	262.50 kips	North face (west): formation of third shear crack
---	---	299.00 kips	North face (east): formation of third shear crack
12:44 PM	209 kips	347.18 kips	Failure over tilt-saddle support

APPENDIX E. CAPACITY CALCULATIONS

E.1 OVERVIEW

Appendix E provides the calculations used to estimate the capacities of the corbels according to the empirical method in ACI 318-14, the STM provisions in ACI 318-14, and AASHTO LRFD Design Specifications STM provisions. The following sections provide the procedures and results for each of these calculations for each specimen:

- Section E.2 defines the notation that is used in this appendix.
- Section E.3 details the empirical method calculations.
- Section E.4 describes the STM method from ACI 318-14.
- Section E.5 shows calculations for the conservative STM AASHTO method.
- Section E.6 examines the unconservative STM AASHTO method.

E.2 NOTATION

This section introduces the variables used in the calculations. Note that the variable names might vary from method to method to match the notation used in each code. For all methods, the V_n values correspond to the shear-force capacity of one side of the specimens and therefore represent half of the nominal load-carrying capacity of the double-corbel specimen.

$A_{\text{back}, i}$ = Area of the back face of Node i (where i is stated), in.²

$A_{\text{bearing}, i}$ = Area of the bearing face of Node i (where i is stated), in.²

$A_{\text{inclined}, i}$ = Area of the inclined face of Node i (where i is stated), in.²

A_{pb} = Cross-sectional area of a primary reinforcement bar, in.²

A_s = Total area of the primary reinforcement, in.²

A_{sb} = Cross-sectional area of a secondary reinforcing bar, in.² (ACI 318-14, Empirical)

A_{sh} = Cross-sectional area of a secondary reinforcement bar, in.² (ACI 318-14, STM)

A_{si} = Cross-sectional area of the inclined strut, in.²

A_{type} = Type of Node A

a_v = Shear span, in.

A_v = Cross-sectional area of a secondary reinforcement bar, in.² (AASHTO LRFD, STM)

A_{vfs} = Cross-sectional area of a shear-friction reinforcement bar, in.² (ACI 318-14, Empirical method)

B = Vertical distance of Node B from the corbel-column corner, in.

B_{type} = Type of Node B

b_w = Width of the specimen, in.

c = Depth of the neutral axis at the shear plane, in.

C = Compression force, kips

CC = Crack-control reinforcement ratio

d = Depth of primary reinforcement, in.

$F_{back, i}$ = Calculated capacity of the back face of Node i (where i is stated), kips

$F_{bearing, i}$ = Calculated capacity of the bearing face of Node i (where i is stated), kips

$F_{\text{inclined}, i}$ = Calculated capacity of the inclined face of Node i (where i is stated),
kips

f'_c = Concrete compressive strength, psi

f_{ce} = Effective concrete compressive strength in a strut or nodal zone, ksi

F_s = Calculated capacity of the inclined strut, kips

f_{yp} = steel yield strength of the primary reinforcing bars, ksi

f_{ys} = steel yield strength of the secondary reinforcing bars, ksi

$L_{\text{back}, i}$ = Length of the back face of Node i (where i is state), in.

$L_{\text{bearing}, i}$ = Length of the bearing face of Node i (where i is state), in.

$L_{\text{inclined}, i}$ = Length of the inclined face of Node i (where i is state), in.

M_n = Calculated moment capacity of the specimen, kip-ft (ACI 318-14, Empirical)

N_{pb} = Number of primary reinforcing bars

N_{sb} = Number of secondary reinforcing bars

s_{sh} = Spacing of the secondary reinforcement bars, in. (ACI 318-14, STM)

s_v = Spacing of the secondary reinforcement bars, in. (AASHTO LRFD, STM)

T = Tensile force at the shear plane, kips

V_n = Calculated shear-force capacity of the specimen, kips (ACI 318-14, Empirical)

$V_{n, a}$ = Calculated shear-force capacity of the specimen from Equation 16.5.2.4 a,
kips. (ACI 318-14, Empirical)

$V_{n, AA'}$ = Calculated shear-force capacity of the specimen based on the tensile
capacity of Tie AA', kips

$V_{n, b}$ = Calculated shear-force capacity of the specimen from Equation 16.5.2.4 b, kips (ACI 318-14, Empirical)

$V_{n, \text{back}, i}$ = Calculated shear-force capacity of the specimen based on the back face of Node i (where i is stated), kips

$V_{n, \text{bearing}, i}$ = Calculated shear-force capacity of the specimen based on the bearing face of Node i (where i is stated), kips

$V_{n, c}$ = Calculated shear-force capacity of the specimen from Equation 16.5.2.4 c, kips (ACI 318-14, Empirical)

$V_{n, \text{inclined}, i}$ = Calculated shear-force capacity of the specimen based on the inclined face of Node i (where i is stated), kips

$V_{n, m}$ = Calculated capacity of the specimen through moment capacity, kips (ACI 318-14, Empirical)

$V_{n, Ni}$ = Calculated shear-force capacity of the specimen based on all faces of Node i, kips (ACI 318-14, STM)

$V_{n, s}$ = Calculated shear-force capacity of the specimen based on shear friction, kips (ACI 318-14, Empirical)

$V_{n, st}$ = Calculated shear-force capacity of the specimen based on the inclined strut, kips (ACI 318-14, STM)

V_u = Measured shear-force capacity of the specimen, kips

β_n = Nodal zone coefficient (ACI 318-14, STM)

β_s = Strut coefficient (ACI 318-14, STM)

β_l = Efficiency factor of the concrete for the rectangular stress block

ε_s = Strain in the primary steel reinforcement at the face of the column, (in./in.)

θ = Angle between the inclined strut and the tie, degrees

μ = Coefficient of friction used for shear-friction calculations

υ = Concrete efficiency factor (AASHTO STM)

E.3 CAPACITY CALCULATIONS: ACI 318-14 EMPIRICAL METHOD

Specimen C0

Table E-1. Specimen C0 properties used in the empirical method

Specimen Properties		Equation (where applicable)
f'_c	5250 psi	
f_{yp}	73.37 ksi	
f_{ys}	69.28 ksi	
A_s	3.16 in. ²	$A_{pb} * (N_{pb})$
A_{vfs}	1.6 in. ²	$A_{sb} * (N_{sb})$
b_w	14 in.	
d	22 in.	
a_v	14.5 in.	
μ	1.4	
Test Results		
V_u	320.5 kips	
V_u/V_n	1.16	-OK

Table E-2. Specimen C0 empirical method calculations

Dimensional Limits Check		Equation	Reference*
$V_{n,a}$	323.40 kips	$0.2f'_c b_w d$	Eqn. 16.2.5.4 [a]
$V_{n,b}$	277.20 kips	$(480+0.08f'_c) b_w d$	Eqn. 16.2.5.4 [b]
$V_{n,c}$	492.80 kips	$1600b_w d$	Eqn. 16.2.5.4 [c]
Shear Friction Check			
$V_{n,s}$	479.78 kips	$\mu A_{vfs} f_{ys} + \mu A_s f_{yp}$	Eqn. 22.9.4.2
Moment Capacity Check			
β_1	0.79	$0.85 - ((0.05(f'_c - 4000))/1000)$	Table 22.2.2.4.3
c	4.71 in.	$(1000A_s f_{yp}) / (0.85f'_c \beta_1 b_w)$	Section 22.2.2.4.1
a	3.71 in.	$\beta_1 c$	Section 22.2.2.4.1
C	231.85 kips	$0.85f'_c a b_w$	
T	231.85 kips	$A_s f_{ys}$	
M_n	389.21 kip-ft	$C(c - (a/2)) + T(d - c)$	
$V_{n,m}$	322.10 kip	$12M_n / a_v$	
V_n	277.20 kip	$\min(V_{n,a}, V_{n,b}, V_{n,c}, V_{n,s}, V_{n,m})$	

* Equation, section, and table numbers refer to those in ACI 318-14.

Specimen C1

Table E-3. Specimen C1 properties used in the empirical method

Specimen Properties		Equation (where applicable)
f'_c	6490 psi	
f_{yp}	70.58 ksi	
f_{ys}	67.18 ksi	
A_s	3.16 in. ²	$A_{pb} * (N_{pb})$
A_{vfs}	1.2 in. ²	$A_{sb} * (N_{sb})$
b_w	14 in.	
d	22 in.	
a_v	13 in.	
μ	1.4	
Test Results		
V_u	376.94 kips	
V_u/V_n	1.22	-OK

Table E-4. Specimen C1 empirical method calculations

Dimensional Limits Check		Equation	Reference*
$V_{n,a}$	399.78 kips	$0.2f'_c b_w d$	Eqn. 16.2.5.4 [a]
$V_{n,b}$	307.75 kips	$(480+0.08f'_c) b_w d$	Eqn. 16.2.5.4 [b]
$V_{n,c}$	492.80 kips	$1600b_w d$	Eqn. 16.2.5.4 [c]
Shear Friction Check			
$V_{n,s}$	425.11 kips	$\mu A_{vfs} f_{ys} + \mu A_s f_{yp}$	Eqn. 22.9.4.2
Moment Capacity Check			
β_1	0.73	$0.85 - ((0.05(f'_c - 4000))/1000)$	Table 22.2.2.4.3
c	3.98 in.	$(1000A_s f_{yp}) / (0.85f'_c \beta_1 b_w)$	Section 22.2.2.4.1
a	2.89 in.	$\beta_1 c$	Section 22.2.2.4.1
C	223.03 kips	$0.85f'_c a b_w$	
T	223.03 kips	$A_s f_{ys}$	
M_n	382.05 kip-ft	$C(c - (a/2)) + T(d - c)$	
$V_{n,m}$	352.66 kip	$12M_n / a_v$	
V_n	307.75 kip	$\min(V_{n,a}, V_{n,b}, V_{n,c}, V_{n,s}, V_{n,m})$	

* Equation, section, and table numbers refer to those in ACI 318-14.

Specimen C2

Table E-5. Specimen C2 properties used in the empirical method

Specimen Properties		Equation (where applicable)
f'_c	6830 psi	
f_{yp}	70.58 ksi	
f_{ys}	67.18 ksi	
A_s	3.16 in. ²	$A_{pb} * (N_{pb})$
A_{vfs}	1.6 in. ²	$A_{sb} * (N_{sb})$
b_w	14 in.	
d	22 in.	
a_v	13 in.	
μ	1.4	
Test Results		
V_u	401.11 kips	
V_u/V_n	1.27	-OK

Table E-6. Specimen C2 empirical method calculations

Dimensional Limits Check		Equation	Reference*
$V_{n,a}$	420.73 kips	$0.2f'_c b_w d$	Eqn. 16.2.5.4 [a]
$V_{n,b}$	316.13 kips	$(480+0.08f'_c) b_w d$	Eqn. 16.2.5.4 [b]
$V_{n,c}$	492.80 kips	$1600b_w d$	Eqn. 16.2.5.4 [c]
Shear Friction Check			
$V_{n,s}$	462.73 kips	$\mu A_{vfs} f_{ys} + \mu A_s f_{yp}$	Eqn. 22.9.4.2
Moment Capacity Check			
β_1	0.71	$0.85 - ((0.05(f'_c - 4000))/1000)$	Table 22.2.2.4.3
c	3.87 in.	$(1000A_s f_{yp}) / (0.85f'_c \beta_1 b_w)$	Section 22.2.2.4.1
a	2.74 in.	$\beta_1 c$	Section 22.2.2.4.1
C	223.03 kips	$0.85f'_c a b_w$	
T	223.03 kips	$A_s f_{ys}$	
M_n	383.39 kip-ft	$C(c - (a/2)) + T(d - c)$	
$V_{n,m}$	353.90 kip	$12M_n / a_v$	
V_n	316.13 kip	$\min(V_{n,a}, V_{n,b}, V_{n,c}, V_{n,s}, V_{n,m})$	

* Equation, section, and table numbers refer to those in ACI 318-14.

Specimen C3

Table E-7. Specimen C3 properties used in the empirical method

Specimen Properties		Equation (where applicable)
f'_c	5590 psi	
f_{yp}	70.58 ksi	
f_{ys}	67.18 ksi	
A_s	3.16 in. ²	$A_{pb} * (N_{pb})$
A_{vfs}	0 in. ²	$A_{sb} * (N_{sb})$
b_w	14 in.	
d	22 in.	
a_v	13 in.	
μ	1.4	
Test Results		
V_u	347.18 kips	
V_u/V_n	1.22	-OK

Table E-8. Specimen C3 empirical method calculations

Dimensional Limits Check		Equation	Reference*
$V_{n,a}$	344.34 kips	$0.2f'_c b_w d$	Eqn. 16.2.5.4 [a]
$V_{n,b}$	285.58 kips	$(480+0.08f'_c) b_w d$	Eqn. 16.2.5.4 [b]
$V_{n,c}$	492.80 kips	$1600b_w d$	Eqn. 16.2.5.4 [c]
Shear Friction Check			
$V_{n,s}$	312.24 kips	$\mu A_{vfs} f_{ys} + \mu A_s f_{yp}$	Eqn. 22.9.4.2
Moment Capacity Check			
β_1	0.77	$0.85 - ((0.05(f'_c - 4000))/1000)$	Table 22.2.2.4.3
c	4.35 in.	$(1000A_s f_{yp}) / (0.85f'_c \beta_1 b_w)$	Section 22.2.2.4.1
a	3.35 in.	$\beta_1 c$	Section 22.2.2.4.1
C	223.03 kips	$0.85f'_c a b_w$	
T	223.03 kips	$A_s f_{ys}$	
M_n	377.73 kip-ft	$C(c - (a/2)) + T(d - c)$	
$V_{n,m}$	348.68 kip	$12M_n / a_v$	
V_n	285.58 kip	$\min(V_{n,a}, V_{n,b}, V_{n,c}, V_{n,s}, V_{n,m})$	

* Equation, section, and table numbers refer to those in ACI 318-14.

E.4 SPECIMEN CALCULATIONS: ACI 318-14 STM

Specimen C0

Table E-9. Specimen C0 properties used in the ACI STM

Specimen Properties		Equation (where applicable)	Explanation (where applicable)*	Meet Requirements? (OK/NG)
f'_c	5250 psi			
f_{yp}	73.37 ksi			
A_s	3.16 in. ²	$A_{pb}^*(N_{pb})$		
b_w	14 in.			
d	22 in.			
a_v	14.5 in.			
A_{sh}	0.4 in. ²			
s_{sh}	3.5 in.			
Formula Calculations for Checks				
β_1	0.79	$0.85 - ((0.05(f'_c - 4000)) / 1000)$	Used to find the strut inclination based on concrete behavior at column face.	
T	231.85 kips	$A_s f_{yp}$		
c	4.71 in.	$(1000T) / (0.85 f'_c \beta_1 b_w)$		
ϵ_s	0.011 in./in.	$0.003(d-c)/c$	Check whether steel has yielded.	-OK
B	1.86 in.	$\beta_1 c / 2$	Node B Location, figure in 3 pages	
θ	48.22 °	$\tan^{-1}(d-B) / (3.5a_v)$	θ , figure in 3 pages	
CC	0.006	$(A_v / b_w s_v) (\sin \theta)$	Eqn. 23.5.3	-OK
a_v/d	0.659		Section 23.2.9	-OK
	0.882	$0.04(f'_c / f_y)(b_w d)$	Eqn. 23.2.9	-OK
Test Results				
V_u	320.5 kips			
V_u/V_n	1.43			-OK

* Equation and section numbers refer to those in ACI 318-14.

Table E-10. Specimen C0 ACI STM (part 1 of 3)

Inclined Node Geometry		Equation (where applicable)	Explanation (where applicable)*
A_{type}	CCT		Node A, figure in 2 pages
$L_{back, A}$	4.00 in.		
$L_{bearing, A}$	8.00 in.		
$L_{inclined, A}$	8.63 in.	$L_{back, A} \cos\theta + L_{bearing, A} \sin\theta$	Figure 23.2.6b.
$A_{back, A}$	56.00 in. ²	$L_{back, A} b_w$	
$A_{bearing, A}$	112.00 in. ²	$L_{bearing, A} b_w$	
$A_{inclined, A}$	120.83 in. ²	$L_{inclined, A} b_w$	
Node A Check			
Back Face			
β_n	0.80		Table 23.9.2
f_{ce}	3.57 ksi	$0.85 \beta_n (f'_c)$	Eqn. 23.9.2
$F_{back, A}$	199.92 kips	$f_{ce} A_{back, A}$	Eqn. 23.9.1
$V_{n, back, A}$	223.74 kips	$F_{back, A} \tan\theta$	
Bearing Face			
$F_{bearing, A}$	399.84 kips	$f_{ce} A_{bearing, A}$	Eqn. 23.9.1
$V_{n, bearing, A}$	399.84 kips	$F_{bearing, A}$	
Inclined Face			
$F_{inclined, A}$	431.36 kips	$f_{ce} A_{inclined, A}$	Eqn. 23.9.1
$V_{n, inclined, A}$	321.66 kips	$F_{inclined, A} \sin\theta$	
$V_{n, NA}$	223.74 kip	$\min(V_{n, back, A}, V_{n, bearing, A}, V_{n, inclined, A})$	

* Equation, section, and table numbers refer to those in ACI 318-14.

Table E-11. Specimen C0 ACI STM (part 2 of 3)

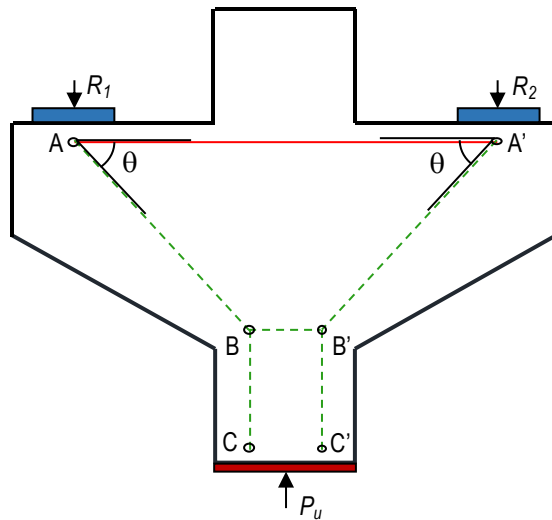
Inclined Node Geometry		Equation (where applicable)	Explanation (where applicable)*
B_{type}	CCC		Node B, figure on next page
$L_{back, B}$	3.71 in.	$\beta_1 c$	Section 23.2.2
$L_{bearing, B}$	7.00 in.		Section 23.2.2
$L_{inclined, B}$	7.69 in.	$L_{back, B} \cos\theta + L_{bearing, B} \sin\theta$	Figure 23.2.6b.
$A_{back, B}$	51.96 in. ²	$L_{back, B} b_w$	
$A_{bearing, B}$	98.00 in. ²	$L_{bearing, B} b_w$	
$A_{inclined, B}$	107.69 in. ²	$L_{inclined, B} b_w$	
Node B Check			
Back Face			
β_n	1.00		Table 23.9.2
f_{ce}	4.46 ksi	$0.85 \beta_n (f'_c)$	Eqn. 23.9.2
$F_{back, B}$	231.85 kips	$f_{ce} A_{back, B}$	Eqn. 23.9.1
$V_{n, back, B}$	259.47 kips	$F_{back, B} \tan\theta$	
Bearing Face			
$F_{bearing, B}$	437.33 in.	$f_{ce} A_{bearing, B}$	Eqn. 23.9.1
$V_{n, bearing, B}$	437.33 kips	$F_{bearing, B}$	
Inclined Face			
$F_{inclined, B}$	480.59 kips	$f_{ce} A_{inclined, B}$	Eqn. 23.9.1
$V_{n, inclined, B}$	358.37 kips	$F_{inclined, B} \sin\theta$	
$V_{n, NB}$	259.47 kip	$\min(V_{n, back, B}, V_{n, bearing, B}, V_{n, inclined, B})$	

* Equation, section, figure, and table numbers refer to those in ACI 318-14.

Table E-12. Specimen C0 ACI STM (part 3 of 3)

Tie Strength		Equation	Reference *
$V_{n, AA'}$	259.47 kips	$T(\tan\theta)$	Eqn. 23.7.2
Strut Strength			
Inclined Face			
A_{si}	107.69 in. ²	$\min(A_{bearing, A}, A_{bearing, B})$	Section 23.4.1
β_s	0.75		Table 23.4.3
f_{ce}	3.35 ksi	$0.85\beta_s f'_c$	Eqn. 23.4.3
F_s	360.44 kips	$f_{ce} A_{si}$	Eqn. 23.4.1
$V_{n, st}$	268.77 kips	$F_s \sin\theta$	
V_n	223.74 kips	$\min(V_{n, AA'}, V_{n, NA}, V_{n, NB}, V_{n, s})$	

* Equation, section and table numbers refer to those in ACI 318-14.



Specimen C1

Table E-13. Specimen C1 properties used in the ACI STM

Specimen Properties		Equation (where applicable)	Explanation (where applicable)*	Meet Requirements? (OK/NG)
f'_c	6490 psi			
f_{yp}	70.58 ksi			
A_s	3.16 in. ²	$A_{pb}^*(N_{pb})$		
b_w	14 in.			
d	22 in.			
a_v	13 in.			
A_{sh}	0.4 in. ²			
s_{sh}	6 in.			
Formula Calculations for Checks				
β_1	0.73	$0.85 - ((0.05(f'_c - 4000))/1000)$	Used to find the strut inclination based on concrete behavior at column face.	
T	223.03 kips	$A_s f_{yp}$		
c	3.98 in.	$(1000T)/(0.85f'_c \beta_1 b_w)$		
ϵ_s	0.014 in./in.	$0.003(d - c)/c$	Check whether steel has yielded.	-OK
B	1.44 in.	$\beta_1 c/2$	Node B Location, figure in 3 pages	
θ	51.25 °	$\tan^{-1}(d - B)/(3.5a_v)$	θ , figure in 3 pages	
CC	0.004	$(A_v/b_w s_v)(\sin\theta)$	Eqn. 23.5.3	-OK
a_v/d	0.591		Section 23.2.9	-OK
	1.133	$0.04(f'_c/f_y)(b_w d)$	Eqn. 23.2.9	-OK
Test Results				
V_u	376.9 kips			
V_u/V_n	1.36			-OK

* Equation and section numbers refer to those in ACI 318-14.

Table E-14. Specimen C1 ACI STM (part 1 of 3)

Inclined Node Geometry		Equation (where applicable)	Explanation (where applicable)*
A_{type}	CCT		Node A, figure in 2 pages
$L_{back, A}$	4.00 in.		
$L_{bearing, A}$	8.00 in.		
$L_{inclined, A}$	8.74 in.	$L_{back, A} \cos\theta + L_{bearing, A} \sin\theta$	Figure 23.2.6b.
$A_{back, A}$	56.00 in. ²	$L_{back, A} b_w$	
$A_{bearing, A}$	112.00 in. ²	$L_{bearing, A} b_w$	
$A_{inclined, A}$	122.40 in. ²	$L_{inclined, A} b_w$	
Node A Check			
Back Face			
β_n	0.80		Table 23.9.2
f_{ce}	4.4132 ksi	$0.85 \beta_n (f'_c)$	Eqn. 23.9.2
$F_{back, A}$	247.14 kips	$f_{ce} A_{back, A}$	Eqn. 23.9.1
$V_{n, back, A}$	307.89 kips	$F_{back, A} \tan\theta$	
Bearing Face			
$F_{bearing, A}$	494.28 kips	$f_{ce} A_{bearing, A}$	Eqn. 23.9.1
$V_{n, bearing, A}$	494.28 kips	$F_{bearing, A}$	
Inclined Face			
$F_{inclined, A}$	540.16 kips	$f_{ce} A_{inclined, A}$	Eqn. 23.9.1
$V_{n, inclined, A}$	421.24 kips	$F_{inclined, A} \sin\theta$	
$V_{n, NA}$	307.89 kip	$\min(V_{n, back, A}, V_{n, bearing, A}, V_{n, inclined, A})$	

* Equation, section, and table numbers refer to those in ACI 318-14.

Table E-15. Specimen C1 ACI STM (part 2 of 3)

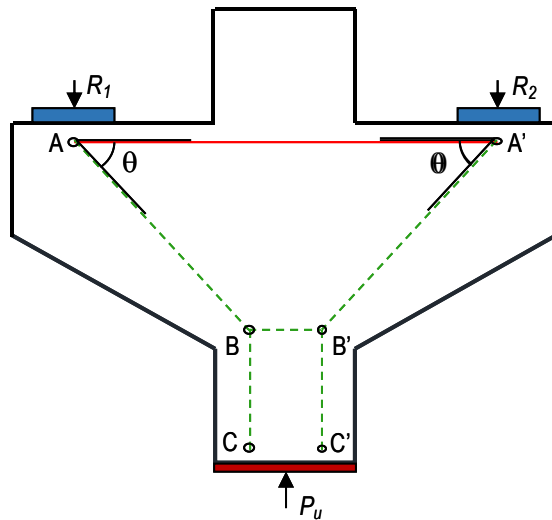
Inclined Node Geometry		Equation (where applicable)	Explanation (where applicable)*
B_{type}	CCC		Node B, figure on next page
$L_{back, B}$	2.89 in.	$\beta_1 c$	Section 23.2.2
$L_{bearing, B}$	7.00 in.		Section 23.2.2
$L_{inclined, B}$	7.27 in.	$L_{back, B} \cos\theta + L_{bearing, B} \sin\theta$	Figure 23.2.6b.
$A_{back, B}$	40.43 in. ²	$L_{back, B} b_w$	
$A_{bearing, B}$	98.00 in. ²	$L_{bearing, B} b_w$	
$A_{inclined, B}$	101.73 in. ²	$L_{inclined, B} b_w$	
Node B Check			
Back Face			
β_n	1.00		Table 23.9.2
f_{ce}	5.52 ksi	$0.85 \beta_n (f'_c)$	Eqn. 23.9.2
$F_{back, B}$	223.03 kips	$f_{ce} A_{back, B}$	Eqn. 23.9.1
$V_{n, back, B}$	277.86 kips	$F_{back, B} \tan\theta$	
Bearing Face			
$F_{bearing, B}$	540.62 in.	$f_{ce} A_{bearing, B}$	Eqn. 23.9.1
$V_{n, bearing, B}$	540.62 kips	$F_{bearing, B}$	
Inclined Face			
$F_{inclined, B}$	561.21 kips	$f_{ce} A_{inclined, B}$	Eqn. 23.9.1
$V_{n, inclined, B}$	437.66 kips	$F_{inclined, B} \sin\theta$	
$V_{n, NB}$	277.86 kip	$\min(V_{n, back, B}, V_{n, bearing, B}, V_{n, inclined, B})$	

* Equation, section, figure, and table numbers refer to those in ACI 318-14.

Table E-16. Specimen C1 ACI STM (part 3 of 3)

Tie Strength		Equation	Reference *
$V_{n, AA'}$	277.86 kips	$T(\tan\theta)$	Eqn. 23.7.2
Strut Strength			
Inclined Face			
A_{si}	101.73 in. ²	$\min(A_{\text{bearing, A}}, A_{\text{bearing, B}})$	Section 23.4.1
β_s	0.75		Table 23.4.3
f_{ce}	4.14 ksi	$0.85\beta_s f'_c$	Eqn. 23.4.3
F_s	420.91 kips	$f_{ce} A_{si}$	Eqn. 23.4.1
$V_{n, st}$	328.24 kips	$F_s \sin\theta$	
V_n	277.86 kips	$\min(V_{n, AA'}, V_{n, NA}, V_{n, NB}, V_{n, s})$	

* Equation, section and table numbers refer to those in ACI 318-14.



Specimen C2

Table E-17. Specimen C2 properties used in the ACI STM

Specimen Properties		Equation (where applicable)	Explanation (where applicable)*	Meet Requirements? (OK/NG)
f'_c	6830 psi			
f_{yp}	70.58 ksi			
A_s	3.16 in. ²	$A_{pb}^*(N_{pb})$		
b_w	14 in.			
d	22 in.			
a_v	13 in.			
A_{sh}	0.4 in. ²			
s_{sh}	3.5 in.			
Formula Calculations for Checks				
β_1	0.71	$0.85 - ((0.05(f'_c - 4000))/1000)$	Used to find the strut inclination based on concrete behavior at column face.	
T	223.03 kips	$A_s f_{yp}$		
c	3.87 in.	$(1000T)/(0.85f'_c \beta_1 b_w)$		
ϵ_s	0.014 in./in.	$0.003(d - c)/c$	Check whether steel has yielded.	-OK
B	1.37 in.	$\beta_1 c/2$	Node B Location, figure in 3 pages	
θ	51.34 °	$\tan^{-1}(d - B)/(3.5a_v)$	θ , figure in 3 pages	
CC	0.006	$(A_v/b_w s_v)(\sin\theta)$	Eqn. 23.5.3	-OK
a_v/d	0.591		Section 23.2.9	-OK
	1.192	$0.04(f'_c/f_y)(b_w d)$	Eqn. 23.2.9	-OK
Test Results				
V_u	401.1 kips			
V_u/V_n	1.44			-OK

* Equation and section numbers refer to those in ACI 318-14.

Table E-18. Specimen C2 ACI STM (part 1 of 3)

Inclined Node Geometry		Equation (where applicable)	Explanation (where applicable)*
A_{type}	CCT		Node A, figure in 2 pages
$L_{back, A}$	4.00 in.		
$L_{bearing, A}$	8.00 in.		
$L_{inclined, A}$	8.75 in.	$L_{back, A} \cos\theta + L_{bearing, A} \sin\theta$	Figure 23.2.6b.
$A_{back, A}$	56.00 in. ²	$L_{back, A} b_w$	
$A_{bearing, A}$	112.00 in. ²	$L_{bearing, A} b_w$	
$A_{inclined, A}$	122.44 in. ²	$L_{inclined, A} b_w$	
Node A Check			
Back Face			
β_n	0.80		Table 23.9.2
f_{ce}	4.6444 ksi	$0.85 \beta_n (f'_c)$	Eqn. 23.9.2
$F_{back, A}$	260.09 kips	$f_{ce} A_{back, A}$	Eqn. 23.9.1
$V_{n, back, A}$	325.15 kips	$F_{back, A} \tan\theta$	
Bearing Face			
$F_{bearing, A}$	520.17 kips	$f_{ce} A_{bearing, A}$	Eqn. 23.9.1
$V_{n, bearing, A}$	520.17 kips	$F_{bearing, A}$	
Inclined Face			
$F_{inclined, A}$	568.67 kips	$f_{ce} A_{inclined, A}$	Eqn. 23.9.1
$V_{n, inclined, A}$	444.08 kips	$F_{inclined, A} \sin\theta$	
$V_{n, NA}$	325.15 kip	$\min(V_{n, back, A}, V_{n, bearing, A}, V_{n, inclined, A})$	

* Equation, section, and table numbers refer to those in ACI 318-14.

Table E-19. Specimen C2 ACI STM (part 2 of 3)

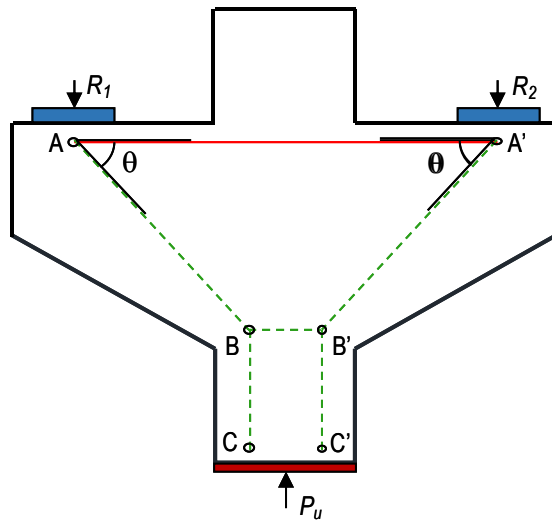
Inclined Node Geometry		Equation (where applicable)	Explanation (where applicable)*
B_{type}	CCC		Node B, figure on next page
$L_{back, B}$	2.74 in.	$\beta_1 c$	Section 23.2.2
$L_{bearing, B}$	7.00 in.		Section 23.2.2
$L_{inclined, B}$	7.18 in.	$L_{back, B} \cos\theta + L_{bearing, B} \sin\theta$	Figure 23.2.6b.
$A_{back, B}$	38.42 in. ²	$L_{back, B} b_w$	
$A_{bearing, B}$	98.00 in. ²	$L_{bearing, B} b_w$	
$A_{inclined, B}$	100.53 in. ²	$L_{inclined, B} b_w$	
Node B Check			
Back Face			
β_n	1.00		Table 23.9.2
f_{ce}	5.81 ksi	$0.85 \beta_n (f'_c)$	Eqn. 23.9.2
$F_{back, B}$	223.03 kips	$f_{ce} A_{back, B}$	Eqn. 23.9.1
$V_{n, back, B}$	278.83 kips	$F_{back, B} \tan\theta$	
Bearing Face			
$F_{bearing, B}$	568.94 in.	$f_{ce} A_{bearing, B}$	Eqn. 23.9.1
$V_{n, bearing, B}$	568.94 kips	$F_{bearing, B}$	
Inclined Face			
$F_{inclined, B}$	583.61 kips	$f_{ce} A_{inclined, B}$	Eqn. 23.9.1
$V_{n, inclined, B}$	455.75 kips	$F_{inclined, B} \sin\theta$	
$V_{n, NB}$	278.83 kip	$\min(V_{n, back, B}, V_{n, bearing, B}, V_{n, inclined, B})$	

* Equation, section, figure, and table numbers refer to those in ACI 318-14.

Table E-20. Specimen C2 ACI STM (part 3 of 3)

Tie Strength		Equation	Reference *
$V_{n, AA'}$	278.83 kips	$T(\tan\theta)$	Eqn. 23.7.2
Strut Strength			
Inclined Face			
A_{si}	100.53 in. ²	$\min(A_{\text{bearing, A}}, A_{\text{bearing, B}})$	Section 23.4.1
β_s	0.75		Table 23.4.3
f_{ce}	4.35 ksi	$0.85\beta_s f'_c$	Eqn. 23.4.3
F_s	437.71 kips	$f_{ce} A_{si}$	Eqn. 23.4.1
$V_{n, st}$	341.81 kips	$F_s \sin\theta$	
V_n	278.83 kips	$\min(V_{n, AA'}, V_{n, NA}, V_{n, NB}, V_{n, s})$	

* Equation, section and table numbers refer to those in ACI 318-14.



Specimen C3

Table E-21. Specimen C3 properties used in the ACI STM

Specimen Properties		Equation (where applicable)	Explanation (where applicable)*	Meet Requirements? (OK/NG)
f'_c	5590 psi			
f_{yp}	70.58 ksi			
A_s	3.16 in. ²	$A_{pb}^*(N_{pb})$		
b_w	14 in.			
d	22 in.			
a_v	13 in.			
A_{sh}	0 in. ²			
s_{sh}	3.5 in.			
Formula Calculations for Checks				
β_1	0.77	$0.85 - ((0.05(f'_c - 4000)) / 1000)$	Used to find the strut inclination based on concrete behavior at column face.	
T	223.03 kips	$A_s f_{yp}$		
c	4.35 in.	$(1000T) / (0.85 f'_c \beta_1 b_w)$		
ϵ_s	0.012 in./in.	$0.003(d - c) / c$	Check whether steel has yielded.	-OK
B	1.68 in.	$\beta_1 c / 2$	Node B Location, figure in 3 pages	
θ	50.93 °	$\tan^{-1}(d - B) / (3.5 a_v)$	θ , figure in 3 pages	
CC	0.000	$(A_v / b_w s_v) (\sin \theta)$	Eqn. 23.5.3	-NG
a_v / d	0.591		Section 23.2.9	-OK
	0.976	$0.04(f'_c / f_y)(b_w d)$	Eqn. 23.2.9	-OK
Test Results				
V_u	347.2 kips			
V_u / V_n	1.48			-OK

* Equation and section numbers refer to those in ACI 318-14.

Table E-22. Specimen C3 ACI STM (part 1 of 3)

Inclined Node Geometry		Equation (where applicable)	Explanation (where applicable)*
A_{type}	CCT		Node A, figure in 2 pages
$L_{back, A}$	4.00 in.		
$L_{bearing, A}$	8.00 in.		
$L_{inclined, A}$	8.73 in.	$L_{back, A} \cos\theta + L_{bearing, A} \sin\theta$	Figure 23.2.6b.
$A_{back, A}$	56.00 in. ²	$L_{back, A} b_w$	
$A_{bearing, A}$	112.00 in. ²	$L_{bearing, A} b_w$	
$A_{inclined, A}$	122.25 in. ²	$L_{inclined, A} b_w$	
Node A Check			
Back Face			
β_n	0.80		Table 23.9.2
f_{ce}	3.8012 ksi	$0.85 \beta_n (f'_c)$	Eqn. 23.9.2
$F_{back, A}$	212.87 kips	$f_{ce} A_{back, A}$	Eqn. 23.9.1
$V_{n, back, A}$	262.20 kips	$F_{back, A} \tan\theta$	
Bearing Face			
$F_{bearing, A}$	425.73 in.	$f_{ce} A_{bearing, A}$	Eqn. 23.9.1
$V_{n, bearing, A}$	425.73 kips	$F_{bearing, A}$	
Inclined Face			
$F_{inclined, A}$	464.69 kips	$f_{ce} A_{inclined, A}$	Eqn. 23.9.1
$V_{n, inclined, A}$	360.76 kips	$F_{inclined, A} \sin\theta$	
$V_{n, NA}$	262.20 kip	$\min(V_{n, back, A}, V_{n, bearing, A}, V_{n, inclined, A})$	

* Equation, section, figure, and table numbers refer to those in ACI 318-14.

Table E-23. Specimen C3 ACI STM (part 2 of 3)

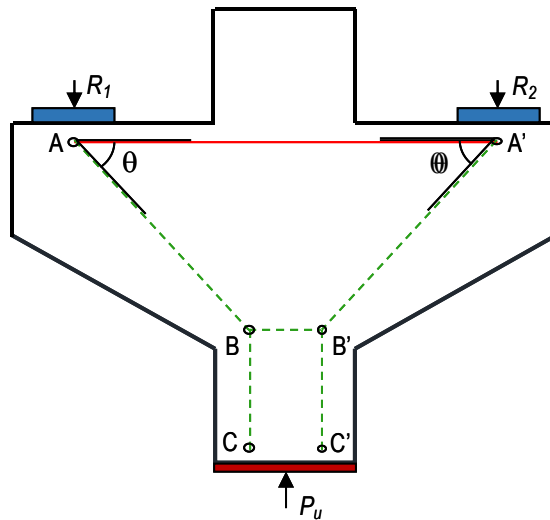
Inclined Node Geometry		Equation (where applicable)	Explanation (where applicable)*
B_{type}	CCC		Node B, figure on next page
$L_{back, B}$	3.35 in.	$\beta_1 c$	Section 23.2.2
$L_{bearing, B}$	7.00 in.		Section 23.2.2
$L_{inclined, B}$	7.55 in.	$L_{back, B} \cos\theta + L_{bearing, B} \sin\theta$	Figure 23.2.6b.
$A_{back, B}$	46.94 in. ²	$L_{back, B} b_w$	
$A_{bearing, B}$	98.00 in. ²	$L_{bearing, B} b_w$	
$A_{inclined, B}$	105.67 in. ²	$L_{inclined, B} b_w$	
Node B Check			
Back Face			
β_n	1.00		Table 23.9.2
f_{ce}	4.75 ksi	$0.85 \beta_n (f'_c)$	Eqn. 23.9.2
$F_{back, B}$	223.03 kips	$f_{ce} A_{back, B}$	Eqn. 23.9.1
$V_{n, back, B}$	274.72 kips	$F_{back, B} \tan\theta$	
Bearing Face			
$F_{bearing, B}$	465.65 in.	$f_{ce} A_{bearing, B}$	Eqn. 23.9.1
$V_{n, bearing, B}$	465.65 kips	$F_{bearing, B}$	
Inclined Face			
$F_{inclined, B}$	502.08 kips	$f_{ce} A_{inclined, B}$	Eqn. 23.9.1
$V_{n, inclined, B}$	389.80 kips	$F_{inclined, B} \sin\theta$	
$V_{n, NB}$	274.72 kip	$\min(V_{n, back, B}, V_{n, bearing, B}, V_{n, inclined, B})$	

* Equation, section, figure, and table numbers refer to those in ACI 318-14.

Table E-24. Specimen C3 ACI STM (part 3 of 3)

Tie Strength		Equation	Reference *
$V_{n, AA'}$	274.72 kips	$T(\tan\theta)$	Eqn. 23.7.2
Strut Strength			
Inclined Face			
A_{si}	105.67 in. ²	$\min(A_{\text{bearing, A}}, A_{\text{bearing, B}})$	Section 23.4.1
β_s	0.6		Table 23.4.3
f_{ce}	2.85 ksi	$0.85\beta_s f'_c$	Eqn. 23.4.3
F_s	301.25 kips	$f_{ce} A_{si}$	Eqn. 23.4.1
$V_{n, st}$	233.88 kips	$F_s \sin\theta$	
V_n	233.88 kips	$\min(V_{n, AA'}, V_{n, NA}, V_{n, NB}, V_{n, s})$	

* Equation, section and table numbers refer to those in ACI 318-14.



E.5 SPECIMEN CALCULATIONS: AASHTO LRFD STM ($\nu = 0.45$)

The tables presented in this section include the STM calculations based on AASHTO LRFD, assuming a conservative concrete efficiency factor of 0.45. Note that the confinement modification factor, m , is taken as 1 in all calculations in this section and Section E.6.

Specimen C0

Table E-25. Specimen C0 properties used in AASHTO STM calculations ($\nu = 0.45$)

Specimen Properties		Equation (where applicable)	Explanation (where applicable)*
f'_c	5250 psi		
f_{yp}	73.37 ksi		
A_s	3.16 in. ²	$A_{pb} * (N_{pb})$	
b_w	14 in.		
d	22 in.		
a_v	14.5 in.		
Formula Calculations for Checks			
β_1	0.79	$0.85 - ((0.05(f'_c - 4000))/1000)$	Used to find the strut inclination based on concrete behavior at column face.
T	231.85 kips	$A_s f_{yp}$	
c	4.71 in.	$(1000T)/(0.85f'_c \beta_1 b_w)$	
ϵ_s	0.011 in./in.	$0.003(d - c)/c$	Check whether steel has yielded.
B	1.86 in.	$\beta_1 c/2$	Node B Location, figure next page
θ	48.22 °	$\tan^{-1}[(d - B)/(3.5 + a_v)]$	θ shown on figure next page
Inclined Node Geometry			Node A, figure next page
A_{type}	CCT		
$L_{back, A}$	4.00 in.		
$L_{bearing, A}$	8.00 in.		
$L_{inclined, A}$	8.63 in.	$L_{back, A} \cos\theta + L_{bearing, A} \sin\theta$	Figure 5.6.3.2-1
$A_{back, A}$	56.00 in. ²	$L_{back, A} b_w$	
$A_{bearing, A}$	112.00 in. ²	$L_{bearing, A} b_w$	
$A_{inclined, A}$	120.83 in. ²	$L_{inclined, A} b_w$	
Test Results			
V_u	320.5 kips		
V_u/V_n	1.51		

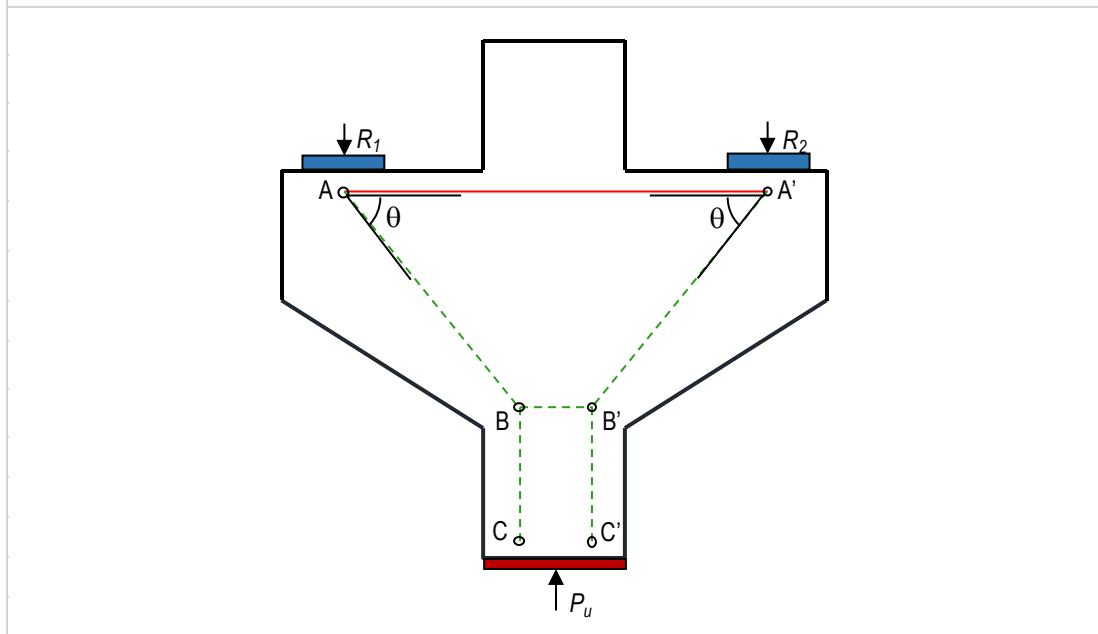
* Figure number refers to those in AASHTO LRFD Bridge Design Specifications.

Table E-26. Specimen C0 AASHTO STM calculations ($\nu = 0.45$)

Tie Strength		Equation	Reference*
$V_{n, AA'}$	259.47 kips	$T(\tan\theta)$	Eqn. 5.6.3.4.1-1
Node A Check			
ν	0.45		Table 5.6.3.5.3
f_{ce}	2.3625 ksi	$\nu(f'_c)$	Eqn. 5.6.3.5.3a-1
$F_{back, A}$	132.30 kips	$f_{ce} A_{back, A}$	Eqn. 5.6.3.5.1-1
$V_{n, back, A}$	148.06 kips	$F_{back, A} \tan\theta$	
$F_{bearing, A}$	264.60 in.	$f_{ce} A_{bearing, A}$	Eqn. 5.6.3.5.1-1
$V_{n, bearing, A}$	264.60 kips	$F_{bearing, A}$	
$F_{inclined, A}$	285.46 kips	$f_{ce} A_{inclined, A}$	Eqn. 5.6.3.5.1-1
$V_{n, inclined, A}$	212.86 kips	$F_{inclined, A} \sin\theta$	
V_n	212.86 kip **	$\min(V_{n, AA'}, V_{n, bearing, A}, V_{n, inclined, A})$	

* Equation and table numbers refer to those in AASHTO LRFD Bridge Design Specification.

** Doesn't include back-face checks that would have controlled.



Specimen C1

Table E-27. Specimen C1 properties used in AASHTO STM calculations ($\nu = 0.45$)

Specimen Properties		Equation (where applicable)	Explanation (where applicable)*
f'_c	6490 psi		
f_{yp}	70.58 ksi		
A_s	3.16 in. ²	$A_{pb} * (N_{pb})$	
b_w	14 in.		
d	22 in.		
a_v	13 in.		
Formula Calculations for Checks			
β_1	0.73	$0.85 - ((0.05(f'_c - 4000))/1000)$	Used to find the strut inclination based on concrete behavior at column face.
T	223.03 kips	$A_s f_{yp}$	
c	3.98 in.	$(1000T)/(0.85f'_c \beta_1 b_w)$	
ϵ_s	0.014 in./in.	$0.003(d - c)/c$	Check whether steel has yielded.
B	1.44 in.	$\beta_1 c/2$	Node B Location, figure next page
θ	51.25 °	$\tan^{-1}[(d - B)/(3.5 + a_v)]$	θ shown on figure next page
Inclined Node Geometry			Node A, figure next page
A_{type}	CCT		
$L_{back, A}$	4.00 in.		
$L_{bearing, A}$	8.00 in.		
$L_{inclined, A}$	8.74 in.	$L_{back, A} \cos\theta + L_{bearing, A} \sin\theta$	Figure 5.6.3.2-1
$A_{back, A}$	56.00 in. ²	$L_{back, A} b_w$	
$A_{bearing, A}$	112.00 in. ²	$L_{bearing, A} b_w$	
$A_{inclined, A}$	122.40 in. ²	$L_{inclined, A} b_w$	
Test Results			
V_u	376.9 kips		
V_u/V_n	1.36		

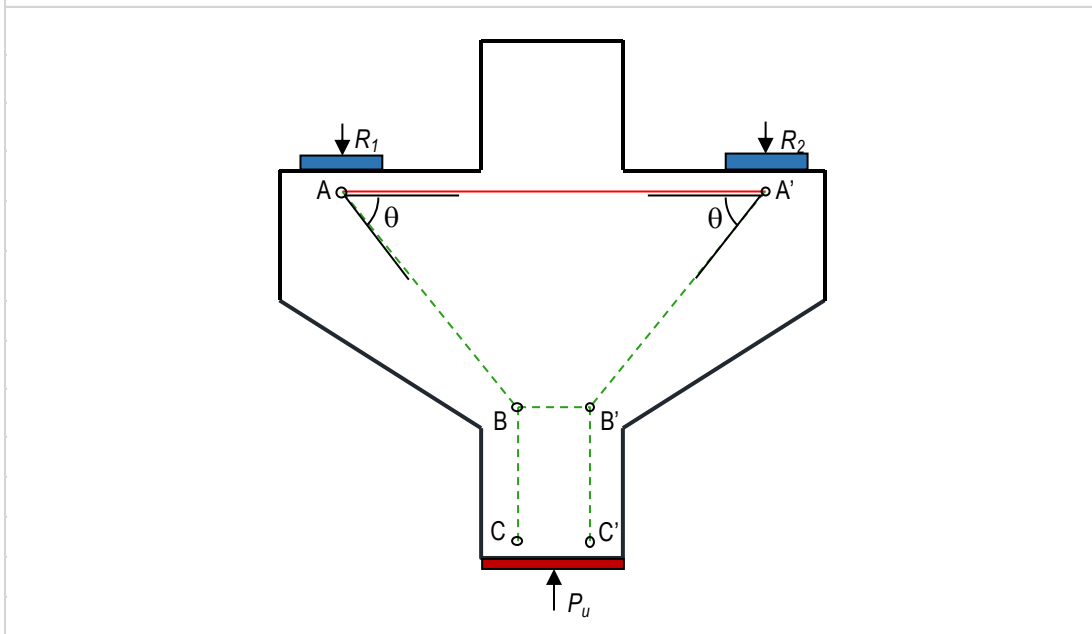
* Figure number refers to those in AASHTO LRFD Bridge Design Specifications.

Table E-28. Specimen C1 AASHTO STM calculations ($\nu = 0.45$)

Tie Strength		Equation	Reference*
$V_{n, AA'}$	277.86 kips	$T(\tan\theta)$	Eqn. 5.6.3.4.1-1
Node A Check			
ν	0.45		Table 5.6.3.5.3
f_{ce}	2.9205 ksi	$\nu(f'_c)$	Eqn. 5.6.3.5.3a-1
$F_{back, A}$	163.55 kips	$f_{ce} A_{back, A}$	Eqn. 5.6.3.5.1-1
$V_{n, back, A}$	203.75 kips	$F_{back, A} \tan\theta$	
$F_{bearing, A}$	327.10 in.	$f_{ce} A_{bearing, A}$	Eqn. 5.6.3.5.1-1
$V_{n, bearing, A}$	327.10 kips	$F_{bearing, A}$	
$F_{inclined, A}$	357.46 kips	$f_{ce} A_{inclined, A}$	Eqn. 5.6.3.5.1-1
$V_{n, inclined, A}$	278.76 kips	$F_{inclined, A} \sin\theta$	
V_n	277.86 kip **	$\min(V_{n, AA'}, V_{n, bearing, A}, V_{n, inclined, A})$	

* Equation and table numbers refer to those in AASHTO LRFD Bridge Design Specification.

** Doesn't include back-face checks that would have controlled.



Specimen C2

Table E-29. Specimen C2 properties used in AASHTO STM calculations ($\nu = 0.45$)

Specimen Properties		Equation (where applicable)	Explanation (where applicable)*
f'_c	6830 psi		
f_{yp}	70.58 ksi		
A_s	3.16 in. ²	$A_{pb} * (N_{pb})$	
b_w	14 in.		
d	22 in.		
a_v	13 in.		
Formula Calculations for Checks			
β_1	0.71	$0.85 - ((0.05(f'_c - 4000))/1000)$	Used to find the strut inclination based on concrete behavior at column face.
T	223.03 kips	$A_s f_{yp}$	
c	3.87 in.	$(1000T)/(0.85f'_c \beta_1 b_w)$	
ϵ_s	0.014 in./in.	$0.003(d - c)/c$	Check whether steel has yielded.
B	1.37 in.	$\beta_1 c/2$	Node B Location, figure next page
θ	51.34 °	$\tan^{-1}[(d - B)/(3.5 + a_v)]$	θ shown on figure next page
Inclined Node Geometry			Node A, figure next page
A_{type}	CCT		
$L_{back, A}$	4.00 in.		
$L_{bearing, A}$	8.00 in.		
$L_{inclined, A}$	8.75 in.	$L_{back, A} \cos\theta + L_{bearing, A} \sin\theta$	Figure 5.6.3.2-1
$A_{back, A}$	56.00 in. ²	$L_{back, A} b_w$	
$A_{bearing, A}$	112.00 in. ²	$L_{bearing, A} b_w$	
$A_{inclined, A}$	122.44 in. ²	$L_{inclined, A} b_w$	
Test Results			
V_u	401.1 kips		
V_u/V_n	1.44		

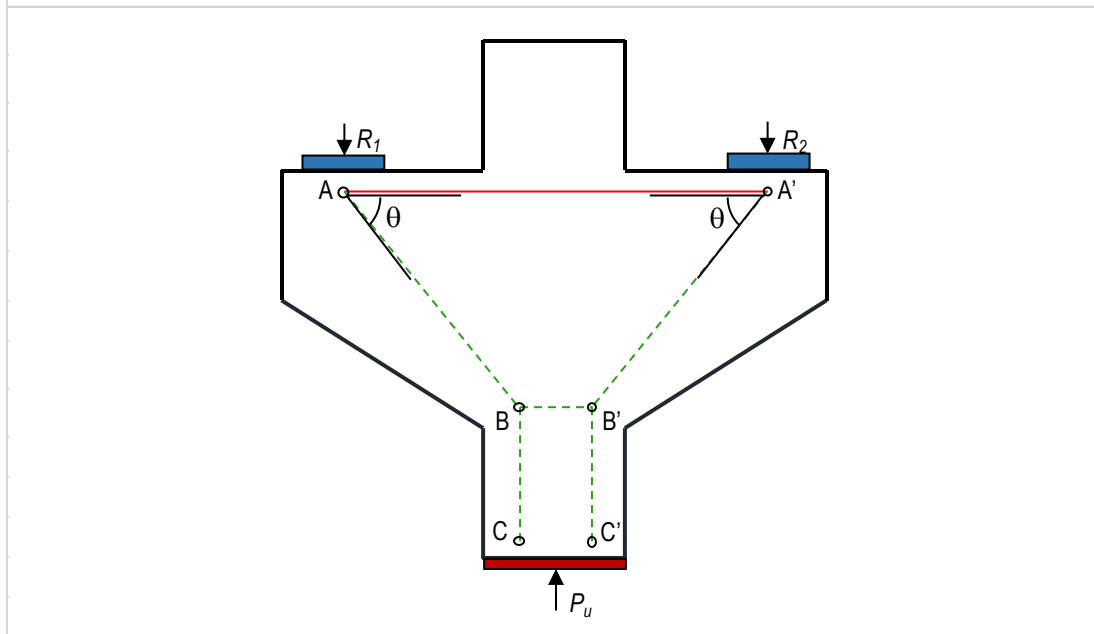
* Figure number refers to those in AASHTO LRFD Bridge Design Specifications.

Table E-30. Specimen C2 AASHTO STM calculations ($\nu = 0.45$)

Tie Strength		Equation	Reference*
$V_{n, AA'}$	278.83 kips	$T(\tan\theta)$	Eqn. 5.6.3.4.1-1
Node A Check			
ν	0.45		Table 5.6.3.5.3
f_{ce}	3.0735 ksi	$\nu(f'_c)$	Eqn. 5.6.3.5.3a-1
$F_{back, A}$	172.12 kips	$f_{ce} A_{back, A}$	Eqn. 5.6.3.5.1-1
$V_{n, back, A}$	215.18 kips	$F_{back, A} \tan\theta$	
$F_{bearing, A}$	344.23 in.	$f_{ce} A_{bearing, A}$	Eqn. 5.6.3.5.1-1
$V_{n, bearing, A}$	344.23 kips	$F_{bearing, A}$	
$F_{inclined, A}$	376.33 kips	$f_{ce} A_{inclined, A}$	Eqn. 5.6.3.5.1-1
$V_{n, inclined, A}$	293.88 kips	$F_{inclined, A} \sin\theta$	
V_n	278.83 kip **	$\min(V_{n, AA'}, V_{n, bearing, A}, V_{n, inclined, A})$	

* Equation and table numbers refer to those in AASHTO LRFD Bridge Design Specification.

** Doesn't include back-face checks that would have controlled.



Specimen C3

Table E-31. Specimen C3 properties used in AASHTO STM calculations ($\nu = 0.45$)

Specimen Properties		Equation (where applicable)	Explanation (where applicable)*
f'_c	5590 psi		
f_{yp}	70.58 ksi		
A_s	3.16 in. ²	$A_{pb} * (N_{pb})$	
b_w	14 in.		
d	22 in.		
a_v	13 in.		
Formula Calculations for Checks			
β_1	0.77	$0.85 - ((0.05(f'_c - 4000))/1000)$	Used to find the strut inclination based on concrete behavior at column face.
T	223.03 kips	$A_s f_{yp}$	
c	4.35 in.	$(1000T)/(0.85f'_c \beta_1 b_w)$	
ϵ_s	0.012 in./in.	$0.003(d - c)/c$	Check whether steel has yielded.
B	1.68 in.	$\beta_1 c/2$	Node B Location, figure next page
θ	50.93 °	$\tan^{-1}[(d - B)/(3.5 + a_v)]$	θ shown on figure next page
Inclined Node Geometry			Node A, figure next page
A_{type}	CCT		
$L_{back, A}$	4.00 in.		
$L_{bearing, A}$	8.00 in.		
$L_{inclined, A}$	8.73 in.	$L_{back, A} \cos\theta + L_{bearing, A} \sin\theta$	Figure 5.6.3.2-1
$A_{back, A}$	56.00 in. ²	$L_{back, A} b_w$	
$A_{bearing, A}$	112.00 in. ²	$L_{bearing, A} b_w$	
$A_{inclined, A}$	122.25 in. ²	$L_{inclined, A} b_w$	
Test Results			
V_u	347.2 kips		
V_u/V_n	1.45		

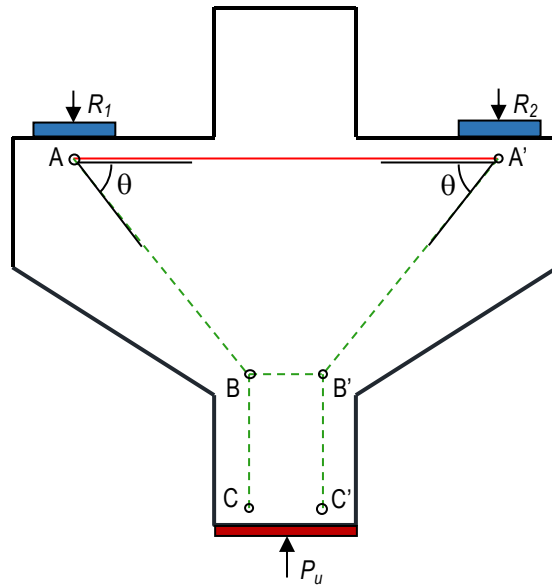
* Figure number refers to those in AASHTO LRFD Bridge Design Specifications.

Table E-32. Specimen C3 AASHTO STM calculations ($\nu = 0.45$)

Tie Strength		Equation	Reference*
$V_{n, AA'}$	274.72 kips	$T(\tan\theta)$	Eqn. 5.6.3.4.1-1
Node A Check			
ν	0.45		Table 5.6.3.5.3
f_{ce}	2.5155 ksi	$\nu(f'_c)$	Eqn. 5.6.3.5.3a-1
$F_{back, A}$	140.87 kips	$f_{ce} A_{back, A}$	Eqn. 5.6.3.5.1-1
$V_{n, back, A}$	173.51 kips	$F_{back, A} \tan\theta$	
$F_{bearing, A}$	281.74 in.	$f_{ce} A_{bearing, A}$	Eqn. 5.6.3.5.1-1
$V_{n, bearing, A}$	281.74 kips	$F_{bearing, A}$	
$F_{inclined, A}$	307.52 kips	$f_{ce} A_{inclined, A}$	Eqn. 5.6.3.5.1-1
$V_{n, inclined, A}$	238.74 kips	$F_{inclined, A} \sin\theta$	
V_n	238.74 kip **	$\min(V_{n, AA'}, V_{n, bearing, A}, V_{n, inclined, A})$	

* Equation and table numbers refer to those in AASHTO LRFD Bridge Design Specification.

** Doesn't include back-face checks that would have controlled.



E.6 SPECIMEN CALCULATIONS: AASHTO STM ($\upsilon > 0.45$)

The tables in this section present the AASHTO LRFD STM calculations for Specimens C0, C1, and C2, assuming a concrete efficiency factor according to Table 5.6.3.5.3a-1 of these specifications. Since the distributed reinforcement in none of the specimens satisfied the crack-control reinforcement requirements of AASHTO LRFD according to Article 5.6.3.6, the use of efficiency factors greater than 0.45 does not conform to the specifications. However, this set of calculations was completed for comparison purposes. For Specimen C3, which did not contain any crack-control reinforcement, the concrete efficiency factor was always taken as 0.45. Therefore, Specimen C3 is not included in this section.

Specimen C0

Table E-33. Specimen C0 properties used in AASHTO STM calculations ($\nu > 0.45$)

Specimen Properties		Equation (where applicable)	Explanation (where applicable)*
f'_c	5250 psi		
f_{yp}	73.37 ksi		
A_s	3.16 in. ²	$A_{pb} * (N_{pb})$	
b_w	14 in.		
d	22 in.		
a_v	14.5 in.		
A_v	0.4 in. ²		
s_v	3.5 in.		
Formula Calculations for Checks			
β_1	0.79	$0.85 - ((0.05(f'_c - 4000))/1000)$	Used to find the strut inclination based on concrete behavior at column face.
T	231.85 kips	$A_s f_{yp}$	
c	4.71 in.	$(1000T)/(0.85f'_c \beta_1 b_w)$	
ϵ_s	0.011 in./in.	$0.003(d-c)/c$	Check whether steel has yielded.
B	1.86 in.	$\beta_1 c/2$	Node B Location, figure next page
θ	48.22 °	$\tan^{-1}[(d-B)/(3.5+a_v)]$	θ shown on figure next page
Inclined Node Geometry			Node A, figure next page
A_{type}	CCT		
$L_{back, A}$	4.00 in.		
$L_{bearing, A}$	8.00 in.		
$L_{inclined, A}$	8.63 in.	$L_{back, A} \cos\theta + L_{bearing, A} \sin\theta$	Figure 5.6.3.2-1
$A_{back, A}$	56.00 in. ²	$L_{back, A} b_w$	
$A_{bearing, A}$	112.00 in. ²	$L_{bearing, A} b_w$	
$A_{inclined, A}$	120.83 in. ²	$L_{inclined, A} b_w$	
Test Results			
V_u	320.5 kips		
V_u/V_n	1.24		

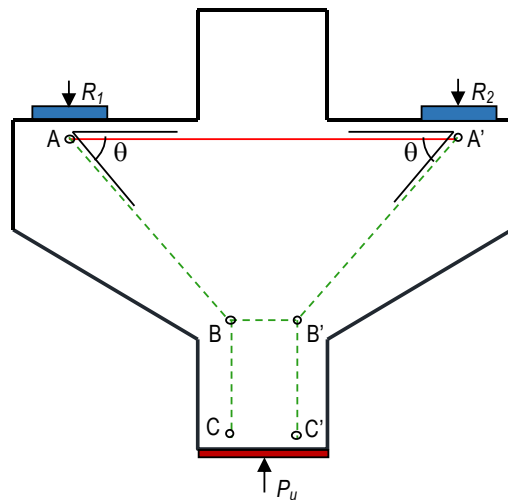
* Figure number refers to those in AASHTO LRFD Bridge Design Specifications.

Table E-34. Specimen C0 AASHTO STM calculations ($\nu > 0.45$)

Tie Strength		Equation	Reference *
$V_{n, AA'}$	259.47 kips	$T(\tan\theta)$	Eqn. 5.6.3.4.1-1
Node A Check			
Back Face			
ν	0.70		Table 5.6.3.5.3a-1
f_{ce}	3.675 ksi	$\nu(f'_c)$	Eqn. 5.6.3.5.3a-1
$F_{back, A}$	205.80 kips	$f_{ce} A_{back, A}$	Eqn. 5.6.3.5.1-1
$V_{n, back, A}$	230.32 kips	$F_{back, A} \tan\theta$	
Bearing Face			
ν	0.70		Table 5.6.3.5.3a-1
f_{ce}	3.675 ksi	$\nu(f'_c)$	Eqn. 5.6.3.5.3a-1
$F_{bearing, A}$	411.60 in.	$f_{ce} A_{bearing, A}$	Eqn. 5.6.3.5.1-1
$V_{n, bearing, A}$	411.60 kips	$F_{bearing, A}$	
Inclined Face			
ν	0.59		Table 5.6.3.5.3a-1
f_{ce}	3.084375 ksi	$\nu(f'_c)$	Eqn. 5.6.3.5.3a-1
$F_{inclined, A}$	372.68 kips	$f_{ce} A_{inclined, A}$	Eqn. 5.6.3.5.1-1
$V_{n, inclined, A}$	277.90 kips	$F_{inclined, A} \sin\theta$	
V_n	259.47 kip **	$\min(V_{n, AA'}, V_{n, Abearing}, V_{n, Ainclined})$	

* Equation and table numbers refer to those in AASHTO LRFD Bridge Design Specifications.

** Doesn't include back-face checks that would have controlled.



Specimen C1

Table E-35. Specimen C1 properties used in AASHTO STM calculations ($\nu > 0.45$)

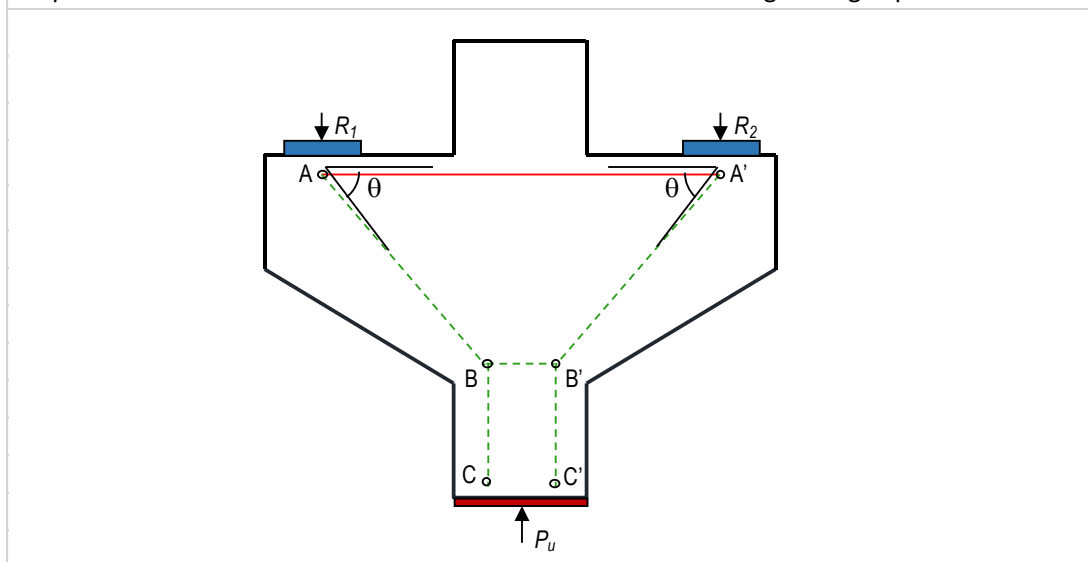
Specimen Properties		Equation (where applicable)	Explanation (where applicable)*
f'_c	6490 psi		
f_{yp}	70.58 ksi		
A_s	3.16 in. ²	$A_{pb}*(N_{pb})$	
b_w	14 in.		
d	22 in.		
a_v	13 in.		
A_v	0.4 in. ²		
s_v	6 in.		
Formula Calculations for Checks			
β_1	0.73	$0.85 - ((0.05(f'_c - 4000))/1000)$	Used to find the strut inclination based on concrete behavior at column face.
T	223.03 kips	$A_s f_{yp}$	
c	3.98 in.	$(1000T)/(0.85f'_c \beta_1 b_w)$	
ϵ_s	0.014 in./in.	$0.003(d-c)/c$	Check whether steel has yielded.
B	1.44 in.	$\beta_1 c/2$	Node B Location, figure next page
θ	51.25 °	$\tan^{-1}[(d-B)/(3.5+a_v)]$	θ shown on figure next page
Inclined Node Geometry			Node A, figure next page
A_{type}	CCT		
$L_{back, A}$	4.00 in.		
$L_{bearing, A}$	8.00 in.		
$L_{inclined, A}$	8.74 in.	$L_{back, A} \cos\theta + L_{bearing, A} \sin\theta$	Figure 5.6.3.2-1
$A_{back, A}$	56.00 in. ²	$L_{back, A} b_w$	
$A_{bearing, A}$	112.00 in. ²	$L_{bearing, A} b_w$	
$A_{inclined, A}$	122.40 in. ²	$L_{inclined, A} b_w$	
Test Results			
V_u	376.9 kips		
V_u/V_n	1.36		

* Figure number refers to those in AASHTO LRFD Bridge Design Specifications.

Table E-36. Specimen C1 AASHTO STM calculations ($\nu > 0.45$)

Tie Strength		Equation	Reference *
$V_{n, AA'}$	277.86 kips	$T(\tan\theta)$	Eqn. 5.6.3.4.1-1
Node A Check			
Back Face			
ν	0.70		Table 5.6.3.5.3a-1
f_{ce}	4.543 ksi	$\nu(f'_c)$	Eqn. 5.6.3.5.3a-1
$F_{back, A}$	254.41 kips	$f_{ce} A_{back, A}$	Eqn. 5.6.3.5.1-1
$V_{n, back, A}$	316.95 kips	$F_{back, A} \tan\theta$	
Bearing Face			
ν	0.70		Table 5.6.3.5.3a-1
f_{ce}	4.543 ksi	$\nu(f'_c)$	Eqn. 5.6.3.5.3a-1
$F_{bearing, A}$	508.82 in.	$f_{ce} A_{bearing, A}$	Eqn. 5.6.3.5.1-1
$V_{n, bearing, A}$	508.82 kips	$F_{bearing, A}$	
Inclined Face			
ν	0.53		Table 5.6.3.5.3a-1
f_{ce}	3.410495 ksi	$\nu(f'_c)$	Eqn. 5.6.3.5.3a-1
$F_{inclined, A}$	417.44 kips	$f_{ce} A_{inclined, A}$	Eqn. 5.6.3.5.1-1
$V_{n, inclined, A}$	325.54 kips	$F_{inclined, A} \sin\theta$	
V_n	277.86 kip	$\min(V_{n, AA'}, V_{n, Abearing}, V_{n, Ainclined})$	

* Equation and table numbers refer to those in AASHTO LRFD Bridge Design Specifications.



Specimen C2

Table E-37. Specimen C2 properties used in AASHTO STM calculations ($\nu > 0.45$)

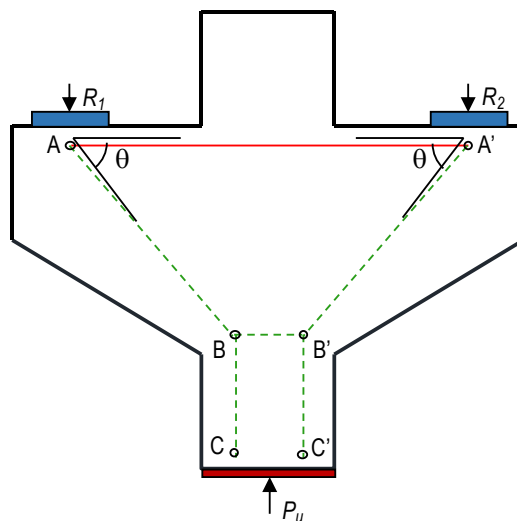
Specimen Properties		Equation (where applicable)	Explanation (where applicable)*
f'_c	6830 psi		
f_{yp}	70.58 ksi		
A_s	3.16 in. ²	$A_{pb} * (N_{pb})$	
b_w	14 in.		
d	22 in.		
a_v	13 in.		
A_v	0.4 in. ²		
s_v	3.5 in.		
Formula Calculations for Checks			
β_1	0.71	$0.85 - ((0.05(f'_c - 4000))/1000)$	Used to find the strut inclination based on concrete behavior at column face.
T	223.03 kips	$A_s f_{yp}$	
c	3.87 in.	$(1000T)/(0.85f'_c \beta_1 b_w)$	
ϵ_s	0.014 in./in.	$0.003(d-c)/c$	Check whether steel has yielded.
B	1.37 in.	$\beta_1 c/2$	Node B Location, figure next page
θ	51.34 °	$\tan^{-1}[(d-B)/(3.5+a_v)]$	θ shown on figure next page
Inclined Node Geometry			Node A, figure next page
A_{type}	CCT		
$L_{back, A}$	4.00 in.		
$L_{bearing, A}$	8.00 in.		
$L_{inclined, A}$	8.75 in.	$L_{back, A} \cos\theta + L_{bearing, A} \sin\theta$	Figure 5.6.3.2-1
$A_{back, A}$	56.00 in. ²	$L_{back, A} b_w$	
$A_{bearing, A}$	112.00 in. ²	$L_{bearing, A} b_w$	
$A_{inclined, A}$	122.44 in. ²	$L_{inclined, A} b_w$	
Test Results			
V_u	401.1 kips		
V_u/V_n	1.44		

* Figure number refers to those in AASHTO LRFD Bridge Design Specifications.

Table E-38. Specimen C2 AASHTO STM calculations ($\nu > 0.45$)

Tie Strength		Equation	Reference *
$V_{n, AA'}$	278.83 kips	$T(\tan\theta)$	Eqn. 5.6.3.4.1-1
Node A Check			
Back Face			
ν	0.70		Table 5.6.3.5.3a-1
f_{ce}	4.781 ksi	$\nu(f'_c)$	Eqn. 5.6.3.5.3a-1
$F_{back, A}$	267.74 kips	$f_{ce} A_{back, A}$	Eqn. 5.6.3.5.1-1
$V_{n, back, A}$	334.72 kips	$F_{back, A} \tan\theta$	
Bearing Face			
ν	0.70		Table 5.6.3.5.3a-1
f_{ce}	4.781 ksi	$\nu(f'_c)$	Eqn. 5.6.3.5.3a-1
$F_{bearing, A}$	535.47 in.	$f_{ce} A_{bearing, A}$	Eqn. 5.6.3.5.1-1
$V_{n, bearing, A}$	535.47 kips	$F_{bearing, A}$	
Inclined Face			
ν	0.51		Table 5.6.3.5.3a-1
f_{ce}	3.473055 ksi	$\nu(f'_c)$	Eqn. 5.6.3.5.3a-1
$F_{inclined, A}$	425.25 kips	$f_{ce} A_{inclined, A}$	Eqn. 5.6.3.5.1-1
$V_{n, inclined, A}$	332.08 kips	$F_{inclined, A} \sin\theta$	
V_n	278.83 kip	$\min(V_{n, AA'}, V_{n, Abearing}, V_{n, Ainclined})$	

* Equation and table numbers refer to those in AASHTO LRFD Bridge Design Specifications.



References

- ACI Committee 318. (2014). *Building Code Requirements for Structural Concrete (ACI 318R-14)*. Farmington Hills, Michigan: American Concrete Institute.
- American Association of State Highway and Transportation Officials (AASHTO). (2016). *AASHTO LRFD Bridge Design Specifications, 7th Edition-with 2015 and 2016 Interim Revisions*. Washington, DC.
- ASTM. (2004). *ASTM C496/C496M: Standard Test Method for Splitting Tensile Strength of Cylindrical Concrete Specimens*. West Conshohocken, PA: ASTM.
- ASTM. (2014). *ASTM C469/C469M: Standard Test Method for Static Modulus of Elasticity and Poisson's Ratio of Concrete in Compression*. West Conshohocken, PA: ASTM.
- ASTM. (2017). *ASTM A370: Standard Test Methods and Definitions for Mechanical Testing of Steel Products*. West Conshohocken, PA: ASTM.
- ASTM. (2017). *ASTM C39/C39M: Standard Test Method for Compressive Strength of Cylindrical Concrete Specimens*. West Conshohocken, PA: ASTM.
- Birkeland, P. W., & Birkeland, H. W. (1966). Connections in Precast Concrete Construction. *Journal of the American Concrete Institute*, 63(3), 345-368.
- Campione, G., La Mendola, L., & Mangiavillano, M. L. (2007). Steel Fiber-Reinforced Concrete Corbels: Experimental Behavior and Shear Strength Prediction. *ACI Structural Journal*, 104(5), 570-579.
- Fattuhi, N. (1994). Reinforced Corbels Made with High-Strength Concrete and Various Secondary Reinforcements. *ACI Structural Journal*, 91(4), 376-383.

- Fattuhi, N. I., & Hughes, B. P. (1989). Ductility of Reinforced Concrete Corbels Containing either Steel Fibers or Stirrups. *ACI Structural Journal*, 86(6), 644-651.
- Foster, S. J., Powell, R. E., & Selim, H. S. (1996). Performance of High-Strength Concrete Corbels. *ACI Structural Journal*, 93(5), 555-563.
- Kriz, L. B., & Rath, C. H. (1965). Connections in Precast Concrete Structures—Strength of Corbels. *PCI Journal*, 10(1), 16-61.
- Marti, P. (1985). Basic Tools of Reinforced Concrete Beam Design. *ACI Structural Journal*, 82(1), 46-56.
- Mattock, A. H., Chen, K. C., & Soongswang, K. (1976). The Behavior of Reinforced Concrete Corbels. *PCI Journal*, 21(2), 52-77.
- Park, R., & Paulay, T. (1975). *Reinforced Concrete Structures*. John Wiley & Sons.
- Ritter, W. (1899). Die Bauweise Hennebique. *Schweizerische Bauzeitung Bd, XXXIII(7)*.
- Schlaich, J. e. (1987). Toward a Consistent Design of Structural Concrete. *PCI Journal*, 32(3), 74-150.
- Yong, Y., Douglas, H., McCloskey, H., & Nawy, E. G. (1985). Reinforced Corbels of High-Strength Concrete. *American Concrete Institute, SP 87*, 197-212.

Vita

Heather Renae Wilson was born in Sacramento, California. She completed her Bachelor of Science in Civil Engineering in 2015 at The University of Alabama in Tuscaloosa, Alabama after graduating from John F. Kennedy High School in Sacramento, California in 2011. During her undergraduate career, Wilson worked as an undergraduate research assistant with Dr. Sriram Aaleti on Ultra-High Performance Concrete (UHPC). In summer 2015, she began her Master of Science studies at The University of Texas at Austin and started working at the Ferguson Structural Engineering Laboratory.

Permanent email: hrwilson2312@gmail.com

This thesis was typed by the author.